AN ABSTRACT OF THE DISSERTATION OF

Terrah M. Owens for the degree of Doctor of Philosophy in Rangeland Ecology and Management presented on November 30, 2023.

Title: Cascading Effects of Anthropogenic Subsidies and Wildfire on Avian Predator Communities and Impacts to Greater Sage-grouse Habitat Selection and Survival

Abstract approved: _____
Jonathan B. Dinkins

The sagebrush biome of western North America faces multiple threats, including land conversion, urban encroachment, resource extraction, conifer expansion, invasive annual grasses, and wildfire. In the Great Basin region, wildfire has surpassed all other sources of habitat loss and fragmentation, burning nearly 90.2 million km2 since the mid-1980s. This loss of sagebrush has contributed to population declines of the greater sage-grouse (Centrocercus urophasianus; hereafter, sage-grouse) which is often used as an umbrella species for the over 350 other species of conservation concern that occur within their range. In addition to the existing threats to the sagebrush biome, sage-grouse are also threatened by increased predation pressure from anthropogenically subsidized predators. I investigated how anthropogenic subsidies and wildfire have altered the landscape and the avian predator community and the subsequent impacts to sage-grouse habitat selection, space use, and survival.

I used count data from a six-year data set (n = 678) and binomial N-mixture, single-species, and multi-species occupancy models to assess how anthropogenic subsidies and wildfire affect density, occupancy and interspecies interactions of

common ravens (Corvus corax; hereafter, ravens), red-tailed hawks (Buteo jaimacensis), and Swainson's hawks in a fire- and human-altered landscape in eastern Oregon. My results indicated anthropogenic subsidies and recent wildfires (≤10 years) were positively associated with the density and occupancy of ravens and red-tailed hawks and were indirectly associated with density and occupancy of Swainson's hawks. The results from multi-species occupancy models provided evidence of resource partitioning between the three species and demonstrated that occupancy probabilities were positively influenced by the presence of an allospecific in altered landscapes. My results indicated that anthropogenic subsidies created generalist predator hotspots, which pose additional threats to sage-grouse, particularly in fire-affected areas.

I used resource selection functions and Cox proportional hazards models to investigate potential additive and interactive effects of wildfire and relative raven density on sage-grouse nest-site selection and survival (n = 169). Raven density did not affect sage-grouse nest-site selection, but female sage-grouse did select nest sites closer to fire footprints (<10 years) and with a higher proportion of burned area (<5 years). Sage-grouse nest survival was negatively influenced as proximity to burned areas (<5 years) and raven density increased. Nest survival was below the range-wide average (0.38) in three out of four of my study areas (0.15–0.28). However, nest survival in the study area with the largest fire footprint was higher (0.51), providing evidence that the effects of fire on sage-grouse nest success may be reduced if nesting areas are located farther away from anthropogenic subsidies that support generalist predators.

I used linear and Cox proportional hazards mixed models to evaluate how landscape composition and configuration affected the spring neighborhood size and survival of adult female sage-grouse. I created minimum convex polygons (n = 107) representing spring neighborhoods between 1 March and 30 June for individual females (n = 76). Neighborhood size varied with the proportion and configuration of anthropogenic footprint, while neighborhood size decreased with an increasing proportion of non-sagebrush and sagebrush cover, but at different rates depending on the configuration. Female survival was negatively affected as the anthropogenic footprint increased and varied in response to the configuration of juniper cover.

My results indicated that anthropogenic and wildfire disturbance affect the nest-site selection and spring space use of female sage-grouse and alter the generalist avian predator community. Landscape heterogeneity and subsidization of generalist predators had direct consequences to sage-grouse adult and nest survival.

Cascading Effects of Anthropogenic Subsidies and Wildfire on Avian Predator Communities and Impacts to Greater Sage-grouse Habitat Selection and Survival

by
Terrah M. Owens

A DISSERTATION

submitted to

Oregon State University

in partial fulfillment of
the requirements for the
degree of

Doctor of Philosophy

Presented November 30, 2023
Commencement June 2024

Doctor of Philosophy dissertation of Terrah M. Owens presented on November 30, 2023

APPROVED:

Major Professor, representing Rangeland Ecology and Management

Head of the Department of Animal and Rangeland Sciences

Dean of the Graduate School

I understand that my thesis will become part of the permanent collection of Oregon State University libraries. My signature below authorizes release of my thesis to any reader upon request.

Terrah M. Owens, Author

ACKNOWLEDGEMENTS

I would like to express my sincere gratitude to my advisor, Jon Dinkins, and my Committee Andrew Olsen, Lisa Ellsworth, Virginia Lesser, and Lori Kayes for their support and guidance throughout this project.

Financial support for this project was provided by the Oregon Department of Fish and Wildlife (ODFW) through Federal Aid in Wildlife Restoration (Pittman-Robertson), the Bureau of Land Management (BLM), U.S. Fish and Wildlife Service (USFWS), and the Oregon Beef Council. I would also like to thank the Department of Animal and Rangeland Sciences for travel awards.

Thank you to the ODFW personnel who made this project possible especially Brian Ratliff, Jason Badger, John Gutcher, Justin Primus, Lee Foster, Mikal Cline, Philip Milburn, Scott Torland, Skyler Vold, and Tom Segal. Also, a big thank you to Glenn Frederick (BLM) and Jacqueline Cupples (USFWS) for their continued support. This project would not have been possible without the help of dedicated technicians. Thank you, Hannah White, Tyler Dungannon, Kris Hernandez, Jackie Dougherty, Rachel Scheffler, Zack Slick, Todd Stansbury, Alex Johnson, Alex Stevens, Stephanie LeQuier, Caleb, Trevor, Derek, Stephanie Loredo, Nathaniel Umphrey, Zac Kendall, Kevin Bott, Bri, and Allison Beck.

I would like to thank my fellow lab mates who have supported me physically, mentally, and spiritually for the last six years. Thank you, Lindsey Perry, Claire Revekant, Alan Harrington, Kayla Ruth, Vanessa Schroeder, Cara Christensen, Shawn Szabo, and Richard Rich. Lastly, I would like to thank my partner Dick

Houghtaling, and my dad Rick Owens, for their unending love and support through this entire process.

TABLE OF CONTENTS

TABLE OF CONTENTS (Continued)

LIST OF FIGURES

LIST OF FIGURES (continued)

Figure Page

LIST OF TABLES

LIST OF TABLES (continued)

CHAPTER 1 - INTRODUCTION

The sagebrush (*Artemisia* spp.) biome stretches across nearly 700,000 km^2 across 14 U.S. states and two Canadian provinces. Considered one of the most imperiled landscapes in North America, it faces multiple threats including climate change, land conversion, urban encroachment, resource extraction, conifer expansion, invasive annual grasses, and wildfire (Doherty et al. 2022, USFWS 2015). These threats also jeopardize nearly 350 plant and animal species of conservation concern that occur in the sagebrush biome (Wisdom et al. 2005). One of the most iconic of these species is the greater sage-grouse (*Centrocercus urophasianus*; hereafter, sage-grouse) which is often considered an umbrella species for the sagebrush ecosystem (Rowland et al. 2006, Barlow et al. 2019, Duchardt et al. 2023). Prior to European settlement, sage-grouse occurred in what are now 13 western states and three Canadian provinces. Now, they occupy less than half of their former range and are extirpated from two US states and one Canadian province (Schroeder et al. 2004, Doherty et al. 2016). The sage-grouse was listed as endangered in Canada in 2008 under the Species at Risk Act (Lungle and Pruss 2008). In contrast, it was not listed in the United States under the Endangered Species Act due to an unprecedented conservation effort, but it remains a species of concern as populations continue to decline due to continued habitat loss and degradation (USFWS 2015).

In the western half of the sage-grouse range, wildfire is the leading cause of habitat loss and fragmentation (Miller at al. 2011, Crist et al. 2023). Nearly 90.2 million km^2 of sagebrush burned between 1984 and 2020, primarily in the Great Basin region (Crist et al. 2023). Sagebrush species experience high mortality during

fire events and, depending on species and location, can take 35 to 120 years to recover fully (Baker 2011). Along with climate change and human fire ignitions (Flannigan et al. 2009, Creutzburg et al. 2015, Coates et al. 2016, Fusco et al. 2022), invasive annual grasses such as cheatgrass (*Bromus tectorum*) and medusahead (*Taeniatherum caput-medusae*), have also contributed to the increase in wildfire activity in the Great Basin (Balch et al. 2013). Large fires (>400 km^2) occasionally occurred before European settlement (Bukowski and Baker 2013) but are now common in the sagebrush biome. Fire return intervals have shortened from ~50 to over 100 years in Wyoming big sagebrush (*A. tridentata wyomingensis*) communities to as few as five years in areas dominated by cheatgrass (Miller et al. 2011, Bradley et al. 2018). Wildfire negatively effects what Taylor et al. (2012) found to be the three main drivers of sage-grouse population growth: adult female survival (Anthony et al. 2022, Foster et al. 2019, Tyrrell et al. 2023), nest survival (Lockyer et al. 2015, Foster et al. 2019, O'Neil et al. 2020, Tyrrell et al. 2023), and brood survival (Anthony et al. 2022, Brussee et al. 2022). In addition, Coates et al. (2016) projected that habitat loss from wildfire and invasive annual grasses will reduce sage-grouse populations by 43% by 2044.

Another major threat to sage-grouse populations is increased predation pressure from human-subsidized generalist predators (Hagen 2011a, Dinkins et al. 2016, Taylor et al. 2017, O'Neil et al. 2018). No single species specializes on predating sage-grouse, but many species including American badgers (*Taxidea taxus*), American kestrels (*Falco sparverius*), black-billed magpies (*Pica hudsonia*), bobcat (*Lynx rufus*), *Buteo* hawk spp., common ravens (*Corvus corax*), coyotes

(*Canis latrans*), golden eagles (*Aquila chrysaetos*), northern harriers (*Circus hudosnius*), raccoons (*Procyon lotor*), red foxes (*Vulpes vulpes*), striped skunks (*Mephitis mephitis*), and weasels (*Mustela* spp.) prey on sage-grouse adults, chicks, and nests (Hagen 2011b, Schroeder et al. 2020). Most of these species are habitat or diet generalists and benefit from anthropogenic subsidization in the form of additional food resources, perching, denning, and nesting sites (Devictor et al. 2008, Terborgh and Estes 2013, Filgueiras et al. 2021). Declines in sage-grouse populations and vital rates have been linked to increases in predator populations, particularly those of the common raven (Bui et al. 2010, Coates and Delehanty 2010, Dinkins et al. 2016, Peebles et al. 2017, Gibson et al. 2018, Kohl et al. 2019, Coates et al. 2020). However, it is unclear how wildfire may be affecting the spatial distribution of anthropogenically subsidized generalist predator communities within sagebrush ecosystems.

The goal of my dissertation was to assess how anthropogenic subsidies and wildfire are affecting sage-grouse by altering the landscape and avian predator community. In Chapter 2, I used count data collected over six years to assess how anthropogenic subsidies and recent wildfire (≤10 years) effect density, occupancy, and interspecies interactions between common ravens, red-tailed hawks (*Buteo jamaicensis*), and Swainson's hawk (*Buteo swainsoni*) within Priority Areas of Conservation (PACs) for sage-grouse in eastern Oregon. In Chapter 3, I used predicted relative raven densities from Chapter 2 to estimate additive and interactive effects of wildfire and raven density on sage-grouse nest-site selection and nest survival. I used the results from resource selection functions and Cox proportional

hazards models to quantify source/sink habitat for sage-grouse nest survival within our chosen PACs. Lastly, in Chapter 4, I used minimum convex polygons to create breeding season neighborhoods for individual adult female sage-grouse. I quantified the amount and configuration of sagebrush, invasive annual grasses, juniper, and anthropogenic footprint within each neighborhood to assess how these factors effect adult female space use and survival during the breeding season.

LITERATURE CITED

Anthony, C. R., L.J. Foster, C. A. Hagen, and K. M. Dugger. 2022. Acute and lagged fitness consequences for a sagebrush obligate in a post mega-fire landscape. Ecology and Evolution 12:e8488.

Baker, W. L. 2011. Pre-EuroAmerican and recent fire in sagebrush ecosystems. Pages 185–201 *in* S. T. Knick and J. W. Connelly, editors. Greater sage-grouse: ecology and conservation of a landscape species and its habitats. Studies in Avian Biology, Volume 38, University of California Press, Berkeley, USA.

Balch, J. K., B. A. Bradley, C. M. D'Antonio, and J. Gómez-Dans. 2013. Introduced annual grass increases regional fire activity across the arid western USA (1980–2009). Global Change Biology 19:173–183.

Barlow, N. L., C. P. Kirol, K. E. Doherty, and B. C. Fedy. 2020. Evaluation of the umbrella species concept at fine spatial scales. The Journal of Wildlife Management 84:237–248.

Bradley, B. A., C. A. Curtis, E. J. Fusco, J. T. Abatzoglou, J. K. Balch, S. Dadashi, and M. Tuanmu. 2018. Cheatgrass (*Bromus tectorum*) distribution in the intermountain western United States and its relationship to fire frequency, seasonality, and ignitions. Biological Invasions 20:1493–1506.

Brussee, B. E., P. S. Coates, S. T. O'Neil, M. L. Casazza, S. P. Espinosa, J. D. Boone, E. M. Ammon, S. C. Gardner, and D. J. Delehanty. 2022. Invasion of annual grasses following wildfire corresponds to maladaptive habitat selection by a sagebrush ecosystem indicator species. Global Ecology and Conservation 37:e02147.

Bui, T. V. D., J. M. Marzluff, and B. Bedrosian. 2010. Common raven activity in relation to land use in western Wyoming: implications for greater sage-grouse reproductive success. The Condor 112:65–78.

Bukowski, B. E., and W. L. Baker. 2013. Historical fire regimes, reconstructed from land-survey data, led complexity and fluctuation in sagebrush landscapes. Ecological Applications 23:546–564.

Coates, P. S., and D. J. Delehanty. 2010. Nest predation of greater sage-grouse in relation to microhabitat factors and predators. Journal of Wildlife Management 74:240–248.

Coates, P. S., M. A. Ricca, B. G. Prochazka, M. L. Brooks, K. E. Doherty, T. Kroger, E. J. Blomberg, C. A. Hagen, and M. L. Casazza. 2016. Wildfire, climate, and invasive grass interactions negatively impact an indicator species by reshaping

sagebrush ecosystems. Proceedings of the National Academy of Sciences 113:12745–12750.

Coates, P. S., S. T. O'Neil, B. E. Brussee, M. A. Ricca, P. J. Jackson, J. B. Dinkins, K. B. Howe, A. M. Moser, L. J. Foster, and D. J. Delehanty. 2020. Broad-scale impacts of an invasive native predator on a sensitive native prey species within the shifting avian community of the North American Great Basin. Biological Conservation 243:108409.

Creutzburg, M. K., E. B. Henderson, and D. R. Conklin. 2015. Climate change and land management impact rangeland condition and sage-grouse habitat in southeastern Oregon. AIMS Environmental Science 2:203–236.

Crist, M. R., R. Belger, K. W. Davies, D. M. Davis, J. R. Meldrum, D. J. Shinneman, T. E. Remington, J. Welty, and K. E. Mayer. 2023. Trends, impacts, and cost of catastrophic and frequent wildfires in the sagebrush biome. Rangeland Ecology and Management 89:3–19.

Devictor, V., R. Julliard, and F. Jiquet. 2008. Distribution of specialist and generalist species along spatial gradients of habitat disturbance and fragmentation. Oikos 117:507–514.

Dinkins, J. B., M. R. Conover, C. P. Kirol, J. L. Beck, and S. N. Frey. 2016. Effects of common raven and coyote removal and temporal variation in climate on greater sage-grouse nesting success. Biological Conservation 202:50–58.

Doherty, K. E., J. S. Evans, P. S. Coates, L. M. Juliusson, and B. C. Fedy. 2016. Importance of regional variation in conservation planning: a rangewide example of the greater sage-grouse. Ecosphere 7:e01462.

Doherty, K., D. M. Theobald, J. B. Bradford, L. A. Wiechman, G. Bredrosian, C. S. Boyd, M. Cahill, P. S. Coates, M. K. Creutzburg, M. R. Crist, S. P. Finn, A. V. Kumar, C. E. Littlefield, J. D. Maestas, K. L. Prentice, B. G. Prochazka, T. E. Remington, W. D. Sparklin, J. C. Tull, Z. Wurtzbach, and K. A. Zeller. 2022. A sagebrush conservation design to proactively restore America's sagebrush biome. U.S. Geological Survey Open-File Report 2022–1081, 38p.

Duchardt, C. J., A. P. Monroe, D. R. Edmunds, M. J. Holloran, A. G. Holloran, and C. L. Aldridge. 2023. Using neutral landscape models to evaluate the umbrella species concept in an ecotone. Landscape Ecology 38:1447–1462.

Filgueiras, B. K. C., C. A. Peres, F. P. L. Melo, I. R. Leal, and M. Tabarelli. 2021. Winner-loser species replacements in human-modified landscapes. Trends in Ecology and Evolution 36:545–555.

Flannigan, M. D., M. A. Krawchuk, W. J. de Groot, B. M. Wotton, and L. M. Gowman. 2009. Implications of changing climate for global wildland fire. International Journal of Wildland Fire 18:483–507.

Foster, L. J., K. M. Dugger, C. A. Hagen, and D. A. Budeau. 2019. Greater sage-grouse vital rates after wildfire. Journal of Wildlife Management 83:121–134.

Fusco, E. J., J. K. Balch, A. L. Mahood, R. C. Nagy, A. D. Syphard, and B. A. Bradley. 2022. The human-grass-fire cycle: how people and invasives co-occur to drive fire regimes. Frontiers in Ecology and the Environment 20:117–126.

Gibson, D., E. J. Blomberg, M. T. Atamian, S. P. Espinosa, and J. S. Sendinger. 2018. Effects of power lines on habitat use and demography of greater sage-grouse (*Centrocercus urophasianus*). Wildlife Monographs 200:1–41.

Hagen, C. A. 2011a. Greater sage-grouse conservation assessment and strategy for Oregon: a plan to maintain and enhance populations and habitat. Oregon Department of Fish and Wildlife, Salem, Oregon, USA.

Hagen, C. A. 2011b. Predation on greater sage-grouse: Facts, processes, and effects. Chapter 6 *in* S. T. Knick and J. W. Connelly, editors. Greater sage-grouse: ecology and conservation of a landscape species and its habitats. Studies in Avian Biology, Volume 38, University of California Press, Berkeley, USA.

Kohl, M. T., T. A. Messmer, B. A. Crabb, M. R. Guttery, D. K. Dahlgren, R. T. Larsen, S. N. Frey, S. Liguori, and R. J. Baxter. 2019. The effects of electric power lines on the breeding ecology of greater sage-grouse. PLoS ONE 14:e0213669.

Lockyer, Z. B., P. S. Coates, M. L. Casazza, S. Espinosa, and D. J. Delehanty. 2015. Nest-site selection and reproductive success of greater sage-grouse in a fire-affected habitat in northwestern Nevada. Journal of Wildlife Management 79:785–797.

Lungle, K. and S. Pruss. 2008. Recovery Strategy for the Greater Sage-Grouse (*Centrocercus urophasianus urophasianus*) in Canada. In Species at Risk Act Recovery Strategy Series. Parks Canada Agency. Ottawa, Ontario, 43 pp.

Miller, R. F., S. T. Knick, D. A. Pyke, C. W. Meinke, S. E. Hanser, M. J. Wisdom, and A. L. Hild. 2011. Characteristics of sagebrush habitats and limitations to long-term conservation. Pages 145–184 *in* S. T. Knick and J. W. Connelly, editors. Greater sage-grouse: ecology and conservation of a landscape species and its habitats. Studies in Avian Biology, Volume 38, University of California Press, Berkeley, USA.

O'Neil, S. T., P. S. Coates, B. E. Brussee, P. J. Jackson, K. B. Howe, A. M. Moser, L. J. Foster, and D. J. Delehanty. 2018. Broad-scale occurrence of a subsidized avian predator: Reducing impacts of ravens on sage-grouse and other sensitive prey. Journal of Applied Ecology 55:2641–2652.

O'Neil, S. T., P. S. Coates, B. E. Brussee, M. A. Ricca, S. P. Espinosa, S. C. Gardner, and D. J. Delehanty. 2020. Wildfire and the ecological niche: diminishing habitat suitability for an indicator species within semi-arid ecosystems. Global Change Biology 26:6296–6312.

Peebles, L. W., M. R. Conover, and J. B. Dinkins. 2017. Adult sage-grouse numbers rise following raven removal or an increase in precipitation. Wildlife Society Bulletin 41:471–478.

Rowland, M. M., J. M. Wisdom, L. H. Suring, and C. W. Meinke. 2006. Greater sage-grouse as an umbrella species for sagebrush-associated vertebrates. Biological Conservation 129:323–335.

Schroeder, M. A., C. L. Aldridge, A. D. Apa, J. R. Bohne, C. E. Braun, S. D. Bunnell, J. W. Connelly, P. A. Deibert, S. C. Gardner, M. A. Hilliard, G. D. Kobriger, S. M. Mcadam, C. W. Mccarthy, J. J. Mccarthy, D. L. Mitchell, E. V Rickerson, and S. J. Stiver. 2004. Distribution of sage-grouse in North America. The Condor 106:363–376.

Taylor, R. L., B. L. Walker, D. E. Naugle, and L. S. Mills. 2012. Managing multiple vital rates to maximize greater sage-grouse population growth. The Journal of Wildlife Management 76:336-347.

Taylor, J. D., D. Holt, E. K. Orning, and J. K. Young. 2017. Greater sage-grouse nest survival in northwestern Wyoming. The Journal of Wildlife Management 81:1219–1227.

Terborgh, J., and J. A. Estes. 2013. Trophic cascades: predators, prey, and the changing dynamics of nature. Island Press, Washington, D.C.

Tyrrell, E. A., P. S. Coates, B. G. Prochazka, B. E. Brussee, S. P. Espinosa, and J. M. Hull. 2023. Wildfire immediately reduces nest and adult survival of greater sage-grouse. Scientific Reports 13:10970.

U.S. Fish and Wildlife Service. 2015. 50 CFR Part 17 Endangered and Threatened Wildlife and Plants; 12-month findings for petitions to list the greater sage-grouse (*Centrocercus urophasianus*) as threatened or endangered. Docket No. FWS-R6-E.S.-2015-0146. U.S. Department of Interior, Fish and Wildlife Service, Washington, DC, USA.

Wisdom, M. J., M. M. Rowland, and L. H. Suring. 2005. Habitat threats in the sagebrush ecosystem: methods of regional assessment and applications in the Great Basin. Alliance Communitcations Group. Lawrence, KS, USA.

CHAPTER 2 - ANTHROPOGENIC SUBSIDIES AND WILDFIRE EFFECT DENSITY, OCCUPANCY, AND INTERSPECIES INTERACTIONS OF THREE SYMPATRIC PREDATORS IN A SAGEBRUSH ECOSYSTEM

ABSTRACT

Anthropogenic subsidization and disturbance can benefit generalist avian species by providing additional food, nesting, and perching resources. In the sagebrush biome, anthropogenic subsidization has led to population increases of common ravens (*Corvus corax*; hereafter ravens), red-tailed hawks (*Buteo jamaicensis*), and Swainson's hawks (*Buteo swainsoni*). We used six years of count data to investigate how anthropogenic subsidies and wildfire were affecting the density, occupancy, and interspecific interactions of these three sympatric predators in five sage-grouse Priority Areas of Conservations (PACs) in eastern Oregon. We used binomial N-mixture (abundance) and single- and multi-species occupancy models to account for imperfect detection and environmental variables influence densities and occupancy of each species. Our results indicated anthropogenic subsidies and recent wildfires (≤10 years) were positively associated with the density and occupancy of ravens and red-tailed hawks and were indirectly associated with density and occupancy of Swainson's hawks. Estimated relative raven density and occupancy probability varied by year and ranged from 0.85–1.64 km^{-2} and 0.66–0.94, respectively; estimated relative red-tailed hawk density and occupancy did not vary annually and was 0.52 km^{-2} and 0.78, respectively; and estimated relative Swainson's hawk density and occupancy varied by County and ranged between 0.11–0.28 km^{-2} and 0.62–0.98, respectively. Multi-species occupancy models with anthropogenic and fire variables indicated that interspecies interactions were either independent or positively

associated with the presence of one or both allospecifics. Our results provide evidence that anthropogenic subsidies created generalist predator hotspots in a sagebrush ecosystem fragmented by wildfire, which could pose a threat to prey species of conservation concern.

INTRODUCTION

Humans are the main drivers of global change. While most species are threatened by human activity, some opportunistic species benefit from anthropogenic subsidization (Rodewald et al. 2011, Osterback et al. 2015, Kirby et al. 2016, O'Neil et al. 2018). Access to and quantity of food are the primary sources of subsidization for synanthropic species (Oro et al. 2013). Subsidization may be direct through the intentional feeding of wildlife through bird feeders, ungulate feeding stations, dump sites, gut piles, or agricultural waste (Oro et al. 2013, Kirby et al. 2016, Newsome and Eeden 2017). It may also come from indirect sources such as agriculture supporting high rodent populations, which in turn may support larger predator communities, or landscape alteration that reduces the energy required to search for prey (e.g., linear right-of-ways, perch sites, or edge habitat). Subsidization may include additional nesting and denning sites from physical structures like nest boxes, platforms, and power poles or by deterring predators through human presence. Anthropogenic subsidization leads to population increases and behavioral changes in opportunistic species that can influence community interactions and ecosystem functions and may lead to the proliferation of non-native and native invaders (Oro et al. 2013). Anthropogenic subsidization may create predator hot spots with unintended

consequences. For example, ungulate feeding stations in Poland were linked to increased predation of nests of ground-nesting birds (Selva et al. 2014), and supplementary feeding of wild birds was linked to increased predation on arthropods in southern England (Orros and Fellowes 2012).

Species that benefit from anthropogenic subsidization are usually generalist species in diet or habitat requirements (Devictor et al. 2008, Terborgh and Estes 2013, Filgueiras et al. 2021). They tend to be tolerant of human-caused disturbances and may also respond positively to natural disturbances like extreme weather events and wildfire (Marvier et al. 2004, Clavero et al. 2011, Terborgh and Estes 2013, Albanesi et al. 2014). Wildfire is increasing in frequency and severity due to the effects of climate change (IPES 2019, IPCC 2023). In the cold desert, sagebrush (*Artemisia tridentata* spp.) dominated Great Basin of the United States, climate change, human ignitions, and invasive annual grasses have allowed wildfire to become the dominant source of habitat loss and fragmentation (Miller et al. 2011, Creutzburg et al. 2015, Balch et al. 2017, Smith et al. 2023). Fire return intervals have shortened from 100 years in Wyoming big sagebrush (*A. t. wyomingensis*) plant communities to as little as five years in areas dominated by cheatgrass (*Bromus tectorum*; Miller et al. 2011). Sagebrush has high mortality during fire events and takes 35 to 120 years to recover fully, depending on species and location (Baker 2011, Schlaepfer et al. 2014, Zaiats et al. 2023). There is extensive research on the effects of wildfire on sagebrush-obligate species, particularly the negative impacts to greater sage-grouse (*Centrocercus urophasianus*; hereafter sage-grouse) (Coates et al. 2016, Foster et al. 2019, O'Neil et al. 2018, Brusee et al. 2022, Dudley et al. 2022, Tyrrell et al. 2023). However,

research is lacking on how wildfire affects generalist predators in the sagebrush ecosystem.

The common raven (*Corvus corax*; hereafter, raven) is a large passerine native to North America. They are omnivores and facultative scavengers that occupy a wide range of ecosystems including deserts, forests, open woodlands, and rangelands (Boarman and Heinrich 2020). Historically, ravens inhabited the Great Basin but were sparsely distributed likely due to limited food, perching, and nesting resources. However, anthropogenic subsidies have allowed their populations to increase twenty-fold since 1966 (Dinkins et al. 2021, Harju et al. 2021a). Ravens are efficient predators, and increasing population densities have been linked to population declines of sensitive species, like the sage-grouse, in this region (Peebles et al. 2017). There is extensive research on how anthropogenic subsidies positively affect raven density and occupancy, but more research on how wildfire may affect their populations is needed. Howe et al. (2014) found an association that ravens selected nest sites closer to edges between vegetation cover types which were primarily created by wildfire, and Dinkins et al. (2021) found that initial abundance and carrying capacity of ravens were positively associated with an increasing proportion of area burned in the last three years. Additionally, there is little research on how the avian predator community may be responding to increasing raven populations.

Red-tailed hawks (*Buteo jamaicensis*) and Swainson's hawks (*Buteo swainsoni*) are two generalist predators that inhabit the sagebrush ecosystem. Red-tailed hawks are one of the most widespread raptors in North America, with increasing populations everywhere except Florida and at the northernmost extent of

their range in Canada (Paprocki et al. 2017, Sauer et al. 2019, Preston and Beane 2020). Swainson's hawks are neotropical migrants that breed in central and western North America from April–July and winter in South America. Swainson's hawk populations declined in the 1980s (Littlefield et al. 1984, Herron et al. 1990), but appear to be rebounding except at the easternmost extent of their range in United States (Sauer et al. 2019, Furnas et al. 2022). Both species are diet and habitat generalists, primarily consuming small mammals, birds, reptiles, and insects (Watson et al. 2023) and inhabiting semi-open areas ranging from woodlands, grasslands, deserts to rural and suburban landscapes (Berchard et al. 2020, Preston and Beane 2020). Red-tailed hawks are tolerant of human development as long as food and tall structures for nesting are available (Bosakowski et al. 1996, Knight et al. 1999, Williams et al. 2000). Swainson's hawks are positively associated with agriculture, but territory size and use may differ with the crop cover type, vegetation density, and access to prey (Woodbridge 1991, Babcock 1995, Fleishman et al. 2016, Furnas et al. 2022). Research in forested ecosystems reported mixed responses of red-tailed hawks to wildfire. In southern California, Gao (2020) found that nest persistence declined the year after the 2018 Woolsey Fire, but Hargove and Unitt (2018) found that red-tailed hawk abundance increased five years post-fire after the Cedar Fire in 2003. Swainson's hawks exhibit pyric-carnivory during and immediately following fire events (Murphy and Smith 2007, Hovick et al. 2017). Hovick et al. (2017) found that local Swainson's hawk numbers increased seven-fold after the ignition of prescribed fires in a tall-grass prairie in Oklahoma, suggesting that Swainson's hawks may have

evolved with fire. Despite these findings, little is known about how red-tailed and Swainson's hawks use fire-affected sagebrush landscapes.

When life history requirements of two or more species overlap, they usually avoid direct competition through resource partitioning (Wiens 1977, Dhondt et al. 2012). Previous research indicates that ravens, red-tailed hawks, and Swainson's hawks coexist in the same environments by partitioning food and nesting resources (Bosakowski et al. 1996, Coates et al. 2014, Auto and O'Connell 2016, Watson et al. 2023). For example, Coates et al. (2014) found that ravens were more likely to nest on anthropogenic structures than the two *Buteo* species in southeastern Idaho. Red-tailed hawks nested primarily in cottonwood trees and on transmission towers, while Swainson's hawk primarily nested in juniper, cottonwood, and ornamental trees (Coates et al. 2014). The three species vigorously defend nesting territories against conspecifics but seem to be relatively tolerant of each other (Janes 1984, Sullivan et al. 2011, Shurtliff and Whiting et al. 2021). Distances between raven and red-tailed hawk nests were as close as 0.35 km (Steenhoff et al. 1993, Sullivan et al. 2011, Coates et al. 2014, Shurtliff and Whiting 2021), while Bosakowski et al. (1996) found that red-tailed hawks nested closer to Swainson's hawks than conspecifics.

Wildfires may induce competition between ravens, red-tailed hawks, and Swainson's hawks by limiting nest and perch sites by removing trees or human infrastructure. Conversely, it may further concentrate predators around infrastructure as these are priority areas for protection and, if damaged, are usually replaced. Conversely, fire may reduce competition by removing cover, making it easier to locate prey, or by providing habitat for preferred prey species. To explore how

wildfire and anthropogenic subsidies affect the relative density, occupancy, and interactions between ravens, red-tailed hawks, and Swainson's hawks, we collected count data for each species in a fire- and human-altered landscape in the northwestern Great Basin. We expected to find evidence of competitive interactions between the three species as density and occupancy increased around anthropogenic landscape components. Since wildfire may increase foraging opportunities but may also reduce access to nesting and perching sites, we expected to find evidence of competitive interactions in fire-affected areas. Lastly, we assessed implications for how changes to the generalist predator community may impact local prey species of conservation concern.

STUDY AREA

Our study was part of a larger predator monitoring project related to sage-grouse conservation in Oregon. We completed surveys in five sage-grouse Priority Areas of Conservation (PACs) in Baker and Malheur counties, Oregon (Figure 1). The Baker, Bully Creek, Crowley, Cow Lakes, and Soldier Creek PACs provide habitat for ravens, red-tailed hawks, and Swainson's hawks within the sagebrush ecosystem and have varying anthropogenic and wildfire footprints.

The Baker PAC was located 5km east of Baker City, in Baker County, OR (44°47'N, 117°49'W) with an area of 1,362 km^2. The Bully Creek, Cow Lakes, Crowley, and Soldier Creek PACs were in Malheur County, OR. The Bully Creek and Crowley PACs were 4.1 km northeast (43°51'N, 117°36'W) and 2.5 km south (43°44'N, 118°04'W) of Juntura, OR, respectively. The Bully Creek PAC

encompassed an area of 1,133 km^2, while the Crowley PAC had an area of 1,760 km^2. The Cow Lakes and Soldier Creek PACs were 5.5 km north (42°58'N, 117°03'W) and 3.5 km southwest (43°55'N, 117°07'W) of Jordan Valley, OR, respectively. Cow Lakes had an area of 1,010 km^2, while Soldier Creek had an area of 1,195 km^2. The elevation among the five PACs ranged from 780 m to 1,855 m, with annual average temperatures between -9° C in January to 34° C in July. The average annual rain and snowfall ranged from 25.7 to 34 cm and 47 to 93 cm, respectively. Land ownership varied among the five PACS, with Crowley and Soldier Creek each comprised of 92% public and 8% privately owned land, Bully Creek and Cow Lakes PACs each contained 75% public and 25% privately owned, and the Baker PAC was 34% public and 66% privately owned land.

The dominant overstory vegetation in all of the PACs was Wyoming big sagebrush, low sagebrush (*A. arbuscula*), stiff sagebrush (*A. rigida*), and a small amount of mountain big sagebrush (*A. t. vaseyana*) at the higher elevations. Native understory vegetation consisted of common forbs (*Lupinus, Crepis,* and *Lomatium* spp.) and native bunchgrasses such as bluebunch wheatgrass (*Pseudoroegneria spicata*), giant wildrye (*Leymus cinereus*), Idaho fescue (*Festuca idahoensis*), and Sandberg's bluegrass (*Poa secunda*). Cheatgrass and medusahead were widespread along with other invasive vegetation such as ventenata (*Ventenata dubia*), crested wheatgrass (*Agropyron cristatum*), Russian thistle (*Kali tragus*), and perennial pepperweed (*Lepidium latifolium*).

Wildfire activity varied among our chosen PACs. The Baker PAC had the lowest burned area with four large fires (>4 km^2) impacting 64 km^2 (4.7%) of the

PAC between 2006 and 2014. There were also three fires between 2006 and 2015 with fire perimeters <1 km from the PAC boundary that burned 611 km^2. The Soldier Creek PAC had sixteen fires that burned 76 km^2 (6.3%) in the PAC and 2,103 km^2 adjacent to the PAC between 2007 and 2019. The Cow Lakes PAC was impacted by eleven large fires between 2007 and 2020, burning 207 km^2 (20.5%) in the PAC and 1,171 km^2 adjacent to the PAC. Nineteen large fires burned 394 km^2 (22.4%) in the Crowley PAC and 1,638 km^2 adjacent to the PAC between 2006 and 2018. Lastly, the Bully Creek PAC was impacted by eight major fires between 2006 and 2020, burning 455 km^2 (39.2%) of the PAC and another 328 km^2 adjacent to the PAC.

METHODS

Data Collection

We conducted point count surveys at random locations within the five PACs. Random locations were generated inside the administrative boundary of each PAC using the "Random Points" tool in ArcMap 10.3.1 with a 2.5 km buffer. We chose this buffer to prevent double-counting of individuals on the same day. We removed random locations if a private landowner denied access or if they were logistically too difficult to get to (7 of 175 locations). The physical placement of random locations was held constant among years. Data were collected in the Baker, Bully Creek, and western half of the Crowley PAC from 2017 to 2022 and in the Cow Lakes and Soldier Creek PACs from 2018 to 2022.

We derived our point count protocol from Dinkins et al. (2012). Point count surveys were conducted at random locations two to five times annually from 1 May

until 15 July, depending on personnel, access, and weather. The timing of surveys corresponded with the overlapping incubation, nestling, and fledging periods of common ravens (March–July), red-tailed hawks (March–July), and Swainson's hawks (April–July). Each survey recorded all auditory and visual detections of ravens and *Buteo* spp. in a 360-degree viewshed within 10 minutes. We recorded visual detections alternating between 8 x 42 mm Nikon Prostaff 7s binoculars and the naked eye. We recorded each detection's bearing, distance from the observer, group size, and detection time. We also recorded the observer and survey start and end times to use as variables on detection probability. We did not complete surveys during precipitation events or if the wind speed exceeded 40 kmph.

Landscape, topographic, and anthropogenic variables

We compiled a suite of land cover, topographic, and wildfire variables (Table 1). We quantified percent cover, proportion, topographic, and density variables using circular neighborhoods at three spatial extents: 1) 1.2 km radii which corresponded to our survey window and the average radii of home ranges of nesting red-tailed hawks reported by Johnson (1975), Janes (1984), Fontaine (2002), and Watson et al. (2023); 2) 2.1 km radii which corresponded to mean nearest neighbor distances between red-tailed and Swainson's hawk's nests reported by Berchard et al. (1990) and to the spatial scale used for the habitat analysis of both species by Bosakowski et al. (1996); 3) 3.6 km radii which corresponded to the mean maximum radius of raven territory size reported by Bruggers (1989) and the average radii of home ranges of nesting Swainson's hawks reported by Craighead and Craighead (1956), Fitzner (1978),

Woodbridge (1991), Babcock (1995), Inselman et al. (2016), Fleishman et al. (2016), and Watson et al. (2023). We calculated Euclidean distances to anthropogenic features and fire-affected areas. We calculated distance decay functions using the formula *decay = exp(Euclidean distance to feature(km)/-decay distance)* to account for potential non-linear effects of proximity to feature variables. We calculated all distance decay functions with five decay distance constants (0.5, 1, 2, 5, and 10 km). The value that each decay function approached 0 (no influence on the response) was ~2.4 km, ~4.5 km, ~9.3 km, ~23.1 km, and ~46.1 km, respectively. Decay functions scale distances between 0 and 1 and are interpreted opposite of Euclidean distance variables with larger values indicating closer proximity to the target feature.

Percent cover of annual herbaceous vegetation, bare ground, perennial herbaceous vegetation, non-sagebrush, sagebrush, all shrubs, and trees were obtained from Rangeland Condition Monitoring Assessment and Projection (RCMAP) products for each year from 2016–2021 (Rigge et al. 2021). We derived topographic variables, including a topographic ruggedness index (Sappington et al. 2007), topographic positioning index (Gallant and Wilson 2000, Weiss 2001), and elevation from a 10 m resolution digital elevation model (DEM; USGS 2021).

Differenced normalized burn ratio (dNBR) rasters of wildfires >4 km^2 that occurred between 2006 and 2020 were obtained from Monitoring Trends in Burn Severity (MTBS) for all fires occurring within and up to 3.6 km away from our study areas (MTBS 2023). We derived three types (severity, proportion, distance to) of fire variables at 10-, 5-, 3-, and 1-year time lags. To create a mean maximum burn severity variable, we reclassified dNBR so that all burn severity values of 1

(unburned to low), 2 (low), 3 (moderate), and 4 (high severity) were retained, and all other values were set to 0. If a pixel burned more than once between 2006 and 2020, we retained the highest burn severity value recorded for that pixel. To create our proportion of area burned variable, we reclassified dNBR so that all burn severity values of 1, 2, 3, and 4 were set to 1, and all other values were set to 0. We summarized the mean maximum burn severity and proportion of area burned using circular neighborhoods at the seven spatial scales described above. Fire variables were temporally aligned; for example, surveys from 2017 were given values from aggregated fire data for 10-, 5-, 3-, and 1-year lags from 2006–2016, 2011–2016, 2013–2016, and 2015, respectively.

We calculated the density of all roads (primary and secondary) and the density of primary roads at all seven spatial scales. We obtained road layers from the Oregon Department of Transportation 2021 Oregon Transportation Network and the Idaho Transportation Department All Roads GIS database, last updated in June 2022. Roads were classified as primary using the following procedures. For Oregon, we classified a road as "primary" if it was a paved or dirt road maintained and owned by the state or a county. We also considered roads "primary" if the owner was listed as "unknown" because visual inspection of these roads showed that they were likely high-use, privately owned driveways or farm roads. All unpaved roads that did not fit the above criteria and were owned by the BLM or the U.S. Forest Service were considered "secondary" roads (i.e., two-track roads). For Idaho, we classified roads as "primary" if the observed route was "2wd Low", the observed mode of transportation was "motorized," and the observed road surface was either solid, aggregate, or natural

improved. We considered roads as "secondary" when the route was "4wd High Clearance", "4wd Low", "ATV," or "Unknown." For both state road systems, we classified any road segments as "secondary" if they were not connected to other primary roads. Additional linear and point anthropogenic variables included distance to transmission line and distance to landfill variables, which were obtained from Homeland Infrastructure Foundation-Level Data (HIFLD 2023).

We reclassified the National Land Cover Database (NLCD) 2016 Land Cover raster by setting values of 81 (Pasture/Hay) and 82 (Cultivated Crops) to 1 and all other values to 0. We then used the same procedure on the 2017 United States Department of Agriculture (USDA) Cropland Data Layer with all cultivated crop, orchard, and vineyard categories set to 1 and all other categories set to 0. We then combined the two layers to create an agriculture raster better representing our study areas. We used the new layer to create the proportion of agriculture and distance to agriculture variables.

We used Julian day, observer experience, the survey start time measured in minutes after sunrise, and mean daily maximum temperature (PRISM 2022) as potential variables that could influence detection. Observer experience was a categorical variable based on years of experience: 1 = first year completing surveys, 2 = second year completing surveys, 3 = 3 or more years of experience completing surveys.

Data compilation

We only included count data for each target species within a 1.2 km radius of our survey locations. Areas up to 1.2 km were generally viewable by observers in sagebrush-dominated landscapes, and landscape features used for distance estimation were identifiable based on topographic maps, GPS, and rangefinders (Dinkins et al. 2012, Coates et al. 2020). Additionally, the detection probability for ravens, the smallest of the three species, fell below 0.10 beyond 1.2 km when we fit a detection curve to our data in a distance sampling framework (Royle et al. 2004a, Sillet et al. *In Press*).

We stacked annual count and presence/absence data, treating each year-location combination as a distinct site. This model structure was retained for all analyses and relaxes the between-year closed population assumption and is appropriate to use with multiple years of data when questions are concerned with potential fixed effects that may contribute to species density or occupancy rather than species population dynamics (Fuller et al. 2016, Crum et al. 2017, Royle 2020). However, since each year-location combination was a distinct site, this data structure can be susceptible to spatial autocorrelation. We tested for spatial autocorrelation using Moran's I, comparing total counts at the same survey location across multiple years. We gave each year-location unit an equal weight. For example, a location surveyed in the Baker PAC in all six years had six year-location units, each with a given weight of 0.167.

Modeling strategy

We evaluated land cover, topographic, anthropogenic, and fire variables in our density and single-species occupancy models at multiple spatial scales and distance equations. For both model types, we determined the best-fitting spatial scale or distance equation (e.g., Euclidean distance, 0.5 km decay, 1 km decay to agriculture) for each variable. To do this, we used Akaike's Information Criteria corrected for small sample sizes (AIC_c) to assess univariate models of all distance equations and spatial scales (e.g., annual herbaceous vegetation within a radius of 1.2, 2.1, and 3.6 km), including quadratic forms to assess non-linear relationships. Variables with the lowest AIC_c were deemed informative and moved forward for analysis if an 85% confidence interval did not overlap zero (Arnold 2010). The categorical variables of county, observer experience, study area, and year were only retained if all categories had 85% confidence intervals that did not overlap zero. We tested the remaining variables for multicollinearity with Pearson's correlation matrices and did not use variables with $r \geq |0.6|$ in the same model. We assessed pairs of variables that exhibited multicollinearity with AIC_c, moving the variable with the lowest AIC_c to the final step of our modeling process. All continuous variables were z-standardized, so model coefficients were directly comparable. For both model types, we first fit all four detection variables to the detection sub-model using backward selection. We then retained the best-fitting detection sub-model while fitting variables using backward selection to the density or occupancy sub-models.

Relative density estimation

We estimated relative raven, red-tailed hawk, and Swainson's hawk abundance with binomial N-mixture models (Royle 2004b, Royle 2020) using the pcount function in the R package 'unmarked' v. 1.2.5 (Fiske and Chandler 2011, Kellner et al. 2023). Binomial N-mixture models allow data to be fit using negative binomial (NB), Poisson, and zero-inflated Poisson (ZIP) distributions. The choice of which latent distribution best fits the data was made prior to fitting variables to either the detection or abundance sub-models. Null models for each distribution were fit and then ranked by AIC_c, and the top-ranking distribution was used in the model selection process. However, binomial N-mixture models fit with the NB distribution are often favored by AIC_c over ZIP and Poisson distributions but can be unstable with some data sets and, therefore, may give ecologically unrealistic estimates of abundance (Kéry et al. 2005, Joseph et al. 2009). Models fit with the ZIP distribution should only be used if the target species was absent from >30% of sites; otherwise, models fit with the Poisson distribution are appropriate (Joseph et al. 2009). We fit models to all three distributions, then determined the proportion of sites where each species was absent, evaluated the stability of each model structure, and ranked any remaining models with AIC_c.

In N-mixture models, K defines the upper index of the integrated likelihood for the N-mixture, which needs to be set high enough to not interfere with parameter estimation (Royle 2004b, Kéry et al. 2005, Kéry 2018). We considered N-mixture models stable when abundance estimates no longer increased as the value of K increased. Following Kéry (2018) and Royle (2020), we added 100 to the highest

observed count of the target species in a single survey (ravens K = 120, red-tailed hawks K=105, Swainson's hawks K=102). We checked for model stability by running each model with K values at 120; 150; 200; 500; 1,000; 2,000; and 3,000. If the abundance estimate continued to increase as K increased, we deemed the model unstable and removed that distribution from consideration.

We inspected the residuals for the detection and abundance sub-models to assess model fit using the 'nmixgof' v. 0.1.0 package in R (Knape et al. 2018). We created relative density surfaces for each species by dividing the relative abundance estimates provided by our top-ranked model by the area within our survey locations (4.52 km^2). We then used predicted relative density estimates from these surfaces combined with the final backwards selected models for each species to assess whether one species' density affected another's density. We used AIC_c to rank model sets consisting of the final model for species A, with additive models containing only species B, a quadratic for only species B, only species C, a quadratic for only species C, species B and species C, and an interaction between species B and species C.

Single and Multi-species Occupancy Analyses

To determine which anthropogenic, fire, landscape, and topographic characteristics influenced the occupancy of each species, we fit single species single-season occupancy models that accounted for imperfect detection using the R package "unmarked" v 1.2.5 (Fiske and Chandler 2011, Kellner et al. 2023, MacKenzie et al. 2002, 2017). These models provide marginal occupancy probability of the target species regardless of the presence or absence of an allospecific. We used parametric

bootstrapping with 1,000 iterations to assess model fit for each species (Fuller et al. 2016, MacKenzie et al. 2017).

To investigate co-occurrence between ravens, red-tailed hawks, and Swainson's hawks, we fit the single-season multi-species occupancy model of Rota et al. (2016) using the R package "unmarked" v. 1.2.5. This model estimates species co-occurrence with symmetric interactions – we did not assume that one species was dominant over the other (Rota et al. 2016). Individual detection and occupancy models can be fit for each species to account for differences in detection probabilities, and habitat features that influence occupancy; therefore, we retained the final detection and occupancy submodels for each species from our single species models in the multi-species model. For the pairwise interaction sub-models, a precise positive beta coefficient estimate for a predictor variable indicates that the occupancy probability of Species A increases with the presence of Species B (and vice versa) as the value of the predictor variable increases. A precise negative beta coefficient estimate indicates that occupancy probability of Species A decreases with the presence of Species B as the value of the predictor variable increases. Imprecise beta coefficient estimates indicate that occupancy probability of Species A and B is independent of the presence of the allospecific. We fit single fire and anthropogenic variables from all spatial scales and distance equations on the pairwise interaction sub-models between ravens and red-tailed hawks (CORA×RTHA), ravens and Swainson's hawks (CORA×SWHA), and red-tailed hawks and Swainson's hawk (RTHA×SWHA). To aid with model convergence and inference of species interactions, we used the penalized likelihood from Clipp et al. (2021).

RESULTS

We completed 2,156 surveys at 678 location-year sites between 2017 and 2022. Ravens were the most widespread species, with detections at 44.8% (n = 304) of sites, followed by red-tailed hawks at 30.5% (n = 207) and Swainson's hawks at 11.2% (n = 76). We detected a total of 592 ravens, 282 red-tailed hawks, and 89 Swainson's hawks over the six years of the study. Our data exhibited weak positive spatial autocorrelation with a Moran's I score of 0.188 and $p < 0.01$.

Density

Density estimates did not stabilize with increasing values of K for the NB models of all three species, so those models were removed from consideration. Ravens were detected at more than 30% of location-year sites, so the ZIP model was removed from consideration for that species. Red-tailed hawks were detected at 30.5% of sites and Swainson's hawks were detected at <30% of sites therefore, we included the ZIP and Poisson models in our final model sets for both species. Estimates for the ZIP models were stable at K = 120 for Swainson's hawks and at K = 500 for red-tailed hawks. Density estimates from Poisson models for all three species were stable at K = 120. The ZIP model had lower AIC_c compared to the Poisson model for red-tailed and Swainson's hawks. However, the ZIP models predicted relative densities that were not biologically realistic (Joseph et al. 2009); thus, we report results from models with the Poisson distribution for all three species. Examination of plots of residuals versus fitted values and residual qq-plots showed a good fit for both the detection and abundance sub-models for each species (Figure 2).

Detection of ravens during surveys decreased as survey start time (β = -0.11, 85% CI: -0.16 - -0.05) and Julian day increased (β = -0.05, 85% CI: -0.10 – -0.003). Observer experience and mean maximum daily temperature were not informative predictors for raven detection. After variable selection, we were left with 12 candidate variables for the density sub-model (Table 2). Our final density sub-model contained a fixed effect of year, which indicated that all relative densities between 2018 and 2022 were higher than those in 2017 (Table 3). Mean relative raven density across all sites was 0.85 km^{-2} (85% CI: 0.61–1.18) in 2017, 1.64 km^{-2} (85% CI: 1.23–2.19) in 2018, 1.42 (85% CI: 1.06–1.89) in 2019, 1.37 (85% CI: 1.00–1.87) in 2020, 1.10 (85% CI: 0.79–1.52) in 2021, and 1.31 (85% CI: 0.94–1.82) in 2022. Raven density was positively associated with closer proximity to agriculture with an effect distance of 23.1 km (5 km decay function; β = 0.141, 85% CI: 0.09–0.19). Raven density was negatively associated with increasing topographic ruggedness within 3.6 km (β = -0.21, 85% CI: -0.26 – -0.15) and increasing Euclidean distance away from areas affected by fire within the last ten years (β = -0.16, 85% CI: -0.22 – -0.10; Figure 3). Lastly, raven densities had a quadratic relationship with the density of all roads at 2.1 km (β = -0.11, 85% CI: -0.15 – -0.07 Figure 3).

Julian Day, observer experience, survey start time, or mean maximum daily temperature did not influence the detection of red-tailed hawks. After variable selection, we were left with 9 candidate variables for the density sub-model (Table 2). The estimated mean relative red-tailed hawk density from our final model was 0.52 km^{-2} (85% CI: 0.33 – 0.82) and did not vary by study site or year. Red-tailed hawk densities were positively associated with an increasing proportion of burned area

within 3.6 km in the last five years (β = 0.27, 85% CI: 0.20–0.34) and closer proximity to transmission lines with an effect distance of 23.1 km (5 km decay function; β = 0.28, 85% CI: 0.19–0.37; Figure 4). Red-tailed hawk densities were negatively associated with increasing Euclidean distance away from landfills (β = -0.18, 85% CI: -0.24 – -0.01; Figure 4) and riparian areas (β = -0.18, 85% CI: -0.27 – -0.09). Densities were also negatively associated with increasing perennial herbaceous cover and increasing distance from agriculture, but both variables had 85% confidence intervals that slightly overlapped zero ($Per_{2.1\ km}$ β = -0.09, 85% CI: -0.17–0.001; $DIST\_AG_{Euclid}$ β = -0.10, 85% CI: -0.20–0.0002)

Detection of Swainson's hawks was not influenced by Julian day, observer experience, survey start time, or mean maximum daily temperature. After variable selection we were left with 11 candidate variables for the density sub-model. Or final model indicated that relative Swainson's hawk density was negatively associated with increasing tree cover within 3.6 km (β = -0.41, 85% CI: -0.70 – -0.11), topographic ruggedness within 1.2 km (β = -0.28, 85% CI: -0.54 – -0.02), and Euclidean distance away from riparian areas (β = -0.36, 85% CI: -0.65 – -0.08; Table 3). Swainson's hawk densities varied by county with a mean relative density of 0.28 km^{-2} (85% CI: 0.16–0.50) in Baker County and 0.11 km^{-2} (85% CI: 0.06–0.19) in Malheur County.

Single Species Occupancy

After the variable selection process, we were left with 10, 5, and 11 predictor variables for the raven, red-tailed hawk, and Swainson's hawk occupancy sub-

models, respectively (Table 2). All three final models indicated a good fit based on the residual sum of squares, chi-squared, and Freeman-Tukey tests (Table 4).

Detection of ravens was negatively associated with later survey start times (β = -0.16, 85% CI: -0.23 – -0.08) but was not informed by Julian day, observer experience, or mean maximum temperature. Like the raven density model, the final occupancy model contained a fixed effect of year with occupancy probabilities higher in 2018 through 2022 than those in 2017 (Table 4). Mean occupancy probability was 0.66 (85% CI: 0.54–0.80) in 2017, 0.92 (85% CI: 0.84–0.96) in 2018, 0.90 (85% CI: 0.83–0.95) in 2019, 0.88 (85% CI: 0.74–0.95) in 2020, 0.87 (85% CI: 0.75–0.93) in 2021, and 0.94 (85% CI: 0.81–0.98) in 2022. Raven occupancy was positively associated with an increasing proportion of riparian area within 3.6 km (β = 0.83, 85% CI: 0.01–1.65) and closer proximity to agriculture with an effect distance of 9.3 km (2 km decay function, β = 0.38, 85% CI: 0.05–0.70; Figure 3). Like the density model, raven occupancy had a quadratic relationship with the density of all roads within 2.1 km (β = -0.35, 85% CI: -0.49 – -0.21; Figure 3).

Detection of red-tailed hawks was positively associated with increasing observer experience (second year: β = 0.50, 85% CI: 0.23–0.77; three or more years: β = 0.39, 85% CI: 0.14–0.65) and negatively associated with mean maximum daily temperature although the 85% interval slightly overlapped zero (β = -0.10, 85% CI: -0.20–0.005). Occupancy probability for red-tailed hawks was positively associated with increasing sagebrush cover within 1.2 km (β = 0.47, 85% CI: 0.18–0.86), closer proximity to fire-affected areas within the previous five years with an effect distance of 9.3 km (2 km decay function; β = 0.71, 85% CI: 0.37–1.05; Figure 4), and closer

proximity to transmission lines with an effect distance of 4.5 km (1 km decay function; β = 2.93, 85% CI: 0.01–5.85; Table 4). The overall mean occupancy probability for red-tailed hawks was 0.78 (85% CI: 0.56–0.90).

Detection of Swainson's hawks was not influenced by Julian day, observer experience, survey start time, or mean maximum daily temperature. Occupancy probability for Swainson's hawks was positively associated with increasing sagebrush cover within 3.6 km (β = 0.43, 85% CI: -0.02–0.91). Occupancy was negatively associated with increasing tree cover within 3.6 km (β = -0.64, 85% CI: -1.15 – -0.15), topographic ruggedness within 1.2 km (β = -0.73, 85% CI: -1.28 – -0.22), and increasing Euclidean distance from riparian areas (β = -0.59, 85% CI: -0.98 – -0.21; Table 4). Additionally, Swainson's hawk occupancy had a quadratic relationship with the density of all roads within 2.1 km (β = -0.34, 85% CI: -0.67 – -0.04; Figure 5). Like the density model, occupancy varied by county, with a probability of 0.93 (85% CI: 0.32–1.00) in Baker County and 0.62 (85% CI: 0.24–0.89) in Malheur County.

Species Interactions

The model set assessing how red-tailed hawk and Swainson's hawk densities affect raven density had four models within 2 ΔAIC_c (Table 5). The top-ranked model was the original raven density model, while the second-ranked model indicated a quadratic relationship with red-tailed hawk density, with raven density increasing until red-tailed hawk density reached ~0.8 km^{-2} and then decreasing (β = -0.04, 85% CI: -0.09 – -0.002, Figure 6). The third and fourth-ranked models included an additive term of red-tailed hawk or Swainson's hawk density, respectively. However,

estimates for both terms had 85% confidence intervals that overlapped zero: red-tailed hawk β = 0.04 (85% CI: -0.01–0.09) and Swainson's hawk β = -0.02 (85% CI: -0.08–0.04).

The model set assessing how raven and Swainson's hawk densities affect red-tailed hawk density also had four models within 2 ΔAIC_c (Table 5). The top-ranked model was the additive raven density model which indicated positive relationship with red-tailed hawk density (β = 0.12, 85% CI: 0.03–0.20, Figure 6). The second-ranked model was the original red-tailed hawk model. The third-ranked model was an additive model containing raven and Swainson's hawk density. Raven density was again positively associated with red-tailed hawk density, but the Swainson's hawk estimate had an 85% confidence interval that overlapped zero (β = -0.04, 85% CI: -0.15–0.07). The fourth-ranked model indicated a quadratic relationship between red-tailed hawk density and raven density, but the estimate had an 85% confidence interval that overlapped zero (β = 0.01, 85% CI: -0.04–0.06).

The final model set assessing how raven and red-tailed hawk densities affect Swainson's hawk densities had three models within 2 ΔAIC_c with all three models containing raven density (Table 5). The top-ranked model contained the interaction term between raven and red-tailed hawk density (β = -0.21, 85% CI: -0.36 – -0.06, Figure 6). However, the interaction caused the estimates for tree cover within 3.6 km and topographic ruggedness within 1.2 km to be imprecise. When red-tailed hawk density was held at the mean and raven density increased, Swainson's hawk density was higher and increased faster than when raven density was held at the mean and red-tailed hawk density increased. This indicates that Swainson's hawks may be less

tolerant of red-tailed hawks compared to ravens. The second-ranked model was an additive model with only raven density, which indicated a positive relationship (β = 0.25, 85% CI: 0.09–0.41, Figure 6). The third-ranked model was an additive model containing both raven and red-tailed hawk densities. The estimate for red-tailed hawk was positive and had an 85% confidence interval that slightly overlapped zero (β = 0.15, 85% CI: -0.02–0.37).

In order to reduce the number of variables tested with our multi-species occupancy models, we did not include any fire variables from the one- and three-year time lags because none of these variables were in the final single-species occupancy variable sets for any of the three species. Additionally, since the proportion of burned area and mean maximum burn severity were highly correlated, we only included burn proportion variables in our multi-species models. The intercept only sub-models for pairwise interactions indicated positive relationships between each species (CORA×RTHA β = 0.75 85% CI: 0.04–1.45), CORA×SWHA β = 0.997 85% CI: -0.05–2.05, RTHA×SWHA β = 1.19 85% CI: 0.33–2.04; Figure 7; Table 6). None of the distance to fire with a ten-year time lag, distance to agriculture, or density of primary roads variables affected interactions between the three species. Interspecies interactions between ravens and red-tailed hawks were positively associated with the proportion of burned area within 3.6 km with a ten-year lag (β = 0.38 85% CI: 0.05–1.13), and increasing proximity to fire with a 5-year time lag with an effect distance out to 46.1 km (10 km decay function; β = 0.43, 85% CI:). They also exhibited a quadratic relationship with the density of all roads within 1.2 km (β = -0.42, 85% CI: -0.71 – -0.13; Figure 8). Raven and Swainson's hawk interactions were negatively

affected by the proportion of burned area with a five-year lag within both the 2.1 (β = -0.51, 85% CI -1.00 – -0.01) and 3.6 km scales (β = -0.69, 85% CI: -1.09 – -0.08; Figure 9). Interactions between these two species were positively associated with increasing proximity to transmission lines with an effect distance of 2.4 km (0.5 km decay function; β = 0.56, 85% CI: 0.11–1.01; Figure 10) and increasing density of all roads within 2.1 km (β = 0.53, 85% CI: 0.39–2.46). Red-tailed hawk and Swainson's hawk interactions were positively associated with the proportion of burned area within 3.6 km for both five- (β = 0.79, 85% CI: 0.25–1.14) and ten-year lags (β = 0.51, 85% CI: 0.002–1.02) and within the 1.2 km (β = 0.36, 85% CI: 0.06–0.78) and 2.1 km (β = 0.54, 85% CI: 0.12–0.95) scales with a five-year lag (Figure 8). Interactions between these two species were also positively associated with increasing proximity to transmission lines with an effect distance 46.1 km (10 km decay function; β = 0.59, 85% CI: 0.03–0.96). Red-tailed and Swainon's hawk interactions were negatively associated with increasing proximity to landfills with an effect distance of 2.4 km (0.5 km decay function β = -0.41, 85% CI: -0.53 – -0.29). Lastly, their interactions had a quadratic relationship with the density of all roads within 1.2 km (β = 0.62, 85% CI: 0.15–1.07; Figure 10).

DISCUSSION

Concurrent with previous research, our results provided evidence of resource partitioning between ravens, red-tailed, and Swainson's hawks (Sullivan et al. 2011, Coates et al. 2014, Atuo and O'Connell 2016, Watson et al. 2023) and tolerance of allospecifics (Steenhoff et al. 1993, Bosakowski et al. 1996, Sullivan et al. 2011,

Coates et al. 2014, Shurtliff and Whiting 2021). Only two habitat components associated with higher densities and occupancy of the three species overlapped. Distance to agriculture was positively associated with raven and red-tailed hawk density. We broadly quantified agricultural areas including cropland, vineyards, orchards, hay fields, and stock yards. Finer scale resource partitioning was likely occurring as land uses provide different food sources (i.e. grain, insects, rodents, animal byproducts) and associated infrastructure provides nesting and perching sites. Raven and Swainson's hawk occupancies had similar quadratic responses to road density within 2.1 km. Roads and associated infrastructure can be partitioned as they provide a variety of perching and nesting substrates (i.e. powerlines, power poles, fences) and foraging opportunities like easier prey detection in open areas and carrion from vehicle collisions (Kristan et al. 2004).

Conditional probabilities from our intercept only multi-species occupancy models indicated that the probability of raven, red-tailed, and Swainson's hawk occupancy increased with the presence of an allospecific (Figure 7). This was contrary to findings from long-term studies by Kennedy et al. (2014) and Janes (1984, 1994) who reported little change in occupancy probabilities or territory changes of nesting red-tailed hawks and Swainson's hawks. Both of these studies did not report on nesting ravens and occurred in landscapes that remained relatively static, with no wildfire or increases to the anthropogenic footprint between observation periods. Results from our density and single-species occupancy models demonstrate that density and occupancy of ravens and red-tailed hawks were positively associated with anthropogenic features and wildfire. Additionally, density estimates of each species

were also positively associated with increasing densities of one or both allospecifics (Figure 6). The only exception was the relationship between raven density and red-tailed hawk density which had a quadratic relationship where raven density increased until red-tailed hawk density reached ~0.8 km^{-2} then declined (Figure 6). Additionally, nine of our anthropogenic and wildfire coefficient estimates from our multi-species occupancy model were precise and positive, indicating that occupancy of one species increased with the presence of an allospecific as that variable value increased. These results suggest that ravens, red-tailed hawks, and Swainson's hawks rarely competed and were relatively tolerant of each other's presence. Additionally, it may provide evidence that heterogeneity in land cover types may reduce specialization and promote sympatry (Atuo and O'Connell 2016).

Landcover and anthropogenic associations from our density and single-species occupancy models for ravens agree with previous research in sagebrush ecosystems (Bui et al. 2010, Howe et al. 2014, O'Neil et al. 2018, Harju et al. 2018, Dinkins et al. 2021, Revekant 2021). Additionally, we found further evidence of a potential positive relationship between raven density and fire-affected areas. We found a strong association between red-tailed hawk density and occupancy and areas affected by fire in the last five years. There is limited research on red-tailed hawk response to wildfire; however, Sanderlin et al. (2015) found that red-tailed hawk occurrence increased up to 10 years post-fire in a ponderosa pine forest in northern Arizona. Fire may attract red-tailed hawks by reducing vegetation cover and increasing detection and access to prey. The associations between red-tailed hawks and agriculture (Bosakowski et al. 1996), riparian areas (Atuo and O'Connell 2016), perennial

herbaceous cover (Fontaine 2002, Coates et al. 2014), sagebrush cover (Bosakowski et al. 1996, Coates et al. 2014), and transmission lines (Knight et al. 1999) from our analyses were similar to those found by other researchers in arid ecosystems. The positive association we found with closer proximity to landfills exhibited by red-tailed hawks has not been documented in the sagebrush ecosystem but has been documented in other areas of their range (DeFusco et al. 2008, Schmalfuss and Bonter 2022). Landfills provide reliable food resources for rodents, supporting larger populations than the surrounding natural landscape (Courtney and Fenton 1976, Plaza and Lambertucci 2017) and consequently attracting predators such as red-tailed hawks.

Habitat associations with topographic ruggedness, tree cover, perennial herbaceous vegetation, and riparian habitat from our Swainson's hawk density and single-species occupancy models were similar to those found in other studies (Woodbridge 1991, Inselman et al. 2016). However, unlike majority of previous Swainson's hawk research, we did not find a direct association with cropland (Bosakowski et al. 1996, Coates et al. 2014, Fleishman et al. 2016, Inselman et al. 2016). Three of these studies were explicitly evaluating Swainson's hawk relationships with different cover types of cropland in an agriculture-dominated landscape (Bosakowski et al. 1996, Fleishman et al. 2016, Inselman et al. 2016). We were not focused on the specific use of different cropland types, but rather on how Swainson's hawks responded to anthropogenic subsidies within a sagebrush dominated conservation area. Additionally, our spatial scales were based on the mean core area of breeding season territories for Swainson's hawks which may not have

adequately captured agriculture use in our study areas as they have been documented foraging as far away as 10 to 22 km from nests (Babcock 1995, Fleishman et al. 2016). Swainson's hawk density and occupancy was higher in our Baker County study area compared to the four study areas located in Malheur County. The Baker PAC had the largest anthropogenic footprint, with 66% privately owned land that was primarily used for multiple types of agriculture (i.e., cropland, hay fields, livestock). Therefore, the broad scale of our county variable may have better represented the relationship of Swainson's hawks to agricultural subsidies better than our finer scaled variables. Additionally, we found a positive relationship between Swainson's hawk density and occupancy and increasing proximity to riparian areas. While distance to riparian areas and distance to agriculture were not correlated ($r = 0.004$), many riparian areas were located near or within agricultural lands.

Although Swainson's hawks exhibit pyric-carnivory during or shortly after fires (Hovick et al. 2017, Caven et al. 2023), we did not find any associations between Swainson's hawk density or occupancy and fire at any of our spatial scales or time lags. However, our multi-species occupancy model indicated that Swainson's hawk occupancy was higher when a red-tailed hawk was present as the proportion of burned area increased within both the five- (1.2, 2.1, and 3.6 km) and ten-year (3.6 km only) time lags (Figure 8, 10). Additionally, we found that raven occupancy decreased when a Swainson's hawk was present as the proportion of burned area increased at the five-year time lag (2.1 and 3.6 km; Figure 9). These relationships suggest that Swainson's hawks may be indirectly attracted to wildfire-affected areas

by following allospecifics, similar to multi-species feeding associations of seabirds attracted to whale foraging sites (Gostischa et al. 2021).

Our relative raven density estimates were broadly consistent with those predicted for the Northern Great Basin by Coates et al. (2020). However, our model predicted higher densities in some areas. Predictions from Coates et al. (2020) were modeled from a large amount of data collected in California, Idaho, and Nevada, but had limited data for eastern Oregon (1 year). Given our six-year data set our models provided more robust estimates that were specific to our study areas. Additionally, our detection and abundance sub-models did show a lack of fit in the upper quantile of qq-residual plots, and our detection probability was low (<0.3), which may have biased our relative estimates high making it difficult to make direct comparisons to other studies (Duarte et al. 2018).

Our mean relative red-tailed hawk density of 0.52/km^2 was similar to the lower range of densities (0.47–1.74 km^2) that Williams et al. (2000) found on rangelands in eastern Kansas and lower than densities found by Atuo and O'Connell (2016) on rangelands in Oklahoma (1.37 and 1.77 /km^2). However, both studies were conducted during the winter on known winter ranges for red-tailed hawks, therefore, are not directly comparable. Our densities were likely lower due to territoriality among conspecifics during the breeding season.

Swainson's hawks had the lowest density of the three species we analyzed with 0.28 and 0.11 birds/km^2 for Baker and Malheur County, respectively. This was not unusual given that Swainson's hawks have the most extensive home ranges of the three species (Fitzner 1978, Woodbridge 1991, Babcock 1995, Inselman et al. 2016,

Fleishman et al. 2016, Watson et al. 2023) and are sparsely distributed in arid landscapes (Fitzner 1978, Anderson 1995, Hansen and Flake 1995, Berchard et al. 2020). Previous research on Swainson's hawk density and occupancy were generated from known nest locations (Coates et al. 2014, Kennedy et al. 2014, Furnas et al. 2022) and not directly comparable to our estimates of all individuals. However, extrapolating from nest density studies, our areas appear to support densities of Swainson's hawks similar to the highly subsidized Central Valley of California (15–50 pairs 100 km^{-2}, ~0.08–0.25 individuals km^{-2}; Furnas et al. 2022) which were much higher than those reported for a sagebrush dominated area of southeast Idaho (mean nest density 0.07 10 km^{-2}, ~0.004 individuals km^{-2}; Coates et al. 2014).

Our results provide evidence that predator hotspots may be forming within the northern Great Basin. Spillover predation into adjacent sagebrush dominated landscapes may occur in our study areas, given the opportunistic foraging strategies of these three avian predator species. Diet studies of ravens, red-tailed, and Swainson's hawks illustrate their ability to prey-switch when preferred prey is scarce (Steenhof and Kochert 1988, Behney et al. 2010, Kristan et al. 2010, Harju et al. 2021b, Watson et al. 2023). Reduction in certain prey items has little effect on reproduction and survival for these species, especially if ample nest sites are available (Young et al. 2023). Spillover predation could pose risks to sensitive species, like the sage-grouse, particularly in areas near anthropogenic subsidies recently affected by fire. Additionally, high densities of these three species in parts of the sagebrush ecosystem may reduce the diversity of the avian predator community if they outcompete more specialist species like the Ferruginous hawk (*Buteo regalis*). In

order to prevent conservation conflicts between predators and sensitive prey species, anthropogenic subsidization needs to be addressed and reduced (Brunk et al. 2021). Artificial structures used for nesting or perching should be removed or altered to prevent use by ravens, red-tailed, and Swainson's hawks. Food subsidies, like agriculture waste, gut piles, and roadkill, should be removed quickly or buried. Finally, all precautions should be taken to prevent unwanted human-caused fire ignitions. Removing predators without addressing the root cause for their presence will not reduce competition or predation pressure on sensitive species (Marzluff et al. 2021).

LITERATURE CITED

Albanesi, S., S. Dardanelli, and L. M. Bellis. 2014. Effects of fire disturbance on bird communities and species of mountain Serrano forest in central Argentina. Journal of Forest Research 19:105–114.

Anderson, D. E. 1995. Productivity, food habits, and behavior of Swainson's hawks breeding in southeast Colorado. Journal of Raptor Research 29:158–165.

Arnold. T. 2010. Uninformative parameters and model selection using Akaike's Information Criterion. Journal of Wildlife Management 74:1175–1178.

Atuo, F. A., and T. J. O'Connell. 2017. Spatial heterogeneity and scale-dependent habitat selection for two sympatric raptors in a mixed-grass prairie. Ecology and Evolution 7:6559–6506.

Babcock, K. W. 1995. Home range and habitat use of breeding Swainson's hawks in the Sacramento Valley of California. Journal of Raptor Research 29:193–197.

Baker, W. L. 2011. Pre-EuroAmerican and recent fire in sagebrush ecosystems. Pages 185–201 *in* S. T. Knick and J. W. Connelly, editors. Greater sage-grouse: ecology and conservation of a landscape species and its habitats. Studies in Avian Biology, Volume 38, University of California Press, Berkeley, USA.

Balch, J. K., B. A. Bradley, J. T. Abatzoglou, R. C. Nagy, E. J. Fusco, and A. L. Mahood. 2017. Human-started wildfires expand the fire niche across the United States. PNAS 114:2946–2951.

Behney, A. C., C. W. Boal, H. A. Whitlaw, and D. R. Lucia. 2010. Prey use by Swainson's hawk in the lesser prairie-chicken range of the southern High Plains of Texas. Journal of Raptor Research 44:317–322.

Berchard, M. J., R. L. Knight, D. G. Smith, and R. E. Fitzner. 1990. Nest sites and habitats of sympatric hawks (*Buteo* spp) in Washington. Journal of Field Ornithology 61:159–170.

Berchard, M. J., C. S. Houston, J. H. Sarasola, and A. S. England. 2020. Swainson's hawk (*Buteo swainsoni*), version 1.0. *in* A. F. Poole, editor. Birds of the World, Cornell Lab of Ornithology, Ithaca, NY, USA.

Boarman, W. I., and B. Heinrich. 2020. Common raven (*Corvus corax*), version 1.0. *In* S. M. Billerman, editor) Birds of the World, Cornell Lab of Ornithology Ithaca, NY, USA.

Bosakowski, T., R. D. Ramsey, and D. G. Smith. 1996. Habitat and spatial relationships of nesting Swainson's hawk (*Buteo swainsoni*) and red-tailed

hawks (*Buteo jamaicensis*) in northern Utah. The Great Basin Naturalist 56:341–347.

Bruggers, D. J. 1989. The behavior and ecology of the common raven in northeastern Minnesota (Dissertation). University of Minnesota, Minneapolis, MN.

Brunk, K. M., E. H. West, M. Z. Peery, and A. M. Pidgeon. 2021. Reducing anthropogenic subsidies can curb density of overabundant predators in a protected area. Biological Conservation 256:109081.

Brussee, B. E., P. S. Coates, S. T. O'Neil, M. L. Casazza, S. P. Espinosa, J. D. Boone, E. M. Ammon, S. C. Gardner, and D. J. Delehanty. 2022. Invasion of annual grasses following wildfire corresponds to maladaptive habitat selection by a sagebrush ecosystem indicator species. Global Ecology and Conservation 37:e02147.

Bui, T. V. D., J. M. Marzluff, and B. Bedrosian. 2010. Common raven activity in relation to land use in western Wyoming: implications for greater sage-grouse reproductive success. The Condor 112:65–78.

Caven, A. J., J. D. Wiese, K. King, E. B. Buckley, B. Krohn, H. English, B. Winter, and T. Smith. 2023. Migrating Swainson' hawk (*Buteo swainsoni*) occurrence at spring controlled burns in the central Great Plains. Platte River Natural Resource Reports eJournal 3:1–17.

Clavero, M., L. Brotons, and S. Herrando. 2011. Bird community specialization, bird conservation and disturbance: the role of wildfires. Journal of Animal Ecology 80:128–136.

Clipp, H. L., A. L. Evans, B. E. Kessinger, K. Kellner, and C. T. Rota. 2021. A penalized likelihood for multispecies occupancy models improves predictions of species interactions. Ecology 102:e03520.

Coates, P. S., J. W. Connelly, and D. J. Delehanty. 2008. Predators of greater sage-grouse nests identified by video monitoring. Journal of Field Ornithology 79:421–428.

Coates, P. S., and D. J. Delehanty. 2010. Nest predation of greater sage-grouse in relation to microhabitat factors and predators. Journal of Wildlife Management 74:240–248.

Coates, P. S., K. B. Howe, M. L. Casazza, and D. J. Delehanty. 2014. Landscape alterations Influence differential habitat use of nesting buteos and ravens within sagebrush ecosystem: implications for transmission line development. The Condor 116:341–356.

Coates, P. S., M. A. Ricca, B. G. Prochazka, M. L. Brooks, K. E. Doherty, T. Kroger, E. J. Blomberg, C. A. Hagen, and M. L. Casazza. 2016. Wildfire, climate, and invasive grass interactions negatively impact an indicator species by reshaping sagebrush ecosystems. Proceedings of the National Academy of Sciences 113:12745–12750.

Coates, P. S., S. T. O'Neil, B. E. Brussee, M. A. Ricca, P. J. Jackson, J. B. Dinkins, K. B. Howe, A. M. Moser, L. J. Foster, and D. J. Delehanty. 2020. Broad-scale impacts of an invasive native predator on a sensitive native prey species within the shifting avian community of the North American Great Basin. Biological Conservation 243:108409.

Courtney, P. A., and M. B. Fenton. 1976. The effects of a small rural garbage dump on populations of *Peromyscus leucopus Rafinesque* and other small mammals. Journal or Applied Ecology 13:413–422.

Craighead, J. J., and F. C. Craighead. 1956. Hawks, owls and wildlife. Dover Publications, New York, NY, USA.

Creutzburg, M. K., E. B. Henderson, and D. R. Conklin. 2015. Climate change and land management impact rangeland condition and sage-grouse habitat in southeastern Oregon. AIMS Environmental Science 2:203–236.

Crum, J. N., A. K. Fuller, C. S. Sutherland, E. G. Cooch, and J. Hurst. Estimating occupancy probability of moose using hunter survey data. The Journal of Wildlife Management 81:521–534.

DeFusco, R. P., K. M. Mieczkowski, and C. J. Quillen. 2008. Comparison of non-lethal versus lethal control methods for red-tailed hawks and other bird species at the Waste Management Outer Loop Recycling and Disposal Facility, Louisville, Kentucky, USA. Bird Strike Committee Proceedings 10th Annual Meeting, Orlando, FL.

Devictor, V., R. Julliard, and F. Jiquet. 2008. Distribution of specialist and generalist species along spatial gradients of habitat disturbance and fragmentation. Oikos 117:507–514.

Dewitz, J. 2019. National land cover database (NLCD) 2016 Products. U.S. Geological Survey data release https://doi.org/10.5066/P96HHBIE.

Dinkins, J. B., M. R. Conover, C. P. Kirol, and J. L. Beck, J. L. 2012. Greater sage-grouse (*Centrocercus urophasianus*) select nest sites and brood sites away from avian predators. The Auk 129:600–610.

Dinkins, J. B., M. R. Conover, C. P. Kirol, J. L. Beck, and S. N. Frey. 2016. Effects of common raven and coyote removal and temporal variation in climate on greater sage-grouse nesting success. Biological Conservation 202:50–58.

Dinkins, J. B., L R. Perry, J. L. Beck, and J. D. Taylor. 2021. Increased abundance of the common raven within the ranges of greater and Gunnison sage-grouse: influence of anthropogenic subsidies and fire. Human-Wildlife Interactions.

Doherty, K. E., D. E. Naugle, and B. L. Walker. 2010. Greater sage-grouse nesting habitat: the important of managing at multiple scales. Journal of Wildlife Management 74:1544–1553.

Dhondt, A. A. 2012. Interspecific competition in birds. Vol 2. Oxford Avian Biology.

Duarte, A., M. J. Adams, and J. T. Peterson. 2018. Fitting N-mixture models to count data with unmodeled heterogeneity: bias, diagnostics, and alternative approaches. Ecological Modelling 374:51–59.

Dudley, I. F., P. S. Coates, B. G. Prochazka, D. M. Davis, S. C. Gardner, and D. J. Delehanty. 2022. Maladaptive nest-site selection and reduces nest survival in female sage-grouse following wildfire. Ecosphere 13:e4282.

Duerr, A. E., P. H. Bloom, K. Ross, T. A. Miller, M. A. Braham, A. L. Fesnock, and T. E. Katzner. 2021. Influence of anthropogenic subsidies on movements of common ravens. Human-Wildlife Interactions 15:9.

Filgueiras, B. K. C., C. A. Peres, F. P. L. Melo, I. R. Leal, and M. Tabarelli. 2021. Winner-loser species replacements in human-modified landscapes. Trends in Ecology and Evolution 36:545–555.

Fiske, I. and R. Chandler. 2011. "unmarked": an R package for fitting hierarchical methods of wildlife occurrence and abundance. Journal of Statistical Software 43:1–23.

Fitzner, R. E. 1978. Behavioral ecology of the Swainson's hawk (*Buteo swainsoni*) in Washington. Prepared for U.S. Department of Energy. Pacific Northwest Laboratory, Richland, WA, USA.

Fleishman E., J. Anderson, B. G. Dickson, D. Krolick, J. A. Estep, R. L. Anderson, C. S. Elphick, D. S. Dobkin, and D. A. Bell. 2016. Space use by Swainson's hawks (*Buteo swainsoni*) in the Natomas Basin, California. Collabra 2:5.

Fontaine, A. J. 2002. Habitat selection by red-tailed hawks (*Buteo jamaicensis*) in prairie landscapes managed for enhanced waterfowl recruitment. Master's Thesis McGill University, Montreal, QC, Canada.

Foster, L. J., K. M. Dugger, C. A. Hagen, and D. A. Budeau. 2019. Greater sage-grouse vital rates after wildfire. Journal of Wildlife Management 83:121–134.

Fuller, A. K., D. W. Linden, and J. A. Royle. 2016. Management decision making for fisher populations informed by occupancy modeling. The Journal of Wildlife Management 80:794–802.

Furnas, B. J., D. H. Wright, E. N. Tennant, R. M. O'Leary, M. J. Keuhn, P. H. Bloom, and C. L. Battisone. 2022. Rapid growth of the Swainson's Hawk population in California since 2005. Ornithological Applications 124:1–12.

Gallant, J. C., and J. P. Wilson. 2000. Primary topographic attributes. Pages 51–85 *in* J. P Wilson and J. C. Gallant, editors. Terrain analysis: principles and applications. Wiley, New York.

Gao, J. 2020. Effects of Woolsey Fire on nesting territories of southern California red-tailed hawks (*Buteo jamaicensis*). Thesis. Oregon State University, Corvallis, OR.

Gostischa, J., A. Massolo, and R. Constantine. 2021. Multi-species feeding association dynamics driven by a large generalist predator. Frontiers in Marine Science 8:739894.

Hansen, R. W., and L. D. Flake. 1995. Ecological relationships between Swainson's and red-tailed hawks in southeastern Idaho. Journal of Raptor Research 29:166–171.

Hagen, C. A. 2011. Greater sage-grouse conservation assessment and strategy for Oregon: a plan to maintain and enhance populations and habitat. Oregon Department of Fish and Wildlife, Salem, Oregon, USA.

Hargrove, L., and P. Unitt. 2018. Responses of birds to large-scale wildfires in southern California. Pages 374–399 *In* (W. D. Shuford, R. E. Gill, and C. M. Handel, editors) Trends and traditions: avifaunal change in western North America. Studies of Western Birds 3. Western Field Ornithologists, Camarillo, CA, USA.

Harju, S. M., P. S. Coates, S. J. Dettenmaier, J. B. Dinkins, P. J. Jackson, and M. P. Chenaille. 2021a. Estimating trends of common raven populations in North America, 1966–2018. Human-Wildlife Interactions 15:248–269.

Harju, S., C. V. Olson, J. Hess, and S. L. Webb. 2021b. Isotopic analysis reveals landscape patterns in the diet of a subsidized predator, the common raven. Ecological Solution and Evidence 2:e12100.

Herron, G. B., C. A. Mortimer, and M. S. Rawlings. 1985. Nevada raptors: their biology and management. Biological Bulletin no. 8, Nevada Department of Wildlife, Reno, NV, USA.

Hovick, T. J., D. A. McGranahan, R. D. Elmore, J. R. Weir, and S. D. Fuhldorf. 2017. Pyric-carnivory: raptor use of prescribed fires. Ecology and Evolution 7:9144–9150.

Howe, K. B., P. S. Coates, and D. J. Delehanty. 2014. Selection of anthropogenic features and vegetation characteristics by nesting common ravens in the sagebrush ecosystem. The Condor 116:35–49.

Idaho Transportation Department (ITD) 2022. Idaho transportation network 2022. ITD OpenData.

Inselman, W. M., S. Datta, J. A. Jenks, R. W. Walker, and T. W. Grovenburg. 2016. Spatial ecology and survival of Swainson's hawks (*Buteo swainsoni*) in the northern Great Plains. Journal of Raptor Research 50:338–350.

IPBES. 2019. Global assessment report on biodiversity and ecosystem services of the Intergovernmental Science-Policy Platform on Biodiversity and Ecosystem Services. Brondizio, E. S., J. Settele, S. Díaz, and H. T. Ngo, editors. IPBES secretariat, Bonn, Germany.

IPCC. 2023. Climate change 2023: synthesis report. A report of the Intergovernmental Panel on Climate Change. Contribution of Working Groups I, II, and III to the sixth assessment of the Intergovernmental Panel on Climate Change. H. Lee, J. Romero, and Core Writing Team, editors. IPCC, Geneva, Switzerland.

Janes, S. W. 1984. Influences of territory composition and interspecific competition on red-tailed hawk reproductive success. Ecology 65:862–870.

Johnson, S. J. 1975. Productivity of the red-tailed hawk in southwestern Montana. The Auk 92:732–736.

Joseph, L. N., C. Elkin, T. G. Martin, and H. P. Possingham. 2009. Modeling abundance using N-mixture models: the importance of considering ecological mechanisms. Ecological Applications 19:631–642.

Kellner, K. F., A. D. Smith, J. A. Royle, M. Kéry, J. L Belant, and R. B. Chandler. 2023. The "unmarked" R package: twelve years of advances in occurrence and abundance modelling in ecology. Methods in Ecology and Evolution 14:1408–1415.

Kennedy, P. L., A. M. Bartuszevige, M. Houle, A. B. Humphrey, K. M Dugger, and J. Williams. 2014. Stable occupancy by breeding hawks (*Buteo* spp.) over 25 years on a privately managed bunchgrass prairie in northeaster Oregon, USA. The Condor 116:435–445.

Kéry, M., J. A. Royle, and H. Schmid. 2005. Modeling avian abundance from replicated counts using binomial mixture models. Ecological Applications 15:1450–1461.

Kéry, M. 2018. Identifiability in N-mixture models: a large-scale screening test with bird data. Ecology 99:281–288.

Kirby, R., M. W. Alldredge, and J. N. Pauli. 2016. The diet of black bears tracks the human footprint across a rapidly developing landscape. Biological Conservation 200:51–59.

Knape, J., D. Arlt, F. Barraquand, Å. Berg, M. Chevalier, T. Pärt, A. Ruete, and M. Zmihorski. 2018. Sensitivity of binomial N-mixture models to overdispersion: the importance of assessing model fit. Methods in Ecology and Evolution 9:2102–2014.

Knight, R. L., R. J. Camp, W. I. Boarman, and H. A. L. Knight. 1999. Predatory bird populations in the east Mojave Desert, California. The Great Basin Naturalist 59:331–338.

Kristan, W. B., W. I. Boarman, and J. J. Crayon. 2004. Diet composition of common ravens across the urban-wildland interface of the west Mojave Desert. Wildlife Society Bulletin 32:244–253.

Littlefield, C. D., S. P. Thompson, and D. E. Bradley. 1984. History and present status of Swainson's hawks in southeast Oregon. Journal of Raptor Research 18:1–5.

MacKenzie, D. I., J. D. Nichols, G. B. Lachman, S. Droege, J. A. Royle, and C. A. Langtimm. 2002. Estimating site occupancy rates when detection probabilities are less than one. Ecology 83:2248–2255.

MacKenzie, D. I., J. D. Nichols, J. A. Royle, K. H. Pollock, L. Bailey, and J. E. Hines. 2017. Occupancy estimation and modeling: inferring patterns and dynamics of species occurrence. Elsevier.

Marvier, M., P. Kareiva, and M. G. Neubert. 2004. Habitat destruction, fragmentation, and disturbance promote invasion by habitat generalists in a multispecies metapopulation. Risk Analysis 24:869–878.

Marzluff, J. M., M. Loretto, C. K. Ho, G. W. Coleman, and M. Restani. 2021. Thinking like a raven: restoring integrity, stability, and beauty to western ecosystems. Human-Wildlife Interactions 15:22.

Miller, R. F., S. T. Knick, D. A. Pyke, C. W. Meinke, S. E. Hanser, M. J. Wisdom, and A. L. Hild. 2011. Characteristics of sagebrush habitats and limitations to long-term conservation. Pages 145–184 *in* S. T. Knick and J. W. Connelly, editors. Greater sage-grouse: ecology and conservation of a landscape species and its habitats. Studies in Avian Biology, Volume 38, University of California Press, Berkeley, USA.

Monitoring Trends in Burn Severity. 2023. MTBS Data Access: Fire Level Geospatial Data (2017, July - last revised). MTBS Project USDA Forest Service/U.S. Geological Survey.

Murphy, R. K., and K. A. Smith. 2007. Swainson's hawks gather to forage at fires on the a northern prairie. Blue Jay 65:78–80.

Newsome, T. M., and L. M. VanEeden. 2017. The effects of food waste on wildlife and humans. Sustainability 9:1269.

O'Neil, S. T., P. S. Coates, B. E. Brussee, P. J. Jackson, K. B. Howe, A. M. Moser, L. J. Foster, and D. J. Delehanty. 2018. Broad-scale occurrence of a subsidized avian predator: Reducing impacts of ravens on sage-grouse and other sensitive prey. Journal of Applied Ecology 55:2641–2652.

Oregon Department of Transportation (ODOT) Geographic Information Service Unit. 2019. Oregon transportation network 2019. Oregon Spatial Data Library.

Oro, D., M. Genovart, G. Tavechhia, M. S. Fowler, and A. Martínez-Abraín. 2013. Ecological and evolutionary implications of food subsidies from humans. Ecology Letters 16:1501–1514.

Orros, M. E., and M. D. E. Fellowes. 2012. Supplementary feeding of wild birds indirectly affects the local abundance of arthropod prey. Basic and Applied Ecology 13:286–293.

Osterback, A. K., D. M. Frechette, S. A. Hayes, S. A. Shaffer, and J. W. Moore. 2015. Long-term shifts in anthropogenic subsidies to gulls and implications for an imperiled fish. Biological Conservation 191:606–613.

Paprocki, N. D. Oleyar, D. Brandes, L. Goodrich, T. Crewe, and S. W. Hoffman. 2017. Combining migration and wintering counts to enhance understanding of population change in a generalist raptor species, the North American red-tailed hawk. The Condor 119:98–107.

Peebles, L. W., M. R. Conover, and J. B. Dinkins. 2017. Adult sage-grouse numbers rise following raven removal or an increase in precipitation. Wildlife Society Bulletin 41:471–478.

Plaza, P. I., and S. A. Lambertucci. 2017. How are garbage dumps impacting vertebrate demography, health, and conservation. Global Ecology and Conservation 12:9–20.

Preston, C. R., and R. D. Beane. 2020. Red-tailed hawk (*Buteo jamaicensis*), version 1.0. *In* (A. F. Poole, editor) Birds of the World, Cornell Lab of Ornithology, Ithaca, NY, USA.

PRISM Climate Group. 2022. Mean maximum temperature. Oregon State University. Data created 2017–2022 https://prism.oregonstate.edu.

Revekant, C. L. 2021. Comparison of common ravens in sage-grouse core and non-core area: assessing predator densities related to anthropogenic features. Thesis. Oregon State University, Corvallis, OR, USA.

Rigge, M. B., B. Bunde, B. H. Shi, and K. Postma. 2021. Rangeland Condition Monitoring Assessment and Projection (RCMAP) Fractional Component Time-Series Across the Western U.S. 1985–2020 (ver. 2.0, October 2021): U.S. Geological Survey data release, https://doi.org/10.5066/P95IQ4BT.

Rodewald, A. D., L. J. Kearns, D. P. Shustack. 2011. Anthropogenic resource subsidies decouple predator-prey relationships. Ecological Applications 21:936–943.

Rota, C. T., M. A. R. Ferreira, R. W. Kays, T. D. Forrester, E. L. Kalies, W. J. McShea, A. W. Parsons, and J. J. Millspaugh. 2016. A multi-species occupancy model for two or more interacting species. Methods in Ecology and Evolution 7:1164–1173.

Royle, J. A., D. K. Dawson, and S. Bates. 2004a. Modeling abundance effects in distance sampling. Ecology 85:1591-1597.

Royle, J. A. 2004b. N-Mixture models for estimating population size from spatially replicated counts. Biometrics 60:108–115.

Royle, J. A. 2020. Modeling population dynamics with count data. Pages 66-156 *in* M. Kéry and J. A. Royle, editors. Applied hierarchical modeling in ecology, volume 2. Elsevier, Academic Press, Cambridge, MA.

Sanderlin, J. S., W. M. Block, and B. E. Strohmeyer. 2015. Long-term post-wildfire correlates with avian community dynamics in ponderosa pine forests.

Proceedings from the 12th Biennial Conference of Research on the Colorado Plateau, U.S. Geological Survey, Reston, VA.

Sappington, J. M., K. M. Longshore, and D. B. Thompson. 2007. Quantifying landscape ruggedness for animal habitat analysis: a case study using bighorn sheep in the Mojave Desert. The Journal of Wildlife Management 71:1419–1426.

Sauer, J. R., D. K. Niven, J. E. Hines, D. J. Ziolkowski, K. L Pardieck, J. E. Fallon, and W. A. Link. 2019. The North American Breeding Bird Survey, results and analysis 1966–2019. USGS Patuxent Wildlife Research Center, Laurel, MD, USA.

Selva, N., T. Berezowska-Cnota, and I. Elguero-Claramunt. 2014. Unforeseen effects of supplementary feeding: ungulate baiting sites as hotspots for ground-nest predation. PLoS ONE 9:e90740

Schlaepfer, D. R., W. K, Lauenroth, and J. B. Bradford. 2014. Natural regeneration processes in big sagebrush (*Artemisia tridentate*). Rangeland Ecology and Management 67:344–357.

Schmalfuss, A. B., and D. N. Bonter. 2022. Response of red-tailed hawks (*Buteo jamaicensis*) and turkey vultures (*Cathartes aura*) to an unintentionally provided, superabundant prey resource. The Journal of Raptor Research 56:313–322.

Shurtliff, Q. R, and J. C. Whiting. 2021. Common raven nesting and spatial distancing on power lines in southeast Idaho, USA. Human-Wildlife Interactions 15:289–303.

Sillett, S. R. B. Chandler, J. A. Royle, and M. Kéry. *In Press*. Hierarchical distance sampling models to estimate population size and habitat-specific abundance of an island endemic. Ecological Applications.

Smith, J. T., B. W. Allred, C. S. Boyd, K. W. Davies, M. O. Jones, A. R. Kleinhesselink, J. D. Maestas, and D. E. Naugle. 2023. Where there's smoke, there fuel: dynamic vegetation data improve predictions of wildfire hazard in the Great Basin. Rangeland Ecology and Management 89:20–32.

Steenhof K., and M. N. Kochert. 1988. Dietary responses of three raptor species to changing prey densities in a natural environment. Journal of Animal Ecology 57:37–48.

Steenhof, K., M. N. Kochert, and J. A. Roppe. 1993. Nesting by raptors and common ravens on electrical transmission line towers. The Journal of Wildlife Management 57:271–281.

Sullivan, B. L., E. L. Kershner, S. P. Finn, A. M. Condon, D. M. Cooper, and D. K. Garcelon. Nest-site characteristics of red-tailed hawks and common ravens on San Clemente Island, California. Journal of Raptor Research 45:252–256.

Terborgh, J., and J. A. Estes. 2013. Trophic cascades: predators, prey, and the changing dynamics of nature. Island Press, Washington, D.C.

Tyrrell, E. A., P. S. Coates, B. G. Prochazka, B. E. Brussee, S. P. Espinosa, and J. M. Hull. 2023. Wildfire immediately reduces nest and adult survival of greater sage-grouse. Scientific Reports 13:10970.

USDA National Agriculture Statistics Service. 2017. Cropland Data Layer 2017. Available at https://nassgeodata.gmu.edu/CropScape/ USDA-NASS, Washington, DC.

U. S. Department of Homeland Security. 2022. Homeland infrastructure foundation-level data (HIFLD). Geospatial Management Office

U.S. Geological Survey. 2021. 30-meter Digital Elevation Models (DEMs). Data collection: U.S. Geological Survey.

Watson, J. W., R. W. Davies, and P. Solar. 2023. Contrasting home range characteristics and prey of sympatric hawks (*Buteo* spp) nesting in the upper Columbia River Basin. Northwestern Naturalist 104:37–47.

Weiss, A. D. 2001. Topographic position and landforms analysis. Poster presentation, ESRI Users Conference, San Diego, CA, USA.

Wiens, J. A. 1977. On competition in variable environments: populations may experience "ecological crunches" in variable climates, nullifying assumptions of competition theory and limiting the usefulness of short-term studies of population patterns. American Scientist 65:590–597.

Williams, C. K., R. D. Applegate, R. S. Lutz, and D. H. Rusch. 2000. A comparison of raptor densities and habitat use in Kansas cropland and rangeland ecosystems. Journal of Raptor Research 34:203–209.

Woodbridge, B. 1991. Habitat selection by nesting Swainson's hawks: a hierarchical approach. Master's Thesis. Oregon State University, Corvallis, OR, USA.

Young, A. C., T. E. Katzner, D. J. Shinneman, and T. N. Johnson. 2023. Implications of tree expansion in shrubland ecosystems for two generalist avian predators. PLoS ONE 18:e0286478

Zaiats, A., M. E. Cattau, D. S. Pilliod, R. Liu, J. M. Requena-Mullor, and T. T. Caughlin. 2023. Forecasting natural regeneration of sagebrush after wildfires using population models and spatial matching. Landscape Ecology 38:1291–1306.

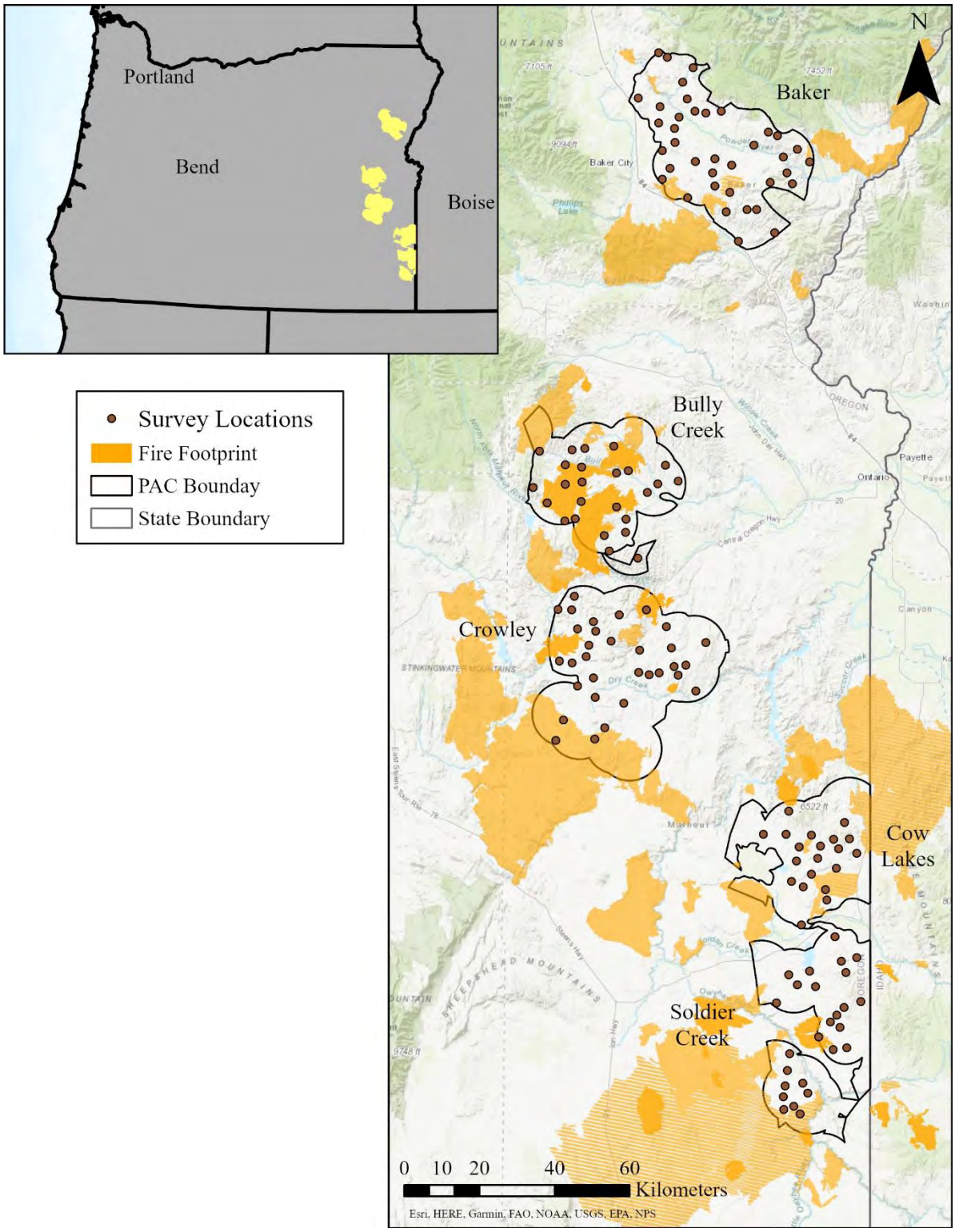

Figure 1. Map of sage-grouse Priority Areas of Conservation (PACs) in Baker and Malheur Counties, OR, USA. Orange polygons represent fire footprints between 2006 and 2020. Dots indicate random locations where count data was collected annually from 2017–2022.

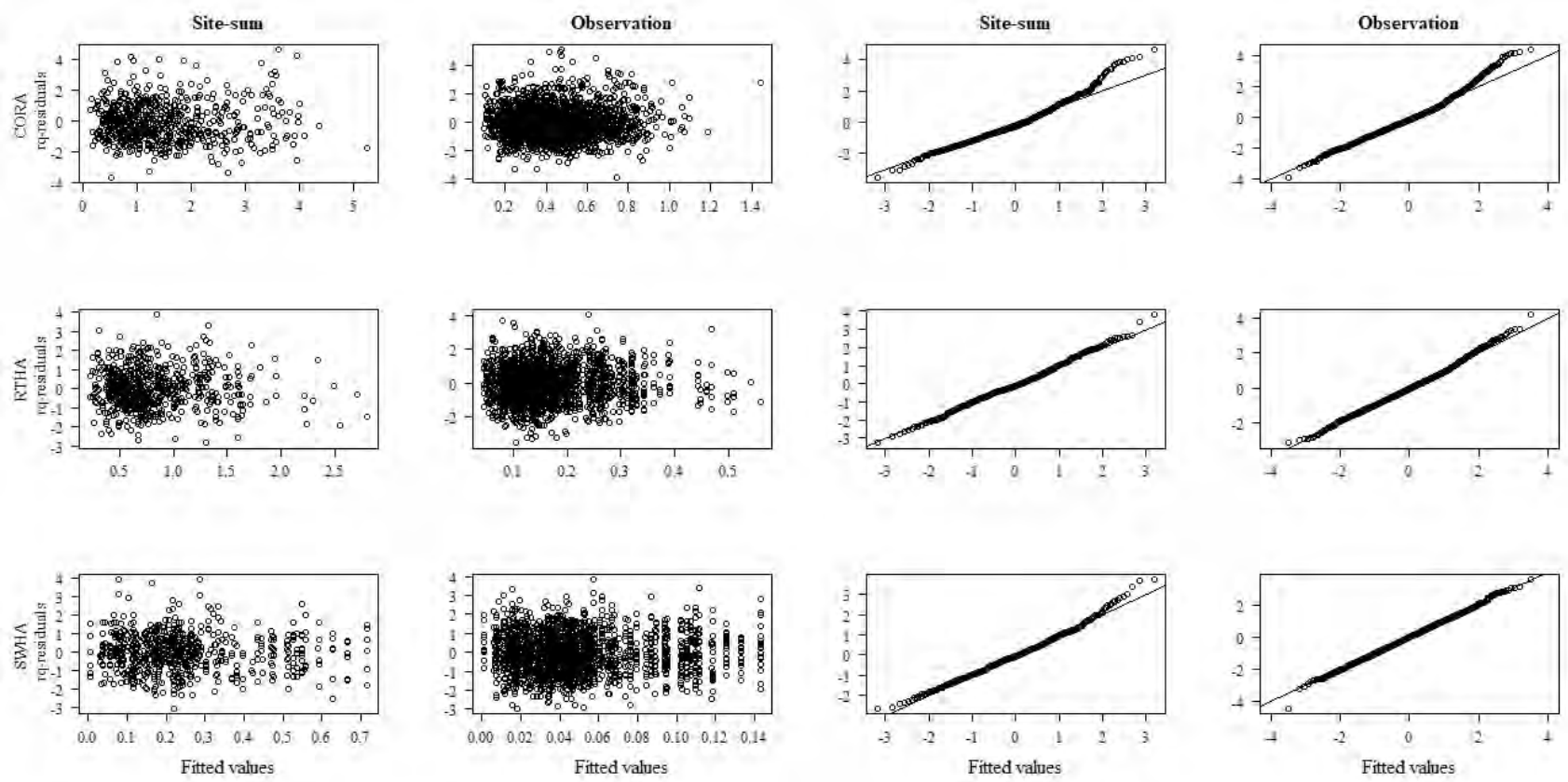

Figure 2. Residual (columns 1 and 2) and qq-plots (columns 3 and 4) of rq-residuals versus fitted values for the density (site-sum) and detection (observation) sub-models from the best-fitting, backward selected, binomial N-mixture models for each species. CORA = common raven, RTHA = red-tailed hawk, SWHA = Swainson's hawk. Count data was collected in Baker and Malheur Counties, Oregon, USA (2017–2022).

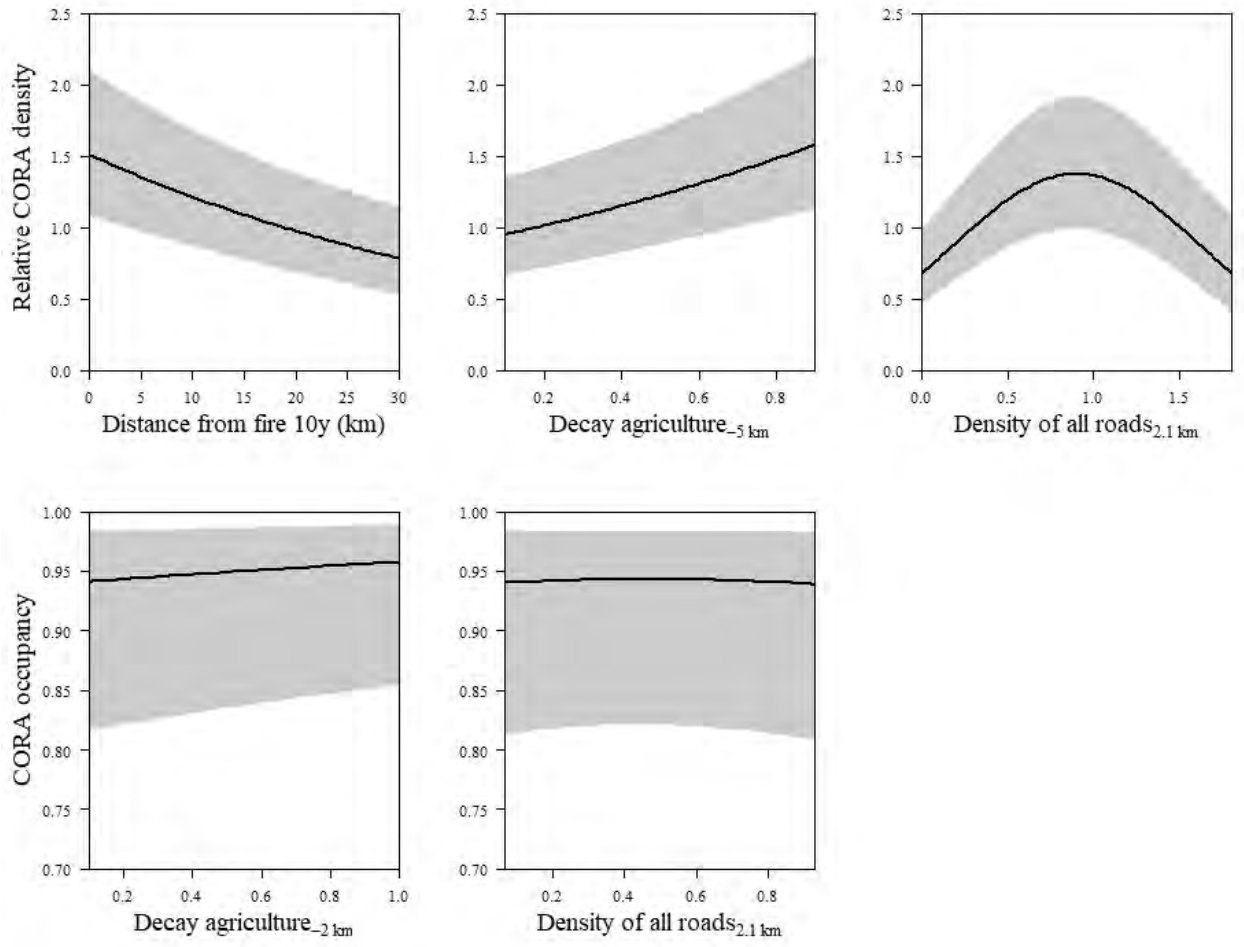

Figure 3. Effects plots with 85% confidence intervals (grey shaded area) of anthropogenic and fire variables from the best fitting raven binomial N-mixture model (top row) and single-species occupancy model (bottom row). Subscripts indicate spatial scale or distance decay equation. Effects plots of distance decay functions with values closer to 1 indicate closer proximity to the target variable. CORA = common raven. Count and occupancy data collected in Baker and Malheur Counties, Oregon, USA (2017–2022).

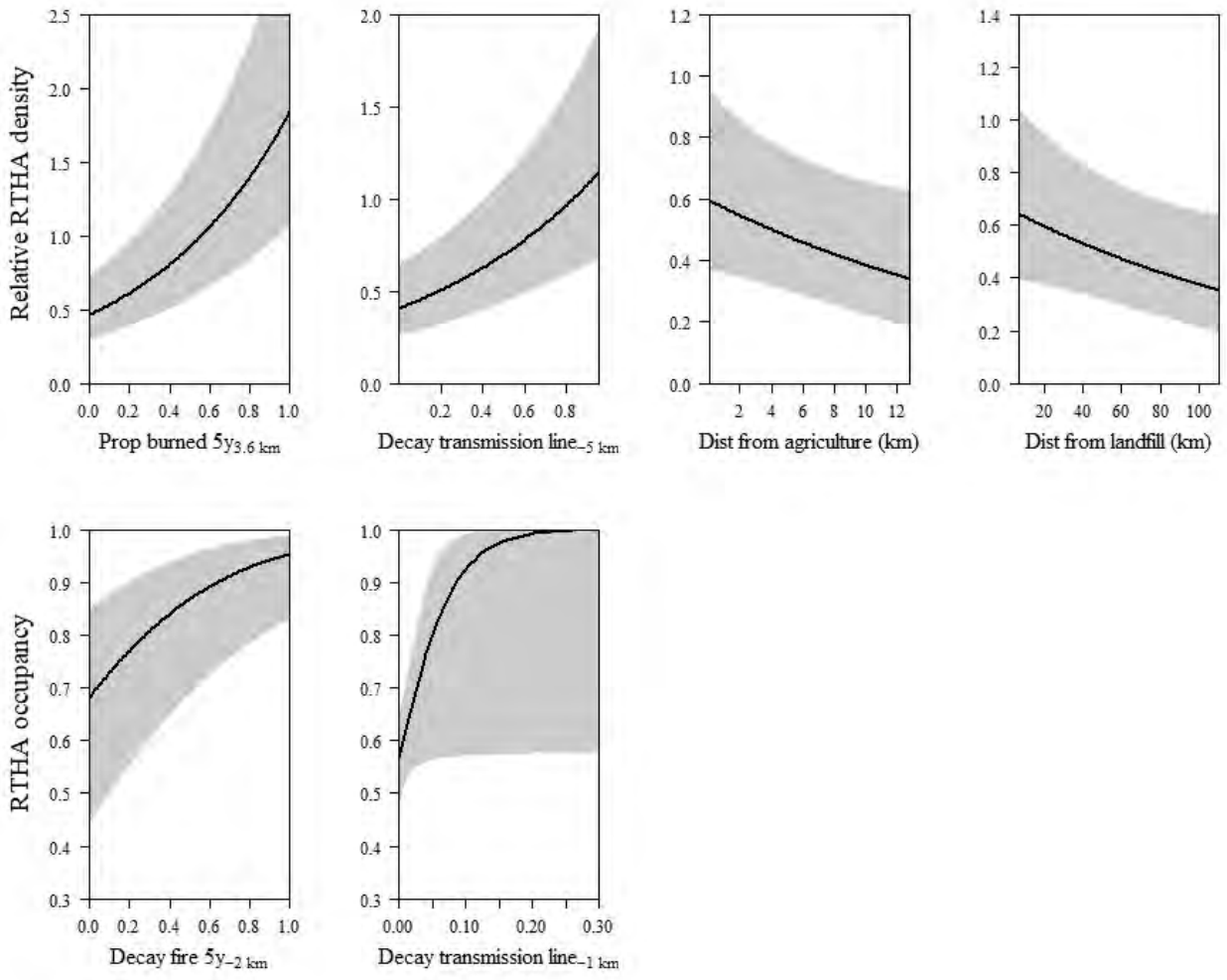

Figure 4. Effects plots with 85% confidence intervals (grey shaded area) of anthropogenic and fire variables from the best fitting red-tailed hawk binomial N-mixture model (top row) and single-species occupancy model (bottom row). Subscripts indicate spatial scale or distance decay equation. Effects plots of distance decay functions with values closer to 1 indicate closer proximity to the target variable. RTHA = common raven. Count and occupancy data collected in Baker and Malheur Counties, Oregon, USA (2017–2022).

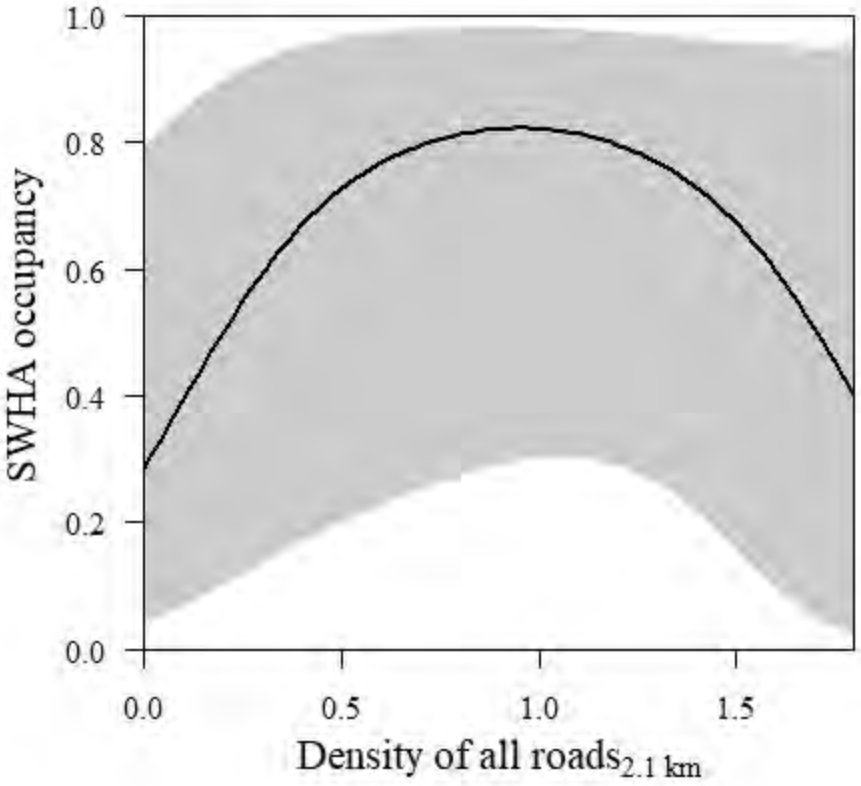

Figure 5. Effects plot with 95% confidence intervals (grey shaded area) of the quadratic relationship between Swainson's hawk occupancy probability and road density within 2.1 km. SWHA = Swainson's hawk. Occupancy data collected in Baker and Malheur Counties, Oregon, USA (2017–2022).

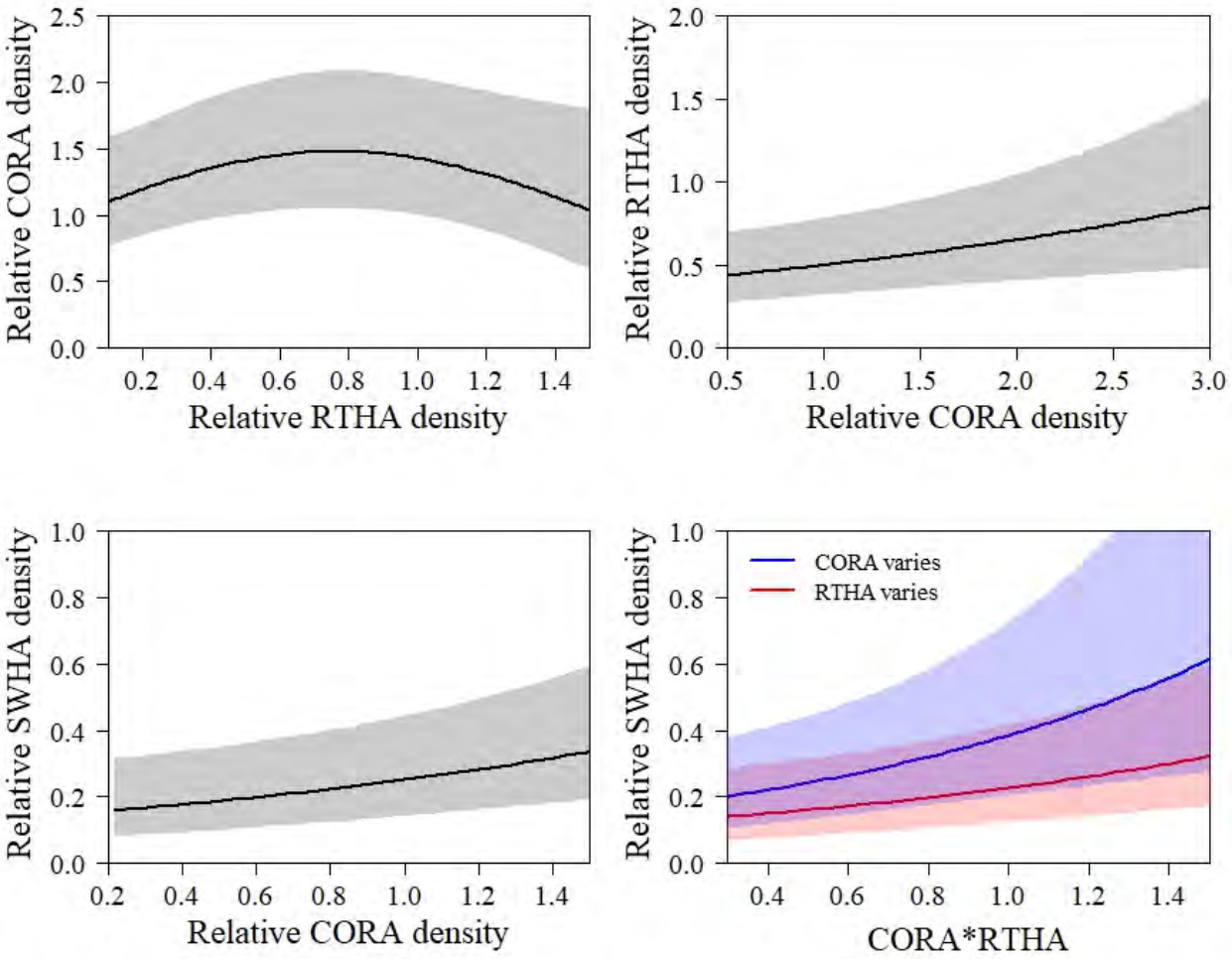

Figure 6. Effects plots with 85% confidence intervals (grey, blue, and red shaded areas) from the best fitting binomial N-mixture models of the effect of red-tailed hawk density on raven density (top left), raven density on red-tailed hawk density (top right), raven density on Swainson's hawk density (bottom left) and the interaction between raven and red-tailed hawk densities on Swainson's hawk density. CORA = common raven, RTHA = red-tailed hawk, SWHA = Swainson's hawk. Count data collected in Baker and Malheur Counties, Oregon, USA (2017–2022).

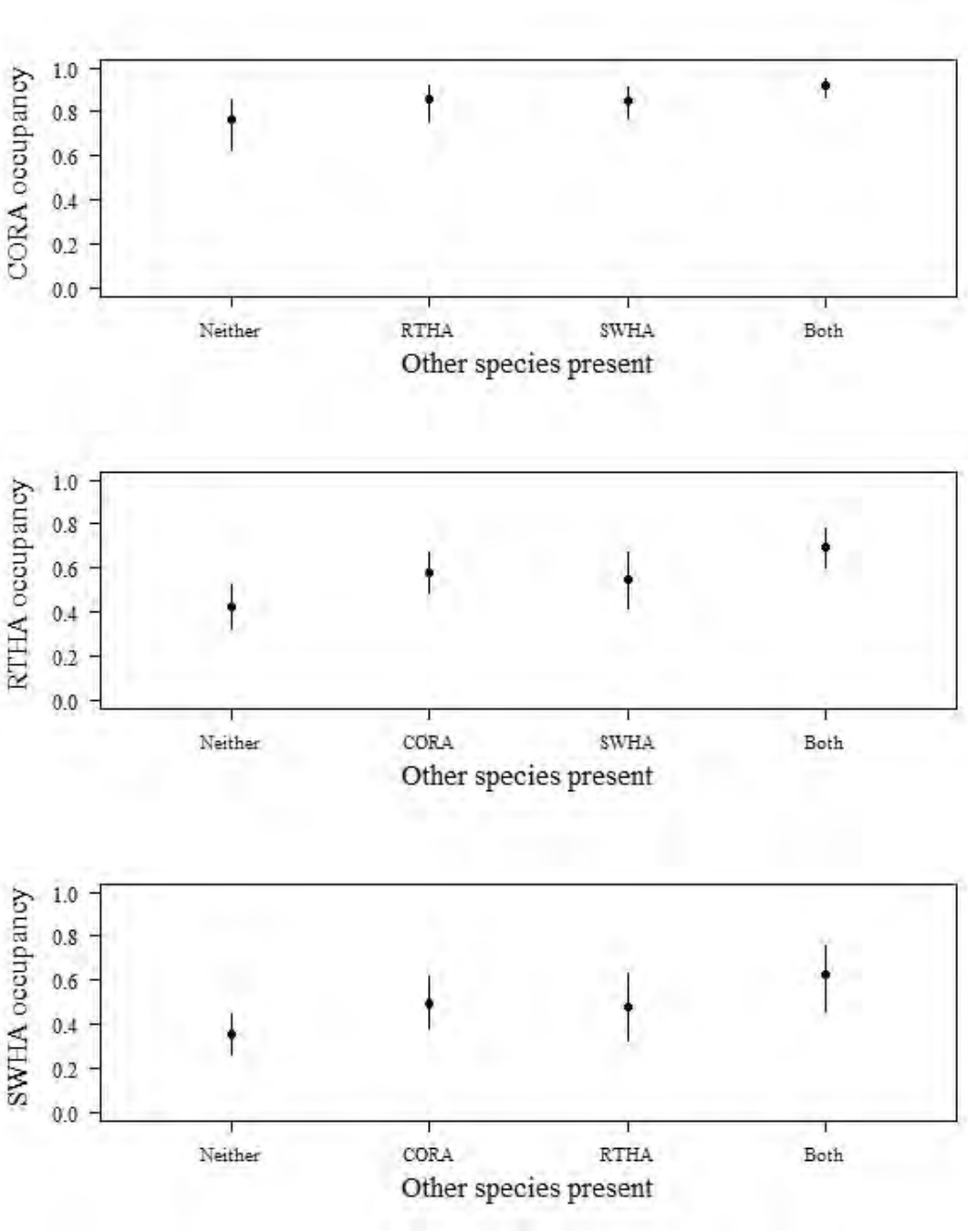

Figure 7. Conditional occupancy probability with 85% confidence intervals (vertical lines) of ravens, red-tailed, and Swainson's hawk, in the absence, presence of one allospecific, and presence of both allospecifics from an intercept-only multi-species model. Each species retained their specific best fitting single-species detection and occupancy sub-models, but no variables were set to pairwise interactions. CORA = common raven, RTHA = red-tailed hawk, SWHA = Swainson's hawk. Occupancy data collected in Baker and Malheur Counties, Oregon, USA (2017–2022).

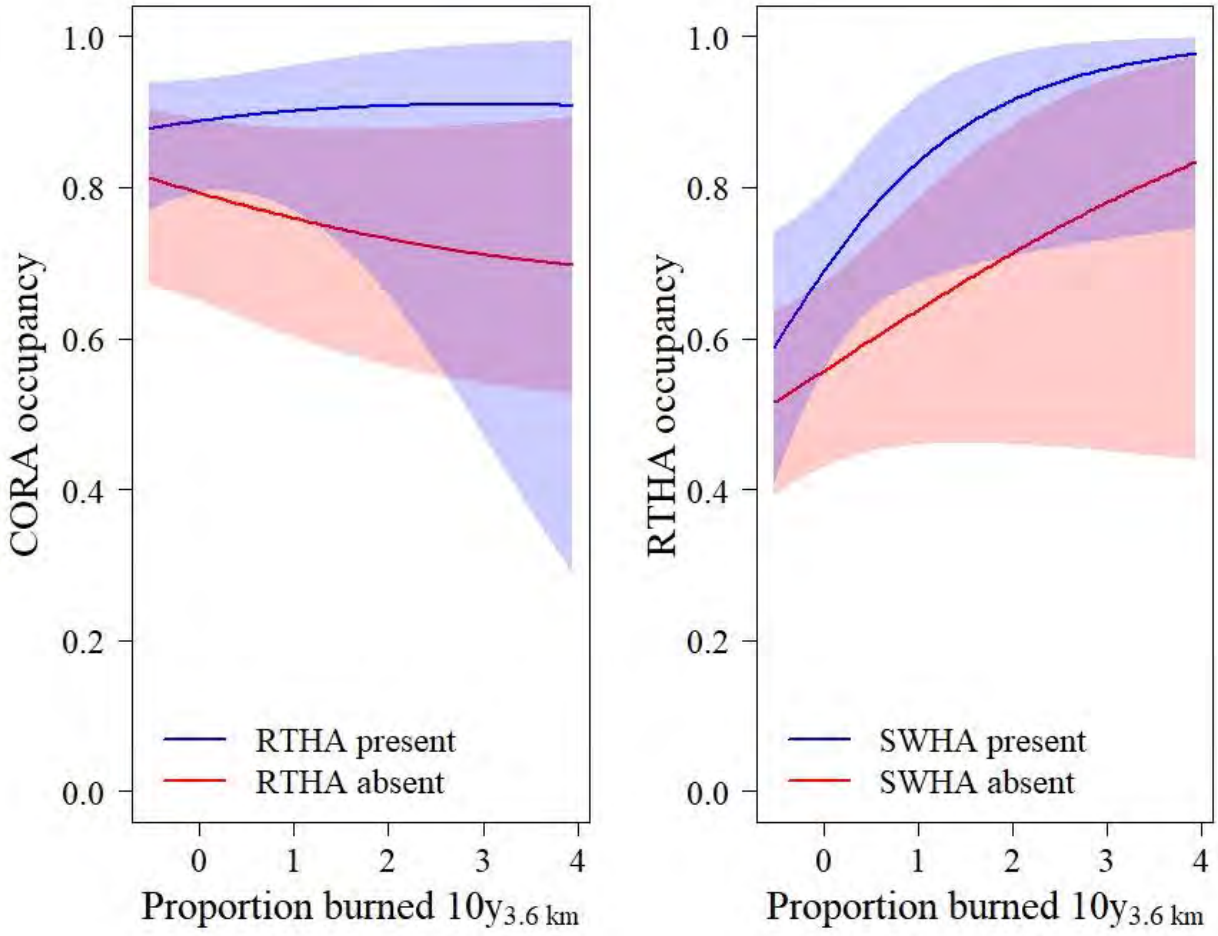

Figure 8. Effects plots with 85% confidence intervals (shaded areas) of conditional occupancy probability from multi-species occupancy models between ravens and red-tailed hawks (left) and between red-tailed and Swainson's hawks (right) as the proportion of burned area in the last ten years within 3.6 km increases. CORA = common ravens, RTHA = red-tailed hawk, SWHA = Swainson's hawk. Occupancy data collected in Baker and Malheur Counties, Oregon, USA (2017–2022).

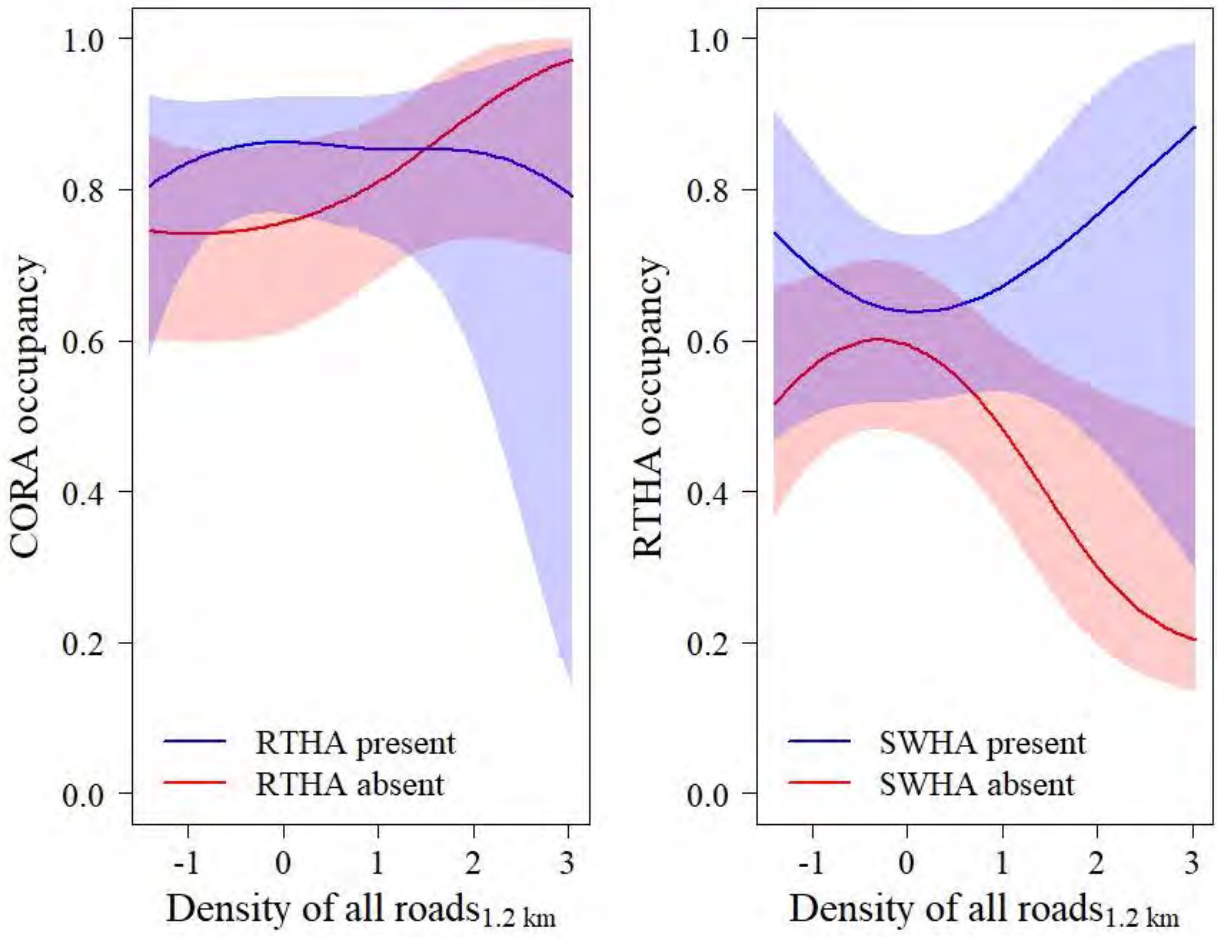

Figure 9. Effects plots with 85% confidence intervals (shaded areas) of conditional occupancy probability from multi-species occupancy models between ravens and red-tailed hawks (left) and between red-tailed and Swainson's hawks (right) with quadratic responses to road density within 1.2 km. CORA = common raven, RTHA = red-tailed hawk, SWHA = Swainson's hawk. Occupancy data collected in Baker and Malheur Counties, Oregon, USA (2017–2022).

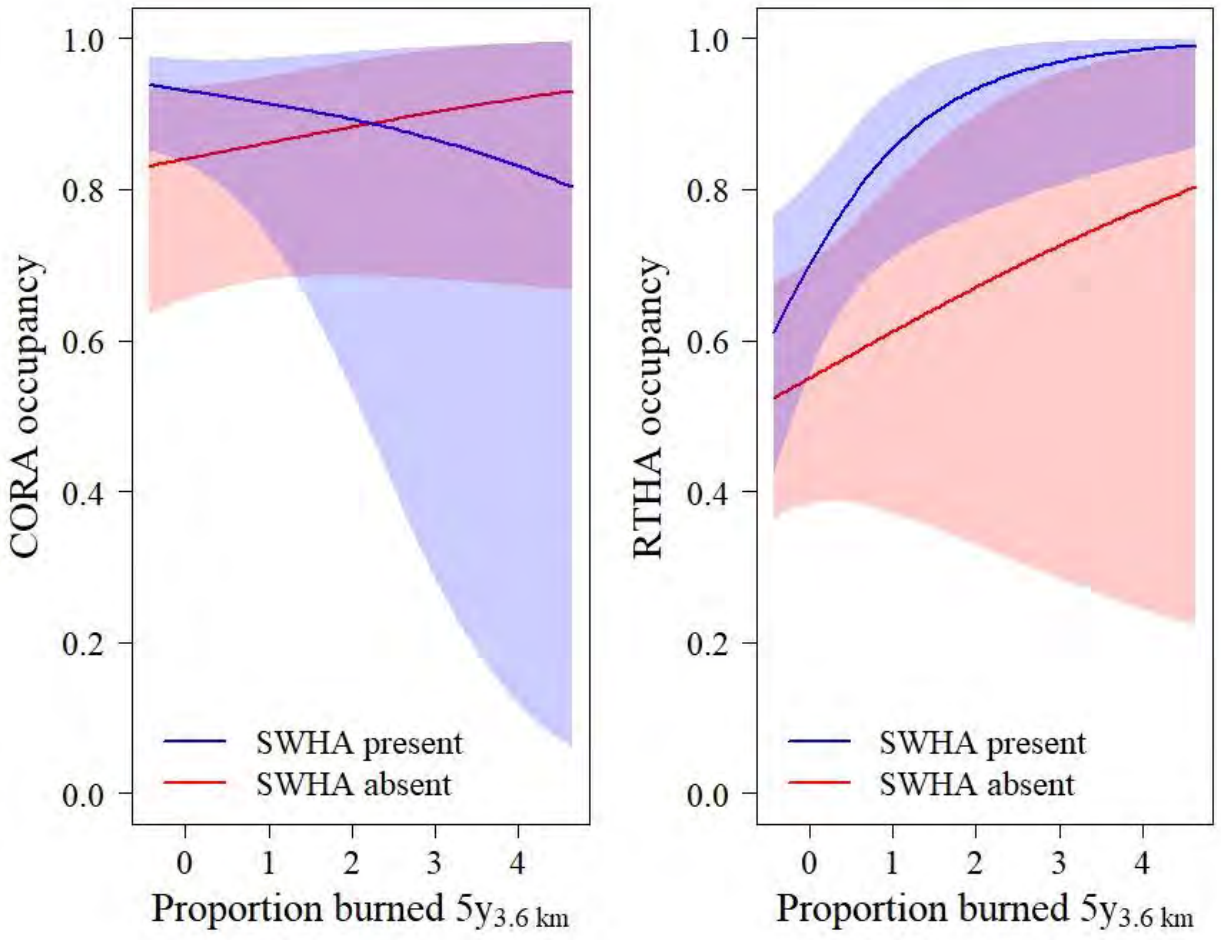

Figure 10. Effects plots with 85% confidence intervals (shaded areas) of conditional occupancy probability from multi-species occupancy models between ravens and red-tailed hawks (left) and between red-tailed and Swainson's hawks (right) as the proportion of burned area in the last five years within 3.6 km increases. CORA = common ravens, RTHA = red-tailed hawk, SWHA = Swainson's hawk. Occupancy data collected in Baker and Malheur Counties, Oregon, USA (2017–2022).

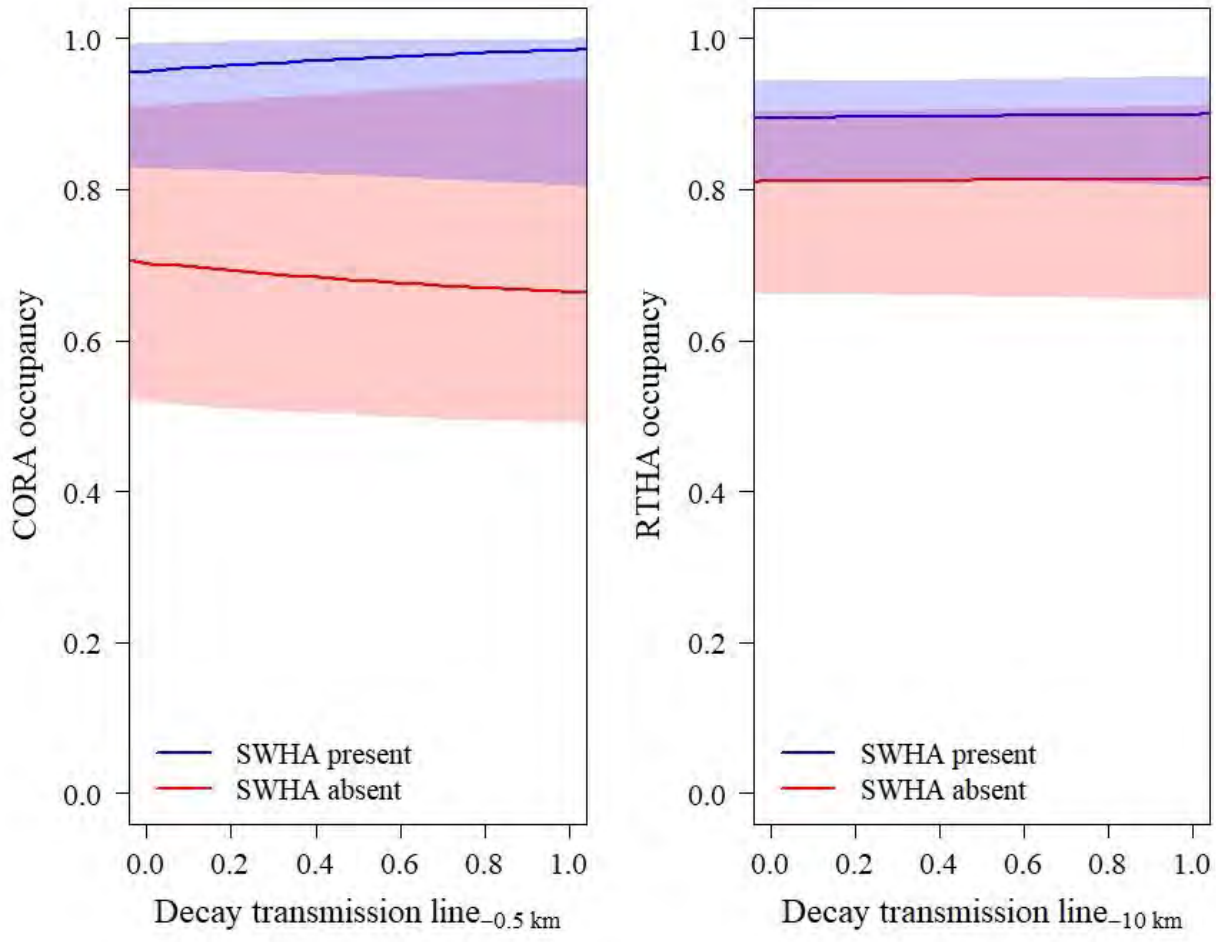

Figure 10. Effects plots with 85% confidence intervals (shaded areas) of conditional occupancy probability from multi-species occupancy models between ravens and Swainson hawks (left) and between red-tailed and Swainson's hawks (right) as proximity to transmission lines increases. Values of decay functions are bounded between 0 and 1 with values closer to 1 indicating closer proximity to the target object. CORA = common ravens, RTHA = red-tailed hawk, SWHA = Swainson's hawk. Occupancy data collected in Baker and Malheur Counties, Oregon, USA (2017–2022).

Table 1. Spatial and climate predictor variables used for modeling relative density and occupancy of ravens, red-tailed hawks, and Swainson's hawks from 2017 to 2022 in Baker and Malheur counties, Oregon, USA.

Predictor Variable	Abbreviation	Year(s)	Data Source(s)
Annual herbaceous vegetation Bare ground Perennial herbaceous vegetation Non-sagebrush Sagebrush Total shrub Tree	Annual Bare Per Nonsage Sage Shrub Tree	2016 – 2021	Rangeland Condition Monitoring Assessment and Projection (RCMAP) (Rigge et al. 2021)
Topographic ruggedness index Topographic positioning index Elevation	TRI TPI Elevation	2021	Derived from 10 m Digital Elevation Model (DEM) (USGS 2021)
Distance to fire Proportion of area burned Mean burn severity	DIST_FIRE_Xy[a] BurnPropXy[a] BurnSevXy[a]	1996 – 2021	Derived from difference Normalized Burn Ratios (dNBR) from Monitoring Trends in Burn Severity (MTBS 2022)
Distance to lek	DIST_LEK	2016 – 2022	Oregon Department of Fish and Wildlife (ODFW 2022) Idaho Department of Fish and Game (IDFG 2002)
Density of primary roads Density of all roads	RoadsPrimary RoadsAll	2019, 2022	Oregon Department of Transportation (ODOT 2019) Idaho Transportation Department (ITD 2022)
Distance to landfill Distance to transmission line	DIST_LAND DIST_POWER	2022	Homeland Infrastructure Foundation-Level Data (HIFLD 2022)
Distance to agriculture Proportion of agriculture	DIST_AG Ag	2016, 2017	National Land Cover Database (Dewitz 2019) Cropland Data Layer (USDA 2017)
Mean daily maximum temperature	Temp	2017 – 2022	PRISM Climate Group (2022)

[a]X in fire variables is equal to 10, 5, 3, or 1 to indicate time lag.

Table 2. Variables used in backward selection for density and occupancy sub-models for ravens, red-tailed hawks, and Swainson's hawks.

	Raven	**Red-tailed hawk**	**Swainson's hawk**
Density	$Perennial_{3.6}$ $Riparian_{1.2}$ $Sage_{3.6}$ $Tree_{3.6}$ $TRI_{3.6}$ $(RoadsAll_{2.1\ km})^2$ $DIST\_FIRE\_10y_{Euclid}$ $DECAY\_AG_{5\ km}$ $DECAY\_POWER_{0.5\ km}$ $DIST\_LAND_{Euclid}$ Year County	$Annual_{3.6}$ $Perennial_{2.1}$ $BurnProp5y_{3.6}$ $(RoadsAll_{3.6\ km})^2$ $DIST\_AG_{Euclid}$ $DECAY\_POWER_{5\ km}$ $DIST\_LAND_{Euclid}$ $DIST\_RIP_{Euclid}$ Elevation	$Perennial_{1.2}$ $Sage_{3.6}$ $Tree_{3.6}$ $TRI_{1.2}$ $(RoadsAll_{2.1\ km})^2$ $DECAY\_FIRE\_3y_{10\ km}$ $DECAY\_AG_{0.5\ km}$ $DECAY\_POWER_{10\ km}$ $DIST\_RIP_{Euclid}$ Elevation County
Occupancy	$Annual_{3.6}$ $Perennial_{3.6}$ $Tree_{2.1}$ $TRI_{3.6}$ $TPI_{1.2}$ $Riparian_{3.6}$ $DECAY\_FIRE\_10y_{2\ km}$ $DECAY\_AG_{2\ km}$ $(RoadsAll_{2.1\ km})^2$ Year	$Annual_{3.6}$ $Perennial_{3.6}$ $Sage_{1.2}$ $DECAY\_FIRE\_5y_{2\ km}$ $DIST\_LAND_{Euclid}$ $DECAY\_POWER_{.1\ km}$	$Bare_{3.6}$ $Sage_{3.6}$ $Tree_{3.6}$ $TRI_{1.2}$ $(RoadsAll_{2.1\ km})^2$ $DECAY\_FIRE\_3y_{10\ km}$ $DECAY\_AG_{0.5\ km}$ $DECAY\_POWER_{10\ km}$ $DIST\_RIP_{Euclid}$ Elevation County

Table 3. Standardized parameter estimates and standard errors (SE) for final backwards selected binomial N-mixture models for relative abundance of ravens, red-tailed hawks, and Swainson's hawks in Baker and Malheur counties, Oregon, USA (2017–2022). An asterisk (*) indicates a parameter estimate with 85% confidence intervals that slightly overlapped zero.

	Raven		**Red-tailed hawk**		**Swainson's hawk**	
	Mean	**SE**	**Mean**	**SE**	**Mean**	**SE**
Density sub-model						
Intercept	1.339	0.224	0.861	0.314	0.242	0.394
$BurnProp5y_{3.6\ km}$			0.270	0.048		
County Malheur					-0.985	0.219
$DIST\_AG_{Euclid}$			-0.100	0.070		
$DECAY\_AG_{5\ km}$	0.141	0.038				
$DIST\_FIRE\_10y_{Euclid}$	-0.157	0.042				
$DIST\_LAND_{Euclid}$			-0.124	0.082		
$DECAY\_POWER_{5\ km}$			0.276	0.062		
$DIST\_RIPARIAN_{Euclid}$			-0.182	0.066		
$Per_{2.1\ km}$			-0.087*	0.061	-0.363	0.146
$RoadsAll_{2.1\ km}$	0.151	0.045				
$(RoadsAll_{2.1\ km})^2$	-0.109	0.028				
$Tree_{3.6\ km}$					-0.405	0.207
$TRI_{1.2\ km}$						
$TRI_{3.6\ km}$	-0.205	0.040			-0.277	0.132
Year 2018	0.683	0.135				
Year 2019	0.554	0.137				
Year 2020	0.526	0.152				
Year 2021	0.275	0.165				
Year 2022	0.498	0.168				
Detection sub-model						
Intercept	-2.510	0.210	-2.730	0.335	-2.740	0.406
Day	-0.054	0.035				
Sunrise	-0.106	0.036				

Table 4. Standardized parameter estimates, standard errors (SE), and fit statistics for final backwards selected single species occupancy models for ravens, red-tailed hawks, and Swainson's hawks in Baker and Malheur counties, Oregon, USA (2017–2022). An asterisk (*) indicates a parameter estimate with an 85% confidence interval that slightly overlapped 0. SSE = sum of squares error.

	Raven		**Red-tailed hawk**		**Swainson's hawk**	
	Mean	**SE**	**Mean**	**SE**	**Mean**	**SE**
Occupancy sub-model						
Intercept	0.785	0.421	1.240	0.691	1.317	1.255
County Malheur					-2.060	1.087
$DECAY\_AG_{2\ km}$	0.382	0.226				
$DECAY\_FIRE\_5y_{2\ km}$			0.709	0.239		
$DECAY\_POWER_{1\ km}$			2.929	2.031		
$DIST\_RIPARIAN_{Euclid}$					-0.591	0.262
$Riparian_{3.6\ km}$	0.832	0.570				
$RoadsAll_{2.1\ km}$	0.317	0.151			0.548	0.316
$(RoadsAll_{2.1\ km})^2$	-0.350	0.099			-0.341	0.202
$Sage_{3.6\ km}$					0.431*	0.306
$Sage_{1.2\ km}$			0.471	0.200		
$Tree_{3.6\ km}$					-0.636	0.330
$TRI_{1.2\ km}$					-0.725	0.355
Year 2018	1.613	0.466				
Year 2019	1.452	0.459				
Year 2020	1.203	0.596				
Year 2021	1.115	0.579				
Year 2022	2.027	0.923				
Detection sub-model						
Intercept	-0.634	0.067	-1.555	0.119	-2.280	0.263
Observer 2			0.502	0.186		
Observer 3			0.392	0.177		
Sunrise	-0.157	0.054				
Temp			-0.095*	0.070		
Fit Statistics	p-value		p-value		p-value	
SSE	0.515		0.430		0.413	
Chi-square	0.733		0.649		0.893	
Freeman-Tukey	0.528		0.522		0.497	

Table 5. Performance of binomial N-mixture models with additive, quadratic, and interactive terms of allospecific densities in Baker and Malheur counties, Oregon, USA (2017–2022). All models contain the base model for the target species. A † indicates models where all parameters had an 85% confidence interval that did not overlap zero. CORA = common raven, RTHA = red-tailed hawk, SWHA = Swainson's hawk.

	Model	K	AIC_c	ΔAIC_c	w_i
CORA	Base	14	4055.80	0.00	0.29
	$RTHA^{2\dagger}$	16	4056.55	0.74	0.20
	RTHA	15	4056.82	1.02	0.17
	SWHA	15	4057.70	1.89	0.11
	$SWHA^2$	16	4058.09	2.28	0.09
	RTHA + SWHA	16	4058.09	2.29	0.09
	RTHA*SWHA	17	4059.44	3.64	0.05
RTHA	$CORA^{\dagger}$	9	2021.38	0.00	0.39
	Base	8	2023.09	1.71	0.17
	CORA + SWHA	10	2023.18	1.80	0.16
	$CORA^2$	10	2023.36	1.98	0.14
	SWHA	9	2025.15	3.76	0.06
	CORA*SWHA	11	2025.18	3.80	0.06
	$SWHA^2$	10	2027.12	5.74	0.02
SWHA	$CORA*RTHA^{\dagger}$	9	845.97	0.00	0.39
	$CORA^{\dagger}$	7	847.37	1.41	0.19
	CORA+RTHA	8	847.85	1.89	0.15
	RTHA	7	848.48	2.52	0.11
	$CORA^2$	8	849.40	3.44	0.07
	Base	6	850.02	4.06	0.05
	$RTHA^2$	8	850.28	4.31	0.04

Table 6. Standardized parameter estimates and standard errors (SE), for variables associated with interactions between ravens, red-tailed hawks, and Swainson's hawks from multi-species occupancy models. Data was collected in Baker and Malheur counties, Oregon, USA (2017–2022). CORA×RTHA = interaction between ravens and red-tailed hawks, CORA×SWHA = interaction between ravens and Swainson's hawks, RTHA×SWHA = interaction between red-tailed and Swainson's hawks.

	CORA×RTHA		**CORA×SWHA**		**RTHA×SWHA**	
	Mean	**SE**	**Mean**	**SE**	**Mean**	**SE**
Intercept only	0.691	0.390	0.788	0.526	0.664	0.441
$BurnProp10y_{3.6\ km}$	0.381	0.219			0.512	0.352
$BurnProp5y_{1.2\ km}$					0.362	0.243
$BurnProp5y_{2.1\ km}$			-0.505	0.325	0.537	0.293
$BurnProp5y_{3.6\ km}$			-0.687	0.443	0.794	0.328
$DECAY\_FIRE\_5y_{10\ km}$	0.329	0.188				
$DECAY\_POWER_{0.5\ km}$			0.561	0.343		
$DECAY\_POWER_{5\ km}$					0.562	0.342
$DECAY\_POWER_{10\ km}$					0.589	0.368
$DECAY\_LAND_{0.5\ km}$					-0.410	0.096
$DECAY\_LAND_{2\ km}$					-0.270	0.186
$RoadsAll_{2.1\ km}$			0.719	0.381		
$(RoadsAll_{1.2\ km})^2$	-0.418	0.238			0.612	0.323
$(RoadsAll_{2.1\ km})^2$	-0.254	0.151				

CHAPTER 3 - ADDITIVE AND INTERACTIVE EFFECTS OF WILDFIRE AND RAVEN DENSITY ON SAGE-GROUSE NEST-SITE SELECTION AND SURVIVAL

ABSTRACT

Wildfire and raven densities are linked to lower sage-grouse nest survival and nest-site selection. However, little is known about the additive or multiplicative effects of raven density on sage-grouse nest survival within fire-affected landscapes. We examined the effects of fire and raven density on greater sage-grouse nest-site selection and survival using resource selection functions and Cox proportional hazards models. Nest-site selection was positively associated with increasing cover of annual herbaceous vegetation, bare ground, perennial herbaceous vegetation, sagebrush cover, proximity to lek, and proximity to areas recently affected by fire (≤10 years). Nest-site selection was negatively associated with increasing cover of non-sagebrush shrubs, proportion of riparian area, topographic ruggedness, road density, and proximity to transmission lines. Raven density was not informative for nest-site selection. Nest survival was positively associated with increasing cover of non-sagebrush shrubs and later initiation dates. Nest survival was negatively associated with increasing road density, northerly aspects, proximity to recently burned areas (≤5 years), and raven density. Source/sink maps of nest survival indicate a lack of habitat characteristics with high relative selection strength (RSS) and high survival in some areas, primarily driven by proximity to anthropogenic subsidies that subsidize raven populations. Our results indicate that raven densities may not highly impact sage-grouse nest survival in fire-affected landscapes if nesting areas are located >8 km from anthropogenic subsidies.

INTRODUCTION

Disturbance is a temporary and discrete event that reshapes community composition and dynamics (White and Pickett 1985, Dornelas 2010). Disturbance can change species richness, abundance, demographic rates (White and Picket 1985, Fontaine and Kennedy 2012, Murphy and Romanuk 2013), and behavior (Fontúrbel et al. 2021, Kreling et al. 2021, Rahman and Candolin 2022). It is often the driving force behind the establishment of invasive species (Bauer 2012, Balch et al. 2013, Simberloff et al. 2013). Native species may also benefit from disturbance and experience population increases within their native range or expand beyond it (Atwood et al. 2004, Vieira-Nieto et al. 2016, Carcos et al. 2019). Human-caused disturbances such as urbanization, land conversion, and resource extraction threaten most ecosystems and species globally (Newbold et al. 2016, IPBES 2019, Rosenberg et al. 2019). However, natural disturbances such as extreme weather events and wildfires are increasing due to climate change's effects and threaten sensitive species and their habitats (IPBES 2019, IPCC 2023). Changes in the abundance and distribution of new species, both native and non-native, after a disturbance, alter the community structure of an area, which can also influence predator-prey dynamics (Wald 1986, Gallett et al. 2007, Dorn and Cook 2015, Labadie et al. 2023). For example, Mumma et al. (2018) found that anthropogenic linear features changed the distribution of gray wolves *(Canis lupus*) in northeastern British Columbia, which resulted in increased predation risk to boreal caribou (*Rangifer trandus caribou*). Interactions between predators and disturbance may lead to additive or synergistic impacts on populations

of prey species (Doherty et al. 2015). These impacts may be numerical, where predator populations increase in disturbed areas, or functional, where the predator population remains stable but reduced cover, changes in behavior, or declines in other prey species result in increased predation intensity. (Holling 1959, Oaten and Murdoch 1975, Didham et al. 2007, Dawes and Souza 2013).

Since the early 1980s, the increased frequency and severity of wildfire has surpassed all other sources of habitat loss and fragmentation in the sagebrush biome of the Great Basin region of North America (Miller et al. 2011, Doherty et al. 2022). Sagebrush (*Artemisia* spp.) species experience high mortality during fire events and, depending on species and location, can take 35 to 120 years to recover fully (Baker 2011). Along with climate change and human fire ignitions (Creutzburg et al. 2015, Fusco et al. 2022), invasive annual grasses, such as cheatgrass (*Bromus tectorum*) and medusahead (*Taeniatherum caput-medusae*), have contributed to the increase in wildfire activity in the Great Basin (Balch et al. 2013). Both invasive grass species flourish in disturbed areas and senesce earlier than native bunchgrasses, creating a bed of fine dry fuel earlier in the spring, increasing wildfire season length. These invasive annual grasses also create a positive feedback cycle resulting in increased fire frequency, which prevents the re-establishment of sagebrush and other native plants (Abatzoglou and Kolden 2011, Chambers et al. 2014). Large fires (>400 km^2) occasionally occurred before European settlement (Bukowski and Baker 2013) but are now common annually in the sagebrush biome. Fire return intervals have shortened from ~100 years in Wyoming big sagebrush (*A. tridentata wyomingensis*) communities to as few as five years in areas dominated by cheatgrass (Miller et al.

2011, Bradley et al. 2018). Loss of sagebrush from wildfire eliminates quality cover, leaving sagebrush-obligate prey species at a higher risk for predation.

The greater sage-grouse (*Centrocercus urophasianus*; hereafter, sage-grouse) is a sagebrush-obligate species endemic to the western United States and south-central Canada and is considered an indicator species for the sagebrush ecosystem (Rowland et al. 2006, Barlow et al. 2020, Duchardt et al. 2023). Before European settlement, sage-grouse occurred in 13 western states and three Canadian provinces. They now occupy less than half of their pre-European settlement range and are extirpated from two U.S. states and one Canadian province (Schroeder et al. 2004, Doherty et al. 2016). The sage-grouse is listed as endangered in Canada but is not listed in the United States due to unprecedented conservation efforts (Lungle and Pruss 2008, USFWS 2015). It remains a species of conservation concern as the loss and fragmentation of sagebrush ecosystems from land conversion, anthropogenic disturbances, and wildfire contribute to local population declines (Johnson et al. 2011, USFWS 2015, Coates et al. 2021).

Female sage-grouse largely avoid areas near anthropogenic disturbance during the breeding season (Dinkins et al. 2014, Gibson et al. 2018, Kirol et al. 2015, Kirol et al. 2020, Coates et al. 2023). For example, Kirol et al. (2015, 2020) found that nesting sage-grouse in Wyoming selected areas with more intact sagebrush cover away from infrastructure associated with energy development. Sage-grouse avoidance of anthropogenic disturbance is also positively associated with avoidance of avian predators (Dinkins et al. 2012, 2014, Gibson et al. 2018). Dinkins et al. (2014) found that female sage-grouse in Wyoming selected areas with lower densities of

anthropogenic features and fewer avian predators, such as American kestrels (*Falco sparverius*), *Buteo* hawk spp., common ravens (*Corvus corax*; hereafter ravens), black-billed magpies (*Pica hudsonia*), northern harriers (*Circus hudsonius*), and golden eagles (*Aquila chrysaetos*). Additionally, Gibson et al. (2018) found that nesting sage-grouse in central Nevada avoided transmission lines, and this avoidance was extended farther in years with higher raven abundance. However, these avoidance behaviors may not carry over to natural disturbances like wildfire. Nest-site selection within burned areas is likely driven by high site fidelity to lekking and nesting areas (Lockyer et al. 2015, O'Neil et al. 2020, Dudley et al. 2022) and linked to reduced sage-grouse adult and nest survival (Byrne 2002, Lockyer et al. 2015, Foster et al. 2019, O'Neil et al. 2020, Tyrrell et al. 2023).

Ravens are a native synanthropic species that have demonstrated population increases within sagebrush ecosystems as a result of anthropogenic subsidization and disturbance (Coates et al. 2020, Dinkins et al. 2021, Duerr et al. 2021, Harju et al. 2021). The ability to capitalize on human-associated subsidies and disturbance has resulted in raven populations that are 6.2 to 23.4 times higher than in 1966 within the sagebrush biome (Harju et al. 2021). Within the range of the sage-grouse, initial abundance estimates and increased carrying capacity of raven populations were linked to anthropogenic subsidies and an increase in the proportion of area burned (Dinkins et al. 2021). In the Great Basin, higher raven densities have been associated with lower elevations and areas closer to human development, agriculture, and transmission lines (Coates et al. 2020). Additionally, Coates et al. (2014) found that ravens were more likely to nest on anthropogenic substrates in southeastern Idaho

compared to *Buteo* hawk species, while Howe et al. (2014) found that nesting ravens selected areas with more non-native vegetation cover, areas closer to transmission lines, and areas with more edge habitat.

Between 1984 and 2020, more than 90,000 km^2 have burned in the sagebrush ecosystem, primarily in the Great Basin (Crist et al. 2023). Between 2003 and 2019, over 5,000 km^2 (6.2%) of the 81,000 km^2 sagebrush-dominated habitat burned in Oregon (Oregon SageCon Partnership 2019). In Oregon, habitat loss and fragmentation connected to increased predation were identified as threats to sage-grouse populations (Hagen 2011a). Ravens are a documented and effective nest predator of sage-grouse (Coates et al. 2008, Coates and Delehanty 2010, Lockyer et al. 2013, Taylor et al. 2017). Their abundance has been linked to declines in sage-grouse lek trends (Peebles et al. 2017) and nest survival (Bui et al. 2010, Coates and Delehanty 2010, Dinkins et al. 2016, Gibson et al. 2018, Kohl et al. 2019, Coates et al. 2020, Coates et al. 2023). Therefore, this combination of habitat loss from wildfire and increasing raven populations may be contributing to the declines of several Oregon sage-grouse populations over the last four decades, with 2020 recorded as the second-lowest estimated state-wide population since 1980 (Vold 2023). Determining the singular, additive, or interactive effects of disturbance and raven density on sage-grouse demographics is critical for selecting the appropriate management strategies for local sage-grouse populations. Our research explored the potential additive and interactive effects of raven density and wildfire with the following questions: 1) is sage-grouse nest-site selection influenced by additive or interactive effects between wildfire and raven density, and 2) do additive or interactive effects of wildfire and

raven density affect sage-grouse nest survival? To address these questions, monitored radio-marked female sage-grouse and quantified local raven density and fire disturbance over five years (2018–2022) in sage-grouse conservation areas in eastern Oregon. We expected nest survival to be the highest for nest sites in areas with low wildfire disturbance and lower raven densities and lowest for nest sites in areas with high wildfire disturbance and higher raven densities. Additionally, we developed source/sink maps for nest survival to quantify the amount of habitat with high relative selection strength (RSS) and high nest survival within our selected sage-grouse conservation areas.

STUDY AREA

We selected our study areas from Oregon sage-grouse Priority Areas of Conservation (PACs) (Figure 1). The Baker, Bully Creek, Crowley, Cow Lakes, and Soldier Creek PACs were selected due to concerns regarding local population declines and significant wildfire activity in the last 20 years. Priority Areas of Conservation were created by the Oregon Department of Fish and Wildlife (ODFW) in 2011 using lek counts and telemetry data to determine areas of high sage-grouse density, seasonal habitats, including winter range, and connectivity corridors (Hagen 2011b, Doherty et al. 2010).

The Baker PAC was located 5 km east of Baker City, in Baker County, OR (44°47'N, 117°49'W) with an area of 1,362 km^2. The Bully Creek, Cow Lakes, Crowley, and Soldier Creek PACs were located in Malheur County, OR. The Bully Creek and Crowley PACs were located 4.1 km northeast (43°51’N, 117°36’W) and

2.5 km south (43°44'N, 118°04'W) of Juntura, OR, respectively. The Bully Creek PAC encompassed an area of 1,133 km^2, while the Crowley PAC had an area of 1,760 km^2. The Cow Lakes and Soldier Creek PACs were located 5.5 km north (42°58'N, 117°03'W) and 3.5 km southwest (43°55'N, 117°07'W) of Jordan Valley, OR, respectively. Cow Lakes had an area of 1,010 km^2, while Soldier Creek had an area of 1,195 km^2. The elevation among the five PACs ranged from 780 m to 1,855 m, with annual average temperatures between -9° C in January to 34° C in July. The average annual rain and snowfall ranged from 25.7 to 34 cm and 47 to 93 cm, respectively. Land ownership varied among the five PACS with Crowley and Soldier Creek each comprised of ~92% public and ~8% privately owned land, Bully Creek and Cow Lakes PACs each contained ~75% public and 25% privately owned, and the Baker PAC was 34% public and 66% privately owned land.

The dominant overstory vegetation in all of the PACs was Wyoming big sagebrush, low sagebrush (*A. arbuscula*), stiff sagebrush (*A. rigida*), and a small proportion of mountain big sagebrush (*A. t. vaseyana*) at the higher elevations. Native understory vegetation consisted of common forbs (*Lupinus, Crepis,* and *Lomatium* spp.) and native bunchgrasses such as bluebunch wheatgrass (*Pseudoroegneria spicata*), giant wildrye (*Leymus cinereus*), Idaho fescue (*Festuca idahoensis*), and Sandberg's bluegrass (*Poa secunda*). Cheatgrass and medusahead were widespread along with other invasive vegetation such as ventenata (*Ventenata dubia*), crested wheatgrass (*Agropyron cristatum*), Russian thistle (*Kali tragus*), and perennial pepperweed (*Lepidium latifolium*).

Wildfire activity and the status of the sage-grouse populations varied among our chosen PACs. The Baker PAC had the least amount of burned area with eleven large fires (>4 km^2) burning 75 km^2 (6%) inside, and 505 km^2 adjacent to the PAC between 1998 and 2015. However, the Baker sage-grouse population is geographically and genetically isolated due to a population decline in 2014, which it has yet to recover from (Vold 2023). The Soldier Creek PAC had eighteen fires burned 101 km^2 (8%) inside and 2,321 km^2 adjacent to the PAC between 1999 and 2020. The sage-grouse population in the Soldier Creek PAC has remained relatively stable since 2012. The Cow Lakes PAC was impacted by fifteen large fires that burned 236 km^2 (23%) inside and 1,509 km^2 adjacent to the PAC between 1996 and 2020. Sage-grouse populations were largely stable between 1993 and 2016 but began declining in 2017, reaching a low in 2018 that drew concern from the Bureau of Land Management (BLM) (BLM 2019, Vold 2023). Lastly, the Bully Creek PAC has been impacted by eight major fires between 1996 and 2020, burning 456 km^2 (40%) inside and 309 km^2 adjacent to PAC, with six fires occurring between 2012 and 2020. The Bully Creek sage-grouse population has remained relatively stable since 2011.

METHODS

Sage-grouse capture and tracking

Using a standard spotlight and hoop net technique, we captured female sage-grouse on foot at night (Giesen et al. 1982, Wakkinen et al. 1992). Beginning in 2017, individuals were primarily captured during the spring lekking season (March–May) and late summer (late-July–August), with occasional captures in the winter

(November–February). Upon capture, we determined the age of each individual based on primary feather molt as either a yearling (first breeding season) or adult (Braun and Schroeder 2015). We marked all individuals with an Oregon Department of Fish and Wildlife (ODFW) aluminum leg band and one of the following transmitters: 1) 22 g VHF necklace (American Wildlife Enterprises, Monticello, FL 32344 USA), 2) RI-2DM 22 g VHF necklace (Holohil Systems Ltd., Carp, Ontario, Canada), 3) 22 g rump-mounted ARGOS/GPS Solar PTT-100 (Microwave Telemetry Inc., Columbia, MD 21045 USA), 4) A Holohil VHF necklace with a PinPoint-75 Avian GPS store-on-board (SOB) 4.1 g tags or PinPoint-120 Avian GPS SOB 4.8 g tags (Lotek Wireless Inc., St. John's, NL A1A 5C6 Canada) with a total weight between 26.1 and 26.8 g, or 5) A Holohil VHF necklace with an attached 5.6 g Pica solar-powered GPS logger capable of remote download (Ecotone Telemetry, Gdynia, Poland) with a total weight of 27.6 g. All five combinations of radio- and GPS-marking equipment totaled < 3% of the female's body weight. We recaptured individuals fitted with Lotek SOB units annually to retrieve data and affix a new SOB unit.

We tracked Argos PTT marked individuals via downloaded locations. Once behavior suggested nest initiation, nests were confirmed using binoculars from approximately 10 m away. We located individuals marked with VHF/SOB units weekly during the nesting period using VHF receivers (Communications Specialists, R-1000, Orange, CA, USA) and 3-way antennas (Communications Specialists, Orange, CA, USA). We used binoculars to locate potential nests from ~10 m away to avoid disturbing VHF-marked nesting females. Once located, nests were monitored from 100 to 150 m. We determined nest fate for Argos PTT marked individuals and

VHF/Lotek SOB individuals after downloaded data or telemetry determined that the female was off the nest. We considered nests successful if ≥1 egg hatched. If we did not locate an individual marked with a VHF/Lotek SOB unit on a nest between 1 April and 15 June, we used the GPS data from the recovered SOB unit (mortality or annual recapture) to locate nests and determine nest survival. We considered nests for these females successful if location data suggested incubation behavior for 27 days.

Landscape, topographic, and anthropogenic variables

We compiled a suite of land cover, topographic, anthropogenic, and wildfire variables to use in our sage-grouse nest-site selection and nest survival analyses (Table 1). We quantified percent cover, proportion, topographic, and density variables using circular neighborhoods at six spatial extents. The radii for the neighborhoods included: 1) 0.09 km, which was the radius of the mean core area used by female sage-grouse around nests found by Dudko et al. (2019); 2) 0.18 km radius, which was the grand mean distance for all use locations for female sage-grouse around nests found by Dudko et al. (2019), 3) 0.57 km radius commonly used to evaluate sage-grouse habitat around nests (Aldridge and Boyce 2007, Dinkins et al. 2014, Kirol et al. 2015, Kirol et al. 2020), 4) 0.81 km radius which was equivalent to the mean distance traveled by nesting ravens found by Harju et al. (2018), 5) 1.47 km which was equivalent to the mean maximum radius of home ranges of breeding ravens found by Smith and Murphy (1973), and 6) 3.6 km which corresponded to the mean maximum radius of raven territory size found by Bruggers (1989).

We calculated Euclidean distances to anthropogenic features and fire-affected areas. We calculated distance decay functions using the formula *decay = exp(Euclidean distance to feature(km)/-decay distance)* to account for potential non-linear effects of proximity to feature variables. We calculated all distance decay functions with five decay distances (0.5, 1, 2, 5, and 10 km). The value that each decay function approached 0 (no influence on the response) was ~2.4 km, ~4.5 km, ~9.3 km, ~23.1 km, and ~46.1 km, respectively. Decay functions scale distances between 0 and 1 and are interpreted opposite of Euclidean distance variables, with larger values indicating closer proximity to the target feature.

Percent cover of annual herbaceous vegetation, bare ground, perennial herbaceous vegetation, non-sagebrush, sagebrush, all shrubs, and trees were obtained from Rangeland Condition Monitoring Assessment and Projection (RCMAP) products for each year from 2016–2021 (Rigge et al. 2021). We derived topographic variables, including a topographic ruggedness index (Sappington et al. 2007), compound topographic index (soil wetness index, Gessler et al. 1995), heat load index (amount of radiation, McCune and Keon 2002), aspect, and elevation from a 10 m resolution digital elevation model (DEM; USGS 2021). Aspect was transformed to a -1 to 1 scale using cos(aspect), so northern aspects had values near 1, and southern aspects had values near -1.

Differenced normalized burn ratio (dNBR) rasters of wildfires >4 km^2 that occurred between 1996 and 2020 were obtained from Monitoring Trends in Burn Severity (MTBS) for all fires occurring within and up to 3.6 km away from our study areas (MTBS 2023). We derived three types (severity, proportion, distance to) of fire

variables at 20, 10, and 5-year time lags. To create a mean maximum burn severity variable, we reclassified dNBR so that all burn severity values of 1 (unburned to low), 2 (low), 3 (moderate), and 4 (high severity) were retained, and all other values were set to 0. If a pixel burned more than once between 1996 and 2020, we retained the highest burn severity value recorded for that pixel. To create our proportion of area burned variable, we reclassified dNBR so that all burn severity values of 1, 2, 3, and 4 were set to 1, and all other values were set to 0. Using circular neighborhoods, we then summarized the mean maximum burn severity and proportion of area burned at the seven spatial scales described above. Fire variables were temporally aligned. For example, data collected in 2018 was given values from aggregated fire data for 20-, 10-, and 5-year lags from 1997–2017, 2007–2017, and 2012–2017, respectively.

We calculated the density of all roads (primary and secondary) and the density of primary roads at all seven spatial scales. We obtained road layers from the Oregon Department of Transportation 2021 Oregon Transportation Network and the Idaho Transportation Department All Roads GIS database, last updated in June 2022. Roads were classified as primary using the following procedures. For Oregon, we classified a road as "primary" if it was a paved or dirt road maintained and owned by the state or a county. We also considered roads "primary" if the owner was listed as "unknown" because visual inspection of these roads showed that they were likely high-use, privately owned driveways or farm roads. All unpaved roads that did not fit the above criteria and were owned by the BLM or the U.S. Forest Service were considered "secondary" roads (i.e., two-track roads). For Idaho, we classified roads as "primary" if the observed route was "2wd Low", the observed mode of transportation

was "motorized," and the observed road surface was either solid, aggregate, or natural improved. We considered roads as "secondary" when the route was "4wd High Clearance", "4wd Low", "ATV," or "Unknown." For both state road systems, we classified any road segments as "secondary" if they were not connected to other primary roads. Additional linear and point anthropogenic variables included distance to transmission line and distance to landfill variables, which were obtained from Homeland Infrastructure Foundation-Level Data (HIFLD 2023).

We reclassified the National Land Cover Database (NLCD) 2016 Land Cover raster by setting values of 81 (Pasture/Hay) and 82 (Cultivated Crops) to 1 and all other values to 0. We then used the same procedure on the 2017 United States Department of Agriculture (USDA) Cropland Data Layer with all cultivated crop, orchard, and vineyard categories set to 1 and all other categories set to 0. We then combined the two layers to create an agriculture raster that better represented our study areas. We used the new layer to create the proportion of agriculture and distance to agriculture variables.

Lastly, sage-grouse exhibit high site fidelity to communal breeding areas, called leks, and usually nest within 10 km of their associated lek (Holloran et al. 2005, Coates et al. 2013). To account for this behavior, we included a distance to active lek variable with Euclidean distance and distance decay equations with 0.5 and 1 km decays. We defined an active lek as any lek with ≥2 males in two or more years between 2016 and 2022 (ODFW 2023, IDFG 2023).

Raven density

Our relative raven density estimates were obtained from count data collected at random locations within our study areas. Ten-minute point count surveys were completed at random locations two to five times annually, between 2017 and 2022. Count data was analyzed with binomial N-mixture models using a Poisson distribution (Royle 2004). Results from these models were used to create predicted surfaces of relative raven density for each year. Full field and analysis methods in Chapter 2.

Modeling strategy

For both sage-grouse nest-site selection and nest survival analyses, we determined the best-fitting spatial scale or distance equation (e.g., Euclidean distance, 0.5 km decay, 1 km decay to agriculture) for each variable. To do this, we used Akaike's Information Criteria corrected for small sample sizes (AIC_c) to assess univariate models of all spatial scales (e.g., annual herbaceous vegetation within a radius of 0.09, 0.18, or 0.57 km) or distance equations. Variables with the lowest AIC_c and variables with only one spatial scale (i.e., aspect, elevation, heat load) were deemed informative and moved forward for analysis if the 85% confidence interval for the beta coefficient did not overlap zero (Arnold 2010). The categorical variables of county, study area, and year were only retained if all categories had 85% confidence intervals that did not overlap zero. We tested the remaining variables for multicollinearity with Pearson's correlation matrices and did not use variables with $r \geq |0.6|$ in the same model. We assessed pairs of variables that exhibited

multicollinearity with AIC_c, moving the variable with the lowest AIC_c to the final step of the modeling process. All continuous variables were z-standardized, so model coefficients were directly comparable.

We wanted to account for as much environmental heterogeneity as possible prior to assessing the effects of fire and raven density. Thus, we used backward selection to create base models for nest-site selection and nest survival from informative anthropogenic, categorical, topographic, and vegetation variables. Following the abovementioned procedures, the best-fitting base models were used as the null model to determine the best-fitting spatial scale or distance equation for fire variables. Informative fire variables and raven density were combined with the base model as additive and interactive terms, which were ranked using AIC_c.

Nest-site selection

We evaluated sage-grouse nest-site selection using generalized linear models to create resource selection functions (RSFs) in a use versus availability design (Manly et al. 2002, Fieberg et al. 2021). An RSF estimates the probability that a resource unit will be selected based on availability (Manly et al. 2002). We completed a sensitivity analysis before model selection to ensure that our models included adequate available locations (Manly et al. 2002, Northrup et al. 2013). To do this, we buffered our study areas by our largest variable spatial scale (3.6 km) to include available habitat for sage-grouse at the periphery of our study areas. We generated random locations within the buffered area to create 11 used versus availability ratios, including 1:1, 1:5, 1:10, and increasing the ratio by five until 1:50. We then ran univariate RSFs for each

ratio with either percent cover of annual herbaceous vegetation or percent cover of sagebrush. We tested the sensitivity of the used versus available ratio with these two variables because they have consistently been found to predict nest-site selection in previous research (Doherty et al. 2010, Connelly et al. 2011, Dinkins et al. 2014, O'Neil et al. 2020). We then examined the coefficient estimates for each model to determine at what ratio of used versus available locations the beta estimates stabilized (i.e., did not change with increasing ratios of used versus available) (Northrup et al. 2013). Once we determined a minimum ratio that resulted in coefficient stability, five additional sets of random locations were generated at that same ratio and analyzed with the same set of univariate models to ensure coefficient estimate and precision stability (Northrup et al. 2013, Long et al. 2014). We evaluated the fit of our base and top ΔAIC_c-ranked fire and raven models using k-fold cross-validation with five folds (Boyce et al. 2002, Johnson et al. 2006, Fieberg et al. 2013).

Nest Survival

We evaluated 28-day nest survival using a Cox proportional hazards (CoxPH) model (Cox 1972) using the "survival" package v. 3.5-5 (Therneau 2023). This time-to-event survival model assesses the probability of an event occurring, in this case, nest failure. CoxPH models produce hazard ratios (H.R.s) with values <1 indicating the variable increases survival and values >1 indicating the variable reduces survival. When we created the base model for nest survival, we also included nest initiation date (Julian day), nesting attempt, and RSS (top ΔAIC_c-ranked RSF model) in addition to the informative variables from the variable selection process. We

evaluated the fit of our base and top ΔAIC_c-ranked fire and raven models using a chi-squared test and the Schoenfeld residual scores for each variable and the global model to ensure they did not violate the proportional hazards assumption.

Identifying source/sink nesting areas

We predicted cumulative 28-day nest survival probabilities for each study area by generating Kaplan-Meier curves from our top ΔAIC_c-ranked CoxPH model. We used these survival probabilities to spatially extrapolate predictions for each study area as a function of each pixel's attribute data according to:

$$S_j(t_e|\mathrm{X}) = (S_{0,j}[t_e])^{\exp(\mathrm{x}\beta_x)}$$

where $S_{0,j}[t_e]$ is the cumulative nest survival probability for each study area (Cleves et al. 2008, DeCesare et al. 2014, Kirol et al. 2015).

We spatially extrapolated predictions from our top ΔAIC_c-ranked RSF model by ignoring the intercept and using an inverse logit link function to bound our RSS estimates between 0 and 1. Subsequently, we increased all values of the predicted surface by one so that values were rescaled between 1 and 2. We then created a new predicted surface by adding the RSS surface to the survival probability surface for each study area. Output from the resulting surface was bound between 0 and 2, with values near 0 representing areas with RSS and low survival, values near 1 corresponding to areas with low RSS and high survival or high RSS and low survival, and values near 2 corresponding to areas with high RSS and high survival.

RESULTS

Sage-grouse nest-site selection

We monitored 169 sage-grouse nests from 75 individuals between 2018 and 2022. After completing the variable selection and multicollinearity assessment steps, we were left with ten landscape, topographic, and anthropogenic variables to create a base nest-site selection model (Table 2). Our base model indicated that female sage-grouse were more likely to select nest sites as annual herbaceous cover increased within 3.6 km, percentage of bare ground within 1.47 km, perennial herbaceous cover within 3.6 km, sagebrush cover within 0.09 km, and closer to active leks. Female sage-grouse were less likely to select nest sites with higher cover of non-sagebrush shrub species within 3.6 km, proportion of riparian habitat within 0.18 km, topographic ruggedness within 0.18 km, density of all road types within 3.6 km, closer to agriculture or closer to transmission lines with a 1 km distance decay (Figure 2). K-fold cross-validation with five folds for our base model resulted in an R^2 of 0.89.

After assessing the best fitting spatial and temporal scales of our fire variables, our final model set included additive and interactive combinations of raven density, Euclidean distance to fire with a ten-year lag, mean maximum burn severity with a five-year lag within 3.6 km, and proportion of area burned with a five-year lag within 3.6 km. There was high correlation between the burn severity and proportion of area burned variables (r = 0.99), but low correlation between distance to fire and burn severity (r = 0.36) or burn proportion (r = 0.36). Four models were <2 ΔAIC_c of

each other (Table 3), indicating model uncertainty. All four models contained Euclidean distance to fire within the last ten years, with sage-grouse selecting nest sites closer to those fire-affected areas (Table 3). The first and second AIC-selected models contained an additive effect at the 3.6 km neighborhood of the proportion of area burned in the last five years and mean maximum burn severity in the last five years, respectively (Table 3). Both models indicate a positive relationship between nest-site selection and increasing proportion of burned area and burn severity (Figure 3). The fourth AIC-selected model included an additive relationship between the proportion of burned area and raven density (Table 3; however, raven density was not an informative predictor ($p = 0.56$). The mean r^2 from K-fold cross-validation for the top four AIC-selected models ranged between 0.90 and 0.97. Since raven density was an uninformative predictor, and the third AIC-selected model was nested within the first and second AIC-selected models, we chose to test the relative selection probabilities from the top two AIC-selected models on nest survival.

Sage-grouse nest survival

We assessed nest survival using the 169 sage-grouse nests from our nest-site selection analysis. After variable selection, we were left with eight variables to create our base nest survival model (Table 2). Our final base model included a fixed effect for study area and showed that sage-grouse nests were 65% (H.R. = 1.65, 95% CI: 1.12 – 2.43) more likely to fail as the density of all roads increased within 0.81 km. Nests with more northerly aspects were also more likely to fail (H.R. = 1.24, CI: 0.93 – 1.63); however, the 95% confidence interval overlapped 1. Nests were 19% less likely to

fail as the percent cover of non-sagebrush shrub species increased at 1.47 km (H.R. = 0.81, 95% CI: 0.66 – 0.98). Nest survival also increased by 1% for each increase in initiation day (H.R. = 0.99, 95% CI: 0.97 – 1.00). From our base model, estimated nest survival in the Baker, Bully Creek, Cow Lakes, and Soldier Creek PACs was 0.23 (95% CI: 0.12 – 0.43), 0.45 (95% CI: 0.32 – 0.63), 0.28 (95% CI: 0.17 – 0.46), and 0.29 (95% CI: 0.18 – 0.46), respectively.

Variable selection for our fire variables left us with distance to fire within the last five years with 0.5, 1, 2, and 5 km decay distances. These were used along with the base model to assess additive and interactive fire and raven density combinations. Five models were within <2 ΔAIC_c of each other and are discussed further (Table 4). The first, second, and third AIC-selected models contained a distance to fire variable with a 1, 0.5, or 2 km decay equation, respectively, and raven density as an additive variable (Table 4). Sage-grouse nests were more likely to fail as raven density increased for all three models, with H.R. = 1.36 (95% CI: 1.08–1.72) for the top-ranked model. The addition of distance to fire and raven density caused the non-sagebrush cover and road density variables to become imprecise. For example, in the model containing distance to fire with a 1 km decay and raven density, the 85% confidence interval for non-sagebrush cover became -0.31–0.06 and -0.06–0.28 for road density. The top-ranked model produced lower estimated nest survival in the Baker PAC (0.15, 95% CI: 0.06–0.35) and increased estimated nest survival in Bully Creek (0.51, 95% CI: 0.37–0.69) but made little change to survival in Cow Lakes (0.27, 95% CI: 0.16–0.47) or Soldier Creek (0.29, 95% CI: 0.18–0.46) (Figure 4). The fourth and fifth AIC-selected models included a single additive term of distance to

fire within five years with 1 and 2 km decay equations, respectively (Table 4). Both models showed that sage-grouse nests closer to areas affected by fire in the last five years were more likely to fail. The base model, the four top AIC-selected fire and raven models, and all variables within these models upheld the proportional hazards assumption (Table 5).

Mapping of nesting source/sink habitat

The amount of source nesting habitat (high selection/high survival) varied by study area. Bully Creek had the highest amount of source nesting habitat with 1,201 km^2 (49.3%), followed by Soldier Creek with 525 km^2 (25%), then Cow Lakes with 151 km^2 (8%), and finally, the Baker PAC had the least with 16 km^2 (0.7%) (Figure 5).

DISCUSSION

Our results provided mixed support for our hypotheses regarding additive and interactive effects of raven densities and wildfire disturbance on sage-grouse nest-site selection and survival. Our 28-day nest survival estimates were well below the range-wide average of 0.38 (Taylor et al. 2012) in the Baker (0.15), Cow Lakes (0.27), and Soldier Creek (0.29) PACs. The top three of our five ΔAIC_c-selected models indicated that sage-grouse nest survival decreased as relative raven density increased, which is consistent with current literature (Bui et al. 2010, Gibson et al. 2018, O'Neil et al. 2018, Coates et al. 2020). Yearly mean relative density estimates in our study areas ranged between 1.10–1.64 ravens km^{-2}, which was higher than estimates from Coates et al. (2020) (0.53 – 1.04 ravens km^{-2}) and much higher than 0.4 ravens/km^2

that corresponded to below-average 38-day nest survival for sage-grouse found by the same study.

We did not find evidence that raven density influenced nest site selection. However, sage-grouse were selecting nest sites with lower road density, away from agriculture, and away from transmission lines, all of which are associated with increased abundance, density, or occupancy of ravens (Bui et al. 2010, Howe et al. 2014, O'Neil et al. 2018, Harju et al. 2018, Dinkins et al. 2021, Revekant 2021, Chapter 2). Our results indicate that sage-grouse may try to avoid areas with higher raven densities, as Dinkins et al. (2012, 2014) found, but cannot find refugia in some areas. There may be a mismatch in spatial scale between where sage-grouse were selecting to nest and anthropogenic subsidies associated with higher raven densities. For example, Gibson et al. (2018) found that the negative impacts of transmission lines on sage-grouse nest survival were contingent on raven abundance, and these impacts could reach up to 12.5 km from the transmission line. Our nest-site selection models indicate that transmission lines negatively influence sage-grouse nest-site selection within five kilometers of the line, which may still leave nests vulnerable to predation in areas with high raven densities.

Maladaptive nest-site selection within fire-affected landscapes has been attributed to female philopatry to lekking and nesting areas (O'Neil et al. 2020, Brussee et al. 2022, Dudley et al. 2022). Our results provide additional evidence for this hypothesis as nest-site selection was positively associated with closer proximity to active leks and fire-affected areas at 5- and 10-year lags. However, nest-site selection was also positively associated with increasing sagebrush cover at 0.90 km

around the nest. These results suggest that even when nesting within fire-affected areas, sage-grouse still select for nest sites with higher sagebrush cover, consistent with findings reported by Schuyler et al. (2022). However, the mismatch of selection scales between sagebrush cover (0.90) and annual herbaceous vegetation, burn proportion, and burn severity (all 3.6 km) found in our models again may leave sage-grouse nests vulnerable to ravens and other predators that forage over large distances.

While distance to fire-affected areas within the last five years was the only fire variable associated with nest survival, the proportion of burned area and mean maximum burn severity were similar between hatched and failed nests for all-time lags. Previous research has shown that nest survival may drop by as much as 51% to 79% post-fire when compared to nest survival rates pre-fire (Dudley et al. 2022, Tyrell et al. 2023). Our study lacked a Before-After-Control-Impact study design, so we could not determine if or by how much nest survival was reduced after fire events in our study areas. However, wildfire probably contributed to our low nest survival in Baker, Cow Lakes, and Soldier Creek. There was at least one fire >4 km^2 that impacted at least one of our study areas every year between 1996 and 2020 (MTBS 2023). Considering it can take four to five years for sage-grouse to begin selecting for unburned or low severity burned areas within a fire footprint (Schuyler et al. 2022), female sage-grouse in our study areas may not be able to adjust to the constantly changing disturbance landscape.

Despite having the largest wildfire footprint, nest survival in the Bully Creek PAC was 0.51, well above the range-wide average. Examination of our nest survival source/sink maps show that Bully Creek has the largest area of source nesting habitat

compared to the other study areas (Figure 5). Our survival model contained study area as an informative parameter which modeled variation among the PACs that we did not account for, such as climate, other predators, disease, and genetics. Local climate patterns and the structure and amount of understory screening vegetation (Webb et al. 2012, Gibson et al. 2016) may be more favorable for nest survival in Bully Creek compared to the other three PACs. However, examination of sage-grouse nest locations mapped onto predicted raven density surfaces show, unlike the Baker and Cow Lakes PACs, the areas where ravens were concentrated were farther away from sage-grouse nesting areas. Therefore, sage-grouse may be able to find refugia away from ravens even in this burned landscape (Figure 6). Sage-grouse nesting areas in Soldier Creek were also largely away from areas of high raven density, but nest survival was below the range-wide average. This, again, may be due to variations in local climate conditions and structure of understory vegetation, or it may indicate that ravens were not the primary nest predators of sage-grouse in Soldier Creek.

Sage-grouse exhibit high site fidelity to nesting and breeding areas (Dunn and Braun 1985, Holloran and Anderson 2005, Coates et al. 2013) even in fragmented landscapes (Schroeder and Robb 2003), which may reduce their ability to respond to disturbance quickly (Knick and Rotenberry 2000). Fire-affected areas, particularly those that are colonized by invasive annual grasses near sage-grouse leks, may turn into sinks for local populations (Battin 2004, Kirol et al. 2015). The frequency and severity of wildfires within the Great Basin is predicted to increase due to the effects of climate change (Creutzburg et al. 2015, Williams et al. 2019, Mansoor et al. 2022). Coates et al. (2016) projected that habitat loss from wildfire and invasive annual

grasses will reduce sage-grouse populations by 43% by 2044. Our results indicate that female sage-grouse in Oregon were nesting within recently (<5 years) burned areas and have lower nest survival, likely contributing to population declines in some areas. Therefore, it is vital to reduce wildfires in nesting habitat (i.e., around leks) and that restoration efforts post-fire are quick and intensive. However, our results also indicate that nest survival may be less affected by wildfires if those nesting areas were located away from anthropogenic sources that increased raven densities. Therefore, in addition to protecting lekking and nesting areas from wildfire and expanding core areas of sagebrush habitat, anthropogenic subsidies should be removed or heavily mitigated beyond 8 km around sage-grouse leks to reduce the impacts of ravens and other human-subsidized predators within sage-grouse nesting areas.

LITERATURE CITED

Abatzoglou, J. T., and C. A. Kolden. 2011. Climate change in western U.S. deserts: potential for increased wildfire and invasive annual grasses. Rangeland Ecology and Management 64:471–478.

Aldridge, C. L., and M. S. Boyce. 2007. Linking occurrence and fitness to persistence: habitat-based approach for endangered greater sage-grouse. Ecological Applications 17:508–526.

Arnold. T. 2010. Uninformative parameters and model selection using Akaike's Information Criterion. Journal of Wildlife Management 74:1175–1178.

Atwood, T. C., H. P. Weeks, T. M. Gehring. 2004. Spatial ecology of coyotes along a suburban-to-rural gradient. Journal of Wildlife Management 68:1000–1009.

Baker, W. L. 2011. Pre-EuroAmerican and recent fire in sagebrush ecosystems. Pages 185–201 *in* S. T. Knick and J. W. Connelly, editors. Greater sage-grouse: ecology and conservation of a landscape species and its habitats. Studies in Avian Biology, Volume 38, University of California Press, Berkeley, USA.

Balch, J. K., B. A. Bradley, C. M. D'Antonio, and J. Gómez-Dans. 2013. Introduced annual grass increases regional fire activity across the arid western USA (1980–2009). Global Change Biology 19:173–183.

Barlow, N. L., C. P. Kirol, K. E. Doherty, and B. C. Fedy. 2020. Evaluation of the umbrella species concept at fine spatial scales. The Journal of Wildlife Management 84:237–248.

Battin, J. 2004. When good animals love bad habitats: ecological traps and the conservation of animal populations. Conservation Biology 18:1482–1491.

Bauer, J. T. 2012. Invasive species: "back-seat drivers" of ecosystem change? Biological Invasions 14:1295–1304.

Boyce, M. S., P. R. Vernier, S. E. Nielsen, and F. K. A. Schmiegelow. 2002. Evaluating resource selection functions. Ecological Modelling 157:281–300.

Bradley, B. A., C. A. Curtis, E. J. Fusco, J. T. Abatzoglou, J. K. Balch, S. Dadashi, and M. Tuanmu. 2018. Cheatgrass (*Bromus tectorum*) distribution in the intermountain western United States and its relationship to fire frequency, seasonality, and ignitions. Biological Invasions 20:1493–1506.

Braun, C. E., and M. A. Schroeder. 2015. Age and sex identification from wings of sage-grouse. Wildlife Society Bulletin 39:182–187.

Bruggers, D. J. 1989. The behavior and ecology of the common raven in northeastern Minnesota (Dissertation). University of Minnesota, Minneapolis, MN.

Brussee, B. E., P. S. Coates, S. T. O'Neil, M. L. Casazza, S. P. Espinosa, J. D. Boone, E. M. Ammon, S. C. Gardner, and D. J. Delehanty. 2022. Invasion of annual grasses following wildfire corresponds to maladaptive habitat selection by a sagebrush ecosystem indicator species. Global Ecology and Conservation 37:e02147.

Bryne, M. W. 2002. Habitat use by female greater sage grouse in relation to fire at Hart Mountain National Antelope Refuge, Oregon. Thesis. Oregon State University, Corvallis, OR, USA.

Bui, T. V. D., J. M. Marzluff, and B. Bedrosian. 2010. Common raven activity in relation to land use in western Wyoming: implications for greater sage-grouse reproductive success. The Condor 112:65–78.

Bukowski, B. E., and W. L. Baker. 2013. Historical fire regimes, reconstructed from land-survey data, led complexity and fluctuation in sagebrush landscapes. Ecological Applications 23:546–564.

Bureau of Land Management (BLM). 2019. Notice of availability of record of decision and approved resource management plan amendment for greater sage-grouse conservation, Wyoming. Federal Register 84:10322–10323.

Carcos, D., J. Nascimbene, M. Campesan, D. Donadello, V. Segat, and L. Marini. 2019. Establishment dynamics of native and exotic plants after disturbance along roadsides. Applied Vegetation Science 2:277–284.

Chambers, J. C., D. A. Pyke, J. D. Maestas, M. Pellant, C. S. Boyd, S. B. Campbell, S. Espinosa, D. W. Havlina, K. E. Mayer, and A. Wuenschel. 2014. Using resistance and resilience concepts to reduce impacts of invasive annual grasses and altered fire regimes on the sagebrush ecosystem and greater sage-grouse: a strategic multi-scale approach. General Technical Report. RMRS-GTR-326. U.S. Department of Agriculture, Forest Service, Rocky Mountain Research Station, Fort Collins, Colorado, USA.

Coates, P. S., J. W. Connelly, and D. J. Delehanty. 2008. Predators of greater sage-grouse nests identified by video monitoring. Journal of Field Ornithology 79:421–428.

Coates, P. S., and D. J. Delehanty. 2010. Nest predation of greater sage-grouse in relation to microhabitat factors and predators. Journal of Wildlife Management 74:240–248.

Coates. P. S., M. L. Casazza, E. J. Blomberg, S. C. Gardner, S. P Espinosa, J. L. Yee, L. Wiechman, and B. J. Halstead. 2013. Evaluating greater sage-grouse seasonal space use relative to leks: implications for surface use designations in sagebrush ecosystems. Journal of Wildlife Management 77:1598–1609.

Coates, P. S., K. B. Howe, M. L. Casazza, and D. J. Delehanty. 2014. Landscape alterations Influence differential habitat use of nesting buteos and ravens within sagebrush ecosystem: implications for transmission line development. The Condor 116:341–356.

Coates, P. S., M. A. Ricca, B. G. Prochazka, M. L. Brooks, K. E. Doherty, T. Kroger, E. J. Blomberg, C. A. Hagen, and M. L. Casazza. 2016. Wildfire, climate, and invasive grass interactions negatively impact an indicator species by reshaping sagebrush ecosystems. Proceedings of the National Academy of Sciences 113:12745–12750.

Coates, P. S., S. T. O'Neil, B. E. Brussee, M. A. Ricca, P. J. Jackson, J. B. Dinkins, K. B. Howe, A. M. Moser, L. J. Foster, and D. J. Delehanty. 2020. Broad-scale impacts of an invasive native predator on a sensitive native prey species within the shifting avian community of the North American Great Basin. Biological Conservation 243:108409.

Coates, P. S., B. G. Prochazka, M. S. O'Donnell, C. L. Aldridge, D. R. Edmunds, A. P. Monroe, M. A. Ricca, G. T. Wann, S. E. Hanser, L. A. Wiechman, and M. P. Chenaille. 2021. Range-wide greater sage-grouse hierarchical monitoring framework–implications for defining population boundaries, trend estimation, and a targeted annual warning system. U. S. Geological Survey Open-File Report 2020–1154, 243 pp.

Coates, P. S., B. P. Prochazka, S. T. O'Neil, S. C. Webster, S. Espinosa, M. A. Ricca, S. R. Mathews, M. Casazza, and D. J. Delehanty. 2023. Geothermal energy production adversely affects a sensitive indicator species within sagebrush ecosystems in western North America. Biological Conservation 280:109889.

Connelly, J. W., E. T. Rinkes, and C. E. Braun. 2011. Characteristics of greater sage-grouse habitats: a landscape species at micro and macro scales. Pages 69–83 *in* S. T. Knick and J. W. Connelly, editors. Greater sage-grouse: ecology and conservation of a landscape species and its habitats. Studies in Avian Biology, Volume 38, University of California Press, Berkeley, USA.

Cox, D. R. 1972. Regression models and life tables (with discussion). Journal of the Royal Statistical Society, Series B 34:187–220.

Creutzburg, M. K., E. B. Henderson, and D. R. Conklin. 2015. Climate change and land management impact rangeland condition and sage-grouse habitat in southeastern Oregon. AIMS Environmental Science 2:203–236.

Crist, M. R., R. Belger, K. W. Davies, D. M. Davis, J. R. Meldrum, D. J. Shinneman, T. E. Remington, J. Welty, and K. E. Mayer. 2023. Trends, impacts, and cost of catastrophic and frequent wildfires in the sagebrush biome. Rangeland Ecology and Management89:3–19.

Dawes, J. H. P., and M. O. Souza. 2013. A derivation of Holling's type I, II, and III functional responses in predator-prey systems. Journal of Theoretical Biology 327:11–22.

DeCesare, N. J., M. Hebblewhite, M. Bradley, D. Hervieux, L. Neufeld, and M. Musiani. 2014. Linking habitat selection and predation risk to spatial variation in survival. Journal of Animal Ecology 83:343–352.

Dewitz, J. 2019. National land cover database (NLCD) 2016 Products. U.S. Geological Survey data release https://doi.org/10.5066/P96HHBIE.

Didham, R. K., J. M. Tylianakis, N. J. Gemmell, T. A. Rand, and R. M. Ewers. 2007. Interactive effects of habitat modification and species invasion on native species decline. TRENDS in Ecology and Evolution 22:489–496.

Dinkins, J. B., M. R. Conover, C. P. Kirol, and J. L. Beck, J. L. 2012. Greater sage-grouse (*Centrocercus urophasianus*) select nest sites and brood sites away from avian predators. The Auk 129:600–610.

Dinkins, J. B., M. R. Conover, C. P. Kirol, J. L. Beck, and S. N. Frey. 2014. Greater sage-grouse (*Centrocercus urophasianus*) select habitat based on avian predators, landscape composition, and anthropogenic features. The Condor 116:629–642.

Dinkins, J. B., M. R. Conover, C. P. Kirol, J. L. Beck, and S. N. Frey. 2016. Effects of common raven and coyote removal and temporal variation in climate on greater sage-grouse nesting success. Biological Conservation 202:50–58.

Dinkins, J. B., L R. Perry, J. L. Beck, and J. D. Taylor. 2021. Increased abundance of the common raven within the ranges of greater and Gunnison sage-grouse: influence of anthropogenic subsidies and fire. Human-Wildlife Interactions.

Doherty, K. E., D. E. Naugle, and B. L. Walker. 2010. Greater sage-grouse nesting habitat: the important of managing at multiple scales. Journal of Wildlife Management 74:1544–1553.

Doherty, T. S., C. R. Dickman, D. G. Nimmo, and E. G. Ritchie. 2015. Multiple threats, or multiplying the threats? Interactions between invasive predators and other ecological disturbances. Biological Conservation 190:60–68.

Doherty, K. E., J. S. Evans, P. S. Coates, L. M. Juliusson, and B. C. Fedy. 2016. Importance of regional variation in conservation planning: a rangewide example of the greater sage-grouse. Ecosphere 7:e01462.

Doherty, K., D. M. Theobald, J. B. Bradford, L. A. Wiechman, G. Bredrosian, C. S. Boyd, M. Cahill, P. S. Coates, M. K. Creutzburg, M. R. Crist, S. P. Finn, A. V. Kumar, C. E. Littlefield, J. D. Maestas, K. L. Prentice, B. G. Prochazka, T. E. Remington, W. D. Sparklin, J. C. Tull, Z. Wurtzbach, and K. A. Zeller. 2022. A sagebrush conservation design to proactively restore America's sagebrush biome. U.S. Geological Survey Open-File Report 2022–1081, 38p.

Dorn, N. J., and M. I. Cook. 2015. Hydrologic disturbance diminishes predator control in wetlands. Ecology 96:2984–2993.

Dornelas, M. 2010. Disturbance and change in biodiversity. Philosophical Transactions of The Royal Society B 365:3719–3727.

Duchardt, C. J., A. P. Monroe, D. R. Edmunds, M. J. Holloran, A. G. Holloran, and C. L. Aldridge. 2023. Using neutral landscape models to evaluate the umbrella species concept in an ecotone. Landscape Ecology 38:1447–1462.

Dudko, J. E., P. S. Coates, and D. J. Delehanty. 2019. Movements of female Sage Grouse *Centrocercus urophasianus* during incubation recess. Ibis 161:222–229.

Dudley, I. F., P. S. Coates, B. G. Prochazka, D. M. Davis, S. C. Gardner, and D. J. Delehanty. 2022. Maladaptive nest-site selection and reduces nest survival in female sage-grouse following wildfire. Ecosphere 13:e4282.

Duerr, A. E., P. H. Bloom, K. Ross, T. A. Miller, M. A. Braham, A. L. Fesnock, and T. E. Katzner. 2021. Influence of anthropogenic subsidies on movements of common ravens. Human-Wildlife Interactions 15:9.

Dunn, P. O., and C. E. Braun. 1985. Natal dispersal and lek fidelity of sage-grouse. The Auk. 102:621–627.

Fieberg, J. R., J. D. Forester, G. M. Street, D. H. Johnson, A. A. ArchMiller, and J. Matthiopoulos. 2017. Used-habitat calibration plots: a new procedure for validating species distribution, resource selection, and step-selection models. Ecography 41:737–752.

Fieberg, J., J. Signer, B. Smith, and T. Avgar. 2021. A 'How to' guide for interpreting parameters in habitat-selection analyses. Journal of Animal Ecology 90:1027–1043.

Fontaine, J. B. and P. L. Kennedy. 2012. Meta-analysis of avian and small-mammal response to fire severity and fire surrogate treatments in U.S. fire-prone forests. Ecological Applications 22:1547–1561.

Fontúrbel, F. E., J. I. Orellana, G. B. Rodríguez-Gómez, C. A. Tabilo, and G. J. Castaño-Villa. 2021. Habitat disturbance can alter forest understory bird activity patterns: a regional-scale assessment with camera traps. Forest Ecology and Management 479:118618.

Foster, L. J., K. M. Dugger, C. A. Hagen, and D. A. Budeau. 2019. Greater sage-grouse vital rates after wildfire. Journal of Wildlife Management 83:121–134.

Fusco, E. J., J. K. Balch, A. L. Mahood, R. C. Nagy, A. D. Syphard, and B. A. Bradley. 2022. The human-grass-fire cycle: how people and invasives co-occur to drive fire regimes. Frontiers in Ecology and the Environment 20:117–126.

Gallett, R., S. Alizon, P. Comte, A. Gutierrez, F. Depaulis, M. van Baalen, E. Michel, and C. D. M. Müller-Graf. 2007. Predation and disturbance interact to shape prey species diversity. The American Naturalist 170:143–154.

Gessler, P. E., I. D. Moore, N. J. McKenzie, and P. J. Ryan. 1995. Soil-landscape modelling and spatial prediction of soil attributes. International Journal of Geographical Information Systems 9:421–432.

Gibson, D., E. J. Blomberg, M. T. Atamian, and J. S. Sedinger. 2016. Nesting habitat selection influences nest and early offspring survival in greater sage-grouse. The Condor 118:689–702.

Gibson, D., E. J. Blomberg, M. T. Atamian, S. P. Espinosa, and J. S. Sendinger. 2018. Effects of power lines on habitat use and demography of greater sage-grouse (*Centrocercus urophasianus*). Wildlife Monographs 200:1–41.

Giesen, K. M., T. J. Schoenberg, and C. E. Braun. 1982. Methods for trapping sage grouse in Colorado. Wildlife Society Bulletin 10:224–231.

Hagen, C. A. 2011a. Predation on greater sage-grouse: Facts, processes, and effects. Chapter 6 *in* S. T. Knick and J. W. Connelly, editors. Greater sage-grouse: ecology and conservation of a landscape species and its habitats. Studies in Avian Biology, Volume 38, University of California Press, Berkeley, USA.

Hagen, C. A. 2011b. Greater sage-grouse conservation assessment and strategy for Oregon: a plan to maintain and enhance populations and habitat. Oregon Department of Fish and Wildlife, Salem, Oregon, USA.

Harju, S. M., C. V. Olson, J. E. Hess, and B. Bedrosian. 2018. Common raven movement and space use: influence of anthropogenic subsidies within greater sage-grouse nesting habitat. Ecosphere 9:e02348.

Harju, S. M., P. S. Coates, S. J. Dettenmaier, J. B. Dinkins, P. J. Jackson, and M. P. Chenaille. 2021. Estimating trends of common raven populations in North America, 1966–2018. Human-Wildlife Interactions 15:248–269.

Holling, C. S. 1959. Some characteristics of simple types of predation and parasitism. Canadian Entomology 91:385–398.

Holloran, M. J. and S. H. Anderson. 2005. Spatial distribution of greater sage-grouse nests in relatively contiguous sagebrush habitats. Condor 107:742–752.

Howe, K. B., P. S. Coates, and D. J. Delehanty. 2014. Selection of anthropogenic features and vegetation characteristics by nesting common ravens in the sagebrush ecosystem. The Condor 116:35–49.

Idaho Transportation Department (ITD) 2022. Idaho transportation network 2022. ITD OpenData.

IPBES. 2019. Global assessment report on biodiversity and ecosystem services of the Intergovernmental Science-Policy Platform on Biodiversity and Ecosystem Services. Brondizio, E. S., J. Settele, S. Díaz, and H. T. Ngo, editors. IPBES secretariat, Bonn, Germany.

IPCC. 2023. Climate change 2023: synthesis report. A report of the Intergovernmental Panel on Climate Change. Contribution of Working Groups I, II, and III to the sixth assessment of the Intergovernmental Panel on Climate Change. H. Lee, J. Romero, and Core Writing Team, editors. IPCC, Geneva, Switzerland.

Johnson, C. J., S. E. Nielsen, E. H. Merrill, T. L. McDonald, and M. S. Boyce. 2006. Resource selection functions based on use-availability data: theoretical motivation and evaluation methods. The Journal of Wildlife Management 70:347–357.

Johnson, D. H., M. J. Holloran, J. W. Connelly, S. E. Hanser, C. L. Amundson, and S. T. Knick. 2011. Influences of environmental and anthropogenic features on greater sage-grouse populations, 1997–2007. Pages 510–553 *in* S. T. Knick and J. W. Connelly, editors. Greater sage-grouse: ecology and conservation of a landscape species and its habitats. Studies in Avian Biology, Volume 38, University of California Press, Berkeley, USA.

Kirol, C. P., J. L. Beck, S. V. Huzurbazar, M. J. Holloran, and S. N. Miller. 2015 Identifying greater sage-grouse source and sink habitats for conservation

planning in an energy development landscape. Ecological Applications 25:968–990.

Kirol, C. P., K. T. Smith, N. E. Graf, J. B. Dinkins, C. W. LeBeau, T. L. Maechtle, A. L. Sutphin, and J. L. Beck. 2020. Greater sage-grouse response to the physical footprint of energy development. The Journal of Wildlife Management 84:989–1001.

Knick, S. T., and J. T. Rotenberry. 2000. Ghosts of habitats passed: contribution of landscape change to current habitats used by shrubland birds. Ecology 81:220–227.

Kohl, M. T., T. A. Messmer, B. A. Crabb, M. R. Guttery, D. K. Dahlgren, R. T. Larsen, S. N. Frey, S. Liguori, and R. J. Baxter. 2019. The effects of electric power lines on the breeding ecology of greater sage-grouse. PLoS ONE 14:e0213669.

Kreling, S. E. S., K. M. Gaynor, A. McInturff, K. L. Calhoun, and J. S. Brashares. 2021. Site fidelity and behavioral plasticity regulate an ungulate's response to extreme disturbance. Ecology and Evolution 11:15683–15694.

Labadie, G., C. Hardy, Y. Boulanger, V. Vanlandeghem, M. Hebblewhite, and D. Fortin. 2023. Global change risks a threatened species due to alteration of predator-prey dynamics. Climate Ecology 3:e4485.

Lockyer, Z. B., P. S. Coates, M. L. Cassaza, S. Espinosa, and D. J. Delehanty. 2013. Greater sage-grouse nest predators in the Virginia Mountains of northwestern Nevada. Journal of Fish and Wildlife Management 4:242–254.

Lockyer, Z. B., P. S. Coates, M. L. Casazza, S. Espinosa, and D. J. Delehanty. 2015. Nest-site selection and reproductive success of greater sage-grouse in a fire-affected habitat in northwestern Nevada. Journal of Wildlife Management 79:785–797.

Long, R. A., R. T. Bowyer, W. P. Porter, P. Mathewson, K. L. Monteith, and J. G. Kie. 2014. Behavior and nutritional condition buffer a large-bodied endotherm against direct and indirect effects of climate. Ecological Monographs 84:513–532.

Lungle, K. and S. Pruss. 2008. Recovery Strategy for the Greater Sage-Grouse (*Centrocercus urophasianus urophasianus*) in Canada. In Species at Risk Act Recovery Strategy Series. Parks Canada Agency. Ottawa, Ontario, 43 pp.

Manly, B. F., J. L. McDonald, D. L. Thomas, T. L. McDonald, and W. P. Erickson. 2002. Resource selection by animals: statistical design and analysis for field studies. Chapman and Hall, London, UK.

Mansoor, S., I. Farooq, M. M. Kachroo, A. E. D. Mahmoud, M. Fawzy, S. M. Popescu, M. N. Alyemeni, C. Sonne, J. Rinklebe, P. Ahmad. 2022. Elevation in wildfire frequencies with respect to climate change. Journal of Environmental Management 301:113769.

McCune, B. and D. Keon. 2002. Equations for potential annual direct incident radiation and heat load. Journal of Vegetation Science 13:603–606.

Miller, R. F., S. T. Knick, D. A. Pyke, C. W. Meinke, S. E. Hanser, M. J. Wisdom, and A. L. Hild. 2011. Characteristics of sagebrush habitats and limitations to long-term conservation. Pages 145–184 *in* S. T. Knick and J. W. Connelly, editors. Greater sage-grouse: ecology and conservation of a landscape species and its habitats. Studies in Avian Biology, Volume 38, University of California Press, Berkeley, USA.

Monitoring Trends in Burn Severity. 2023. MTBS Data Access: Fire Level Geospatial Data (2017, July - last revised). MTBS Project USDA Forest Service/U.S. Geological Survey.

Mumma, M. A., M. P. Gillingham, K. L. Parker, C. J. Johnson, and M. Watters. 2018. Predation risk for boreal woodland caribou in human-modified landscapes: evidence of wolf spatial responses independent of apparent competition. Biological Conservation 228:215–223.

Murphy, G. E. P., and T. N. Romanuk. 2013. A meta-analysis of declines in local species richness from human disturbances. Ecology and Evolution 4:91–103.

Newbold, T., L. N. Hudson, S. L. L. Hill, S. A. Contu, C. L. Gray, J. P. W. Scharlemann, L. Börger, H. R. P. Phillips, D. Sheil, I. Lysenko, and A. Purvis. 2016. Global patterns of terrestrial assemblage turnover within and among land uses. Ecography 39:1151–1163.

Northrup, J. M., M. B. Hooten, C. R. Anderson, and G. Wittemyer. 2013. Practical guidance on characterizing availability in resource selection functions under a use-availability design. Ecology 94:1456–1463.

Oaten, A., and W. W. Murdoch. 1975. Functional response and stability in predator-prey systems. The American Naturalist 109:289–298.

O'Neil, S. T., P. S. Coates, B. E. Brussee, P. J. Jackson, K. B. Howe, A. M. Moser, L. J. Foster, and D. J. Delehanty. 2018. Broad-scale occurrence of a subsidized avian predator: Reducing impacts of ravens on sage-grouse and other sensitive prey. Journal of Applied Ecology 55:2641–2652.

O'Neil, S. T., P. S. Coates, B. E. Brussee, M. A. Ricca, S. P. Espinosa, S. C. Gardner, and D. J. Delehanty. 2020. Wildfire and the ecological niche: diminishing habitat suitability for an indicator species within semi-arid ecosystems. Global Change Biology 26:6296–6312.

Oregon SageCon Partnership. 2019. Oregon sagebrush: status, trends, and ongoing efforts. Proceedings from SageCon Summit 2019. October 4, 2019. Ontario, Oregon, USA.

Oregon Department of Transportation (ODOT) Geographic Information Service Unit. 2019. Oregon transportation network 2019. Oregon Spatial Data Library.

Peebles, L. W., M. R. Conover, and J. B. Dinkins. 2017. Adult sage-grouse numbers rise following raven removal or an increase in precipitation. Wildlife Society Bulletin 41:471–478.

Poessel, S. A., D. M. Barnard, C. Applestein, M. J. Germino, E. A. Ellsworth, D. Major, A. Moser, and T. E. Katzner. 2022. Greater sage-grouse respond positively to intensive post-fire restoration treatments. Ecology and Evolution 12:e8671.

Rahman, T. and U. Candolin. 2022. Linking animal behavior to ecosystem change in disturbed environments. Frontiers in Ecology and Evolution. 10:1–13.

Revekant, C. L. 2021. Comparison of common ravens in sage-grouse core and non-core area: assessing predator densities related to anthropogenic features. Thesis. Oregon State University, Corvallis, OR, USA.

Rigge, M. B., B. Bunde, B. H. Shi, and K. Postma. 2021. Rangeland Condition Monitoring Assessment and Projection (RCMAP) Fractional Component Time-Series Across the Western U.S. 1985–2020 (ver. 2.0, October 2021): U.S. Geological Survey data release, https://doi.org/10.5066/P95IQ4BT.

Rosenberg, K. V., A. M. Dokter, P. J. Blancher, J. R .Sauer, A. C. Smith, P. A. Smith, J. C. Stanton, A. Panjabi, L. Helft, M. Parr, and P. P. Marra. 2019. Decline of the North American avifauna. Science 366:120–124.

Rowland, M. M., J. M. Wisdom, L. H. Suring, and C. W. Meinke. 2006. Greater sage-grouse as an umbrella species for sagebrush-associated vertebrates. Biological Conservation 129:323–335.

Royle, J. A. 2004a. N-Mixture models for estimating population size from spatially replicated counts. Biometrics 60:108-115.

Sappington, J. M., K. M. Longshore, and D. B. Thompson. 2007. Quantifying landscape ruggedness for animal habitat analysis: a case study using bighorn

sheep in the Mojave Desert. The Journal of Wildlife Management 71:1419–1426.

Schroeder, M. A. and L. A. Robb. 2003. Fidelity of greater sage-grouse *Centrocercus urophasianus* to breeding areas in a fragmented landscape. Wildlife Biology 9:291–299.

Schroeder, M. A., C. L. Aldridge, A. D. Apa, J. R. Bohne, C. E. Braun, S. D. Bunnell, J. W. Connelly, P. A. Deibert, S. C. Gardner, M. A. Hilliard, G. D. Kobriger, S. M. Mcadam, C. W. Mccarthy, J. J. Mccarthy, D. L. Mitchell, E. V Rickerson, and S. J. Stiver. 2004. Distribution of sage-grouse in North America. The Condor 106:363–376.

Schuyler, E. M., C. A. Hagen, C. R. Anthony, L. J. Foster, and K. M. Dugger. 2022. Temporal mismatch in space use by a sagebrush obligate species after large-scale wildfire. Ecosphere 13:e4179.

Simberloff, D., J. Martin, P. Genovesi, V. Maris, D. A. Wardle, J. Aronson, F. Courchamp, B. Galil, E. García-Berthou, M. Pascal, P. Pyšek, R. Sousa, E. Tabacchi, and M. Vilá. 2013. Impacts of biological invasions: what's what and the way forward. Trends in Ecology and Evolution 28:58–66.

Smith, D. G., and J. R. Smith. 1973. Breeding ecology of raptors in the eastern Great Basin of Utah. Brigham Young University Science Bulletin, Biological Series 18:1–72.

Taylor, R. L., B. L. Walker, D. E. Naugle, and L. S. Mills. 2012. Managing multiple vital rates to maximize greater sage-grouse population growth. The Journal of Wildlife Management 76:336-347.

Taylor, J. D., D. Holt, E. K. Orning, and J. K. Young. 2017. Greater sage-grouse nest survival in northwestern Wyoming. The Journal of Wildlife Management 81:1219–1227.

Therneau, T. 2023. A package for survival analysis in R. R package version 3.5-5, https://CRAN.R-project.org/package=survival.

Tyrrell, E. A., P. S. Coates, B. G. Prochazka, B. E. Brussee, S. P. Espinosa, and J. M. Hull. 2023. Wildfire immediately reduces nest and adult survival of greater sage-grouse. Scientific Reports 13:10970.

USDA National Agriculture Statistics Service. 2017. Cropland Data Layer 2017. Available at https://nassgeodata.gmu.edu/CropScape/ USDA-NASS, Washington, DC.

U. S. Department of Homeland Security. 2022. Homeland infrastructure foundation-level data (HIFLD). Geospatial Management Office.

U.S. Geological Survey. 2021. 30-meter Digital Elevation Models (DEMs). Data collection: U.S. Geological Survey.

U.S. Fish and Wildlife Service. 2015. 50 CFR Part 17 Endangered and Threatened Wildlife and Plants; 12-month findings for petitions to list the greater sage-grouse (*Centrocercus urophasianus*) as threatened or endangered. Docket No. FWS-R6-E.S.-2015-0146. U.S. Department of Interior, Fish and Wildlife Service, Washington, DC, USA.

Vieira-Nieto, E. H. M., H. L. Vasconcelos, and E. M. Bruna. 2016. Roads increase population growth rates of a native leaf-cutter ant in Neotropical savannahs. Journal of Applied Ecology 53:983–992.

Vold, S. T. 2023. Oregon greater sage-grouse population monitoring: 2023 annual report. Oregon Department of Fish and Wildlife, Hines, OR, USA.

Wakkinen W. L., K. P. Reese, J. W. Connelly, and R. A. Fischer. 1992. An improved spotlighting technique for capturing sage grouse. Wildlife Society Bulletin 20:425–426.

Wald, S. J. 1986. Effect of abiotic disturbance on a lotic predator-prey interaction. Oecologia 69:243–247.

Webb, S. L., C. V. Olson, M. R. Dzialak, S. M. Harju, J. B. Winstead, and D. Lockman. 2012. Landscape features and weather influence nest survival of a ground-nesting bird of conservation concern, the greater sage-grouse in human-altered environments. Ecological Processes 1:1–15.

White, P. S., and S. T. A Pickett. 1985. Natural disturbance and patch dynamics: an introduction. Pages 3–13 *in* S. T. A. Pickett and P. S. White, editors. The ecology of natural disturbance and patch dynamics. Academic Press, Inc., Orlando, FL.

Williams, A. P., J. T. Abatzoglou, A. Gershunov, J. Guzman-Morales, D. A. Bishop, J. K. Balch, and D. P. Lettenmaier. 2019. Observed impacts of anthropogenic climate change on wildfire in California. Earth's Future 7:852–910.

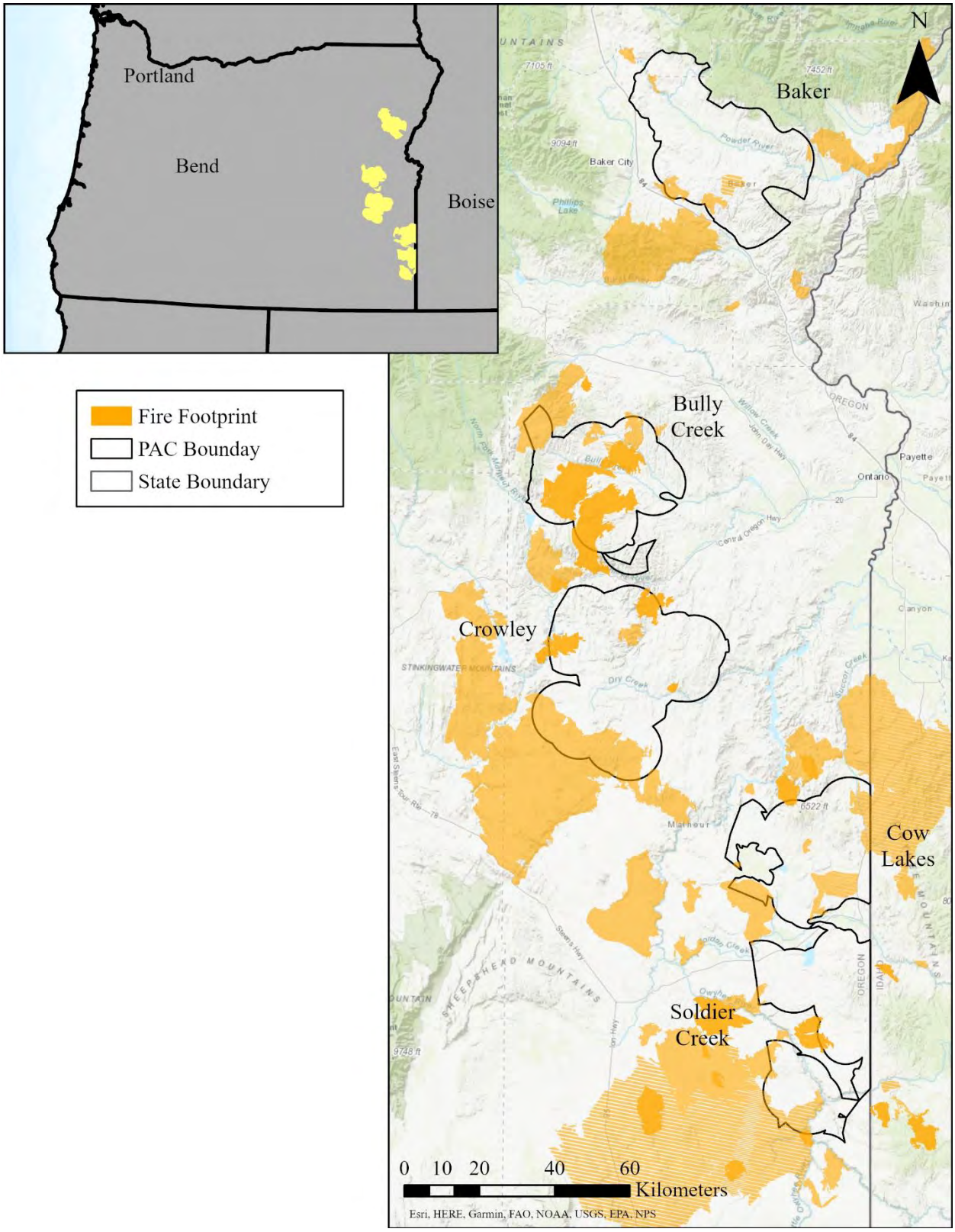

Figure 1. Map of sage-grouse Priority Areas of Conservation (PACs) in Baker and Malheur Counties, OR, USA. Orange polygons represent fire footprints between 2006 and 2020.

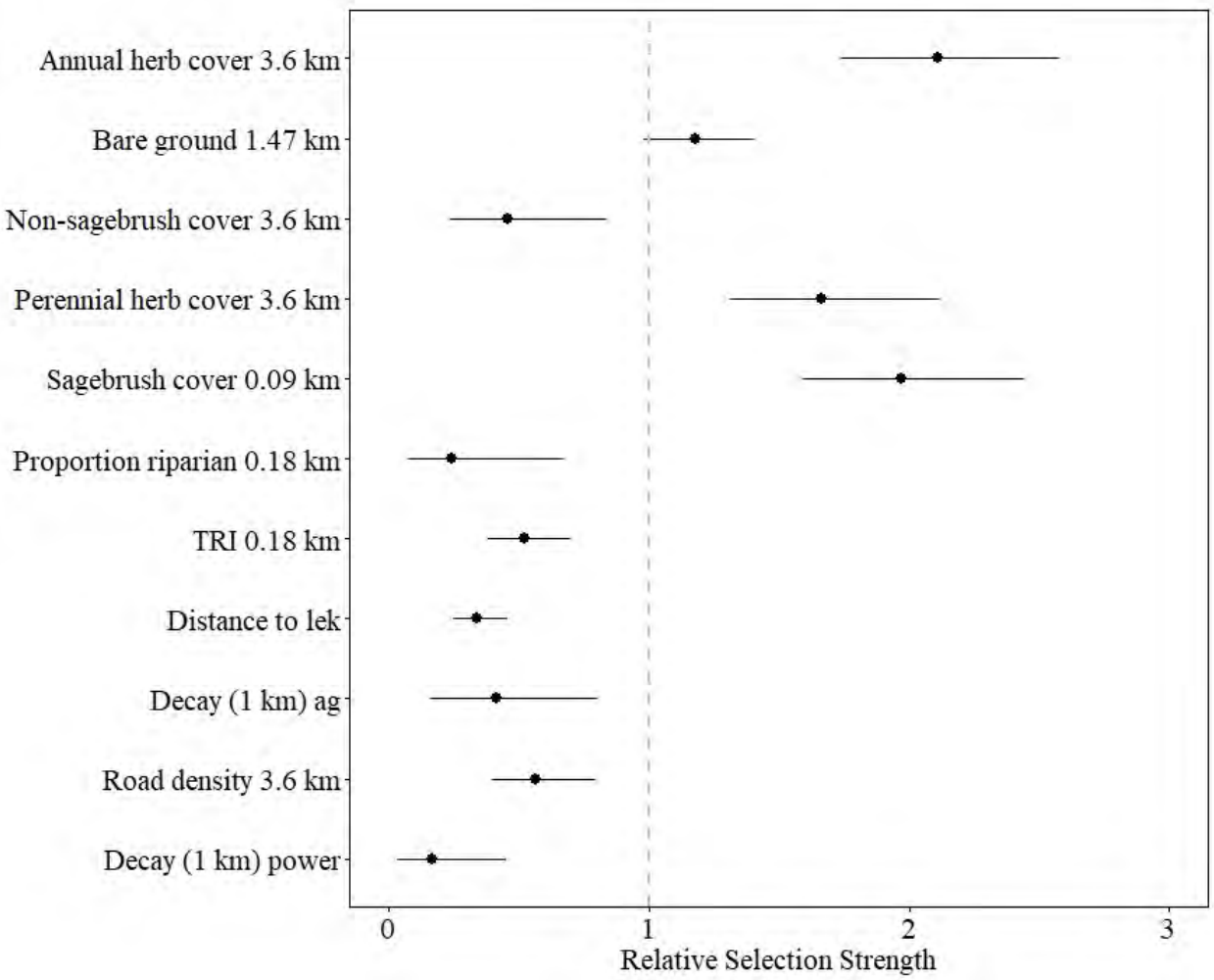

Figure 2. Estimated relative selection strength (RSS) and 95% confidence intervals of variables from the base resource selection function (RSF) model for sage-grouse nest site selection. RSS >1 indicate a positive effect on nest-site selection and RSS <1 indicate a negative effect. Data collected in Baker and Malheur Counties, Oregon, USA (2018–2022).

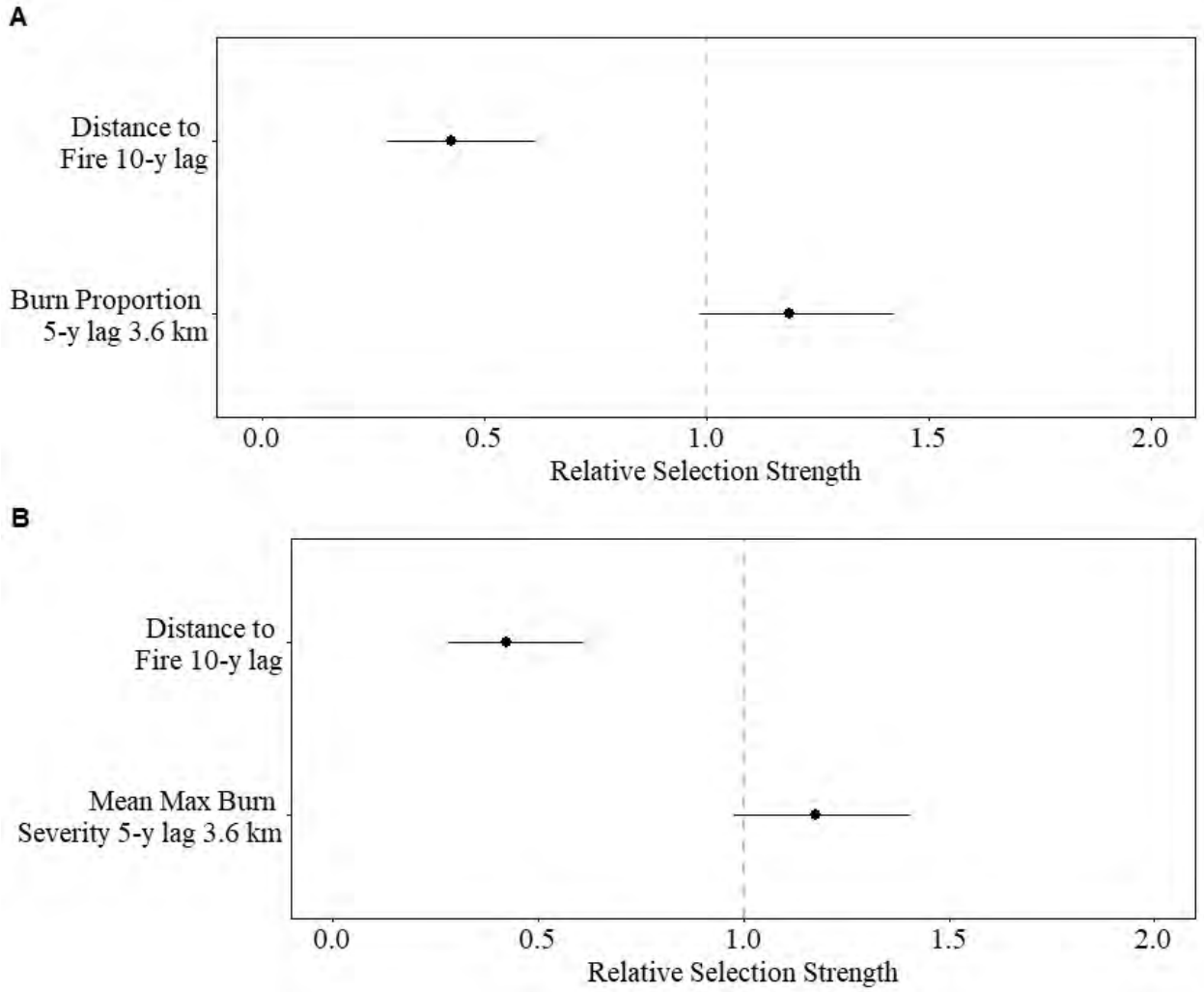

Figure 3. Estimated relative selection strength (RSS) and 85% confidence intervals for fire variables from top AIC-selected RSF (A) and second AIC-selected RSF (B). RSS >1 indicate a positive effect on nest-site selection and RSS <1 indicate a negative effect. Data collected in Baker and Malheur Counties, Oregon, USA (2018–2022).

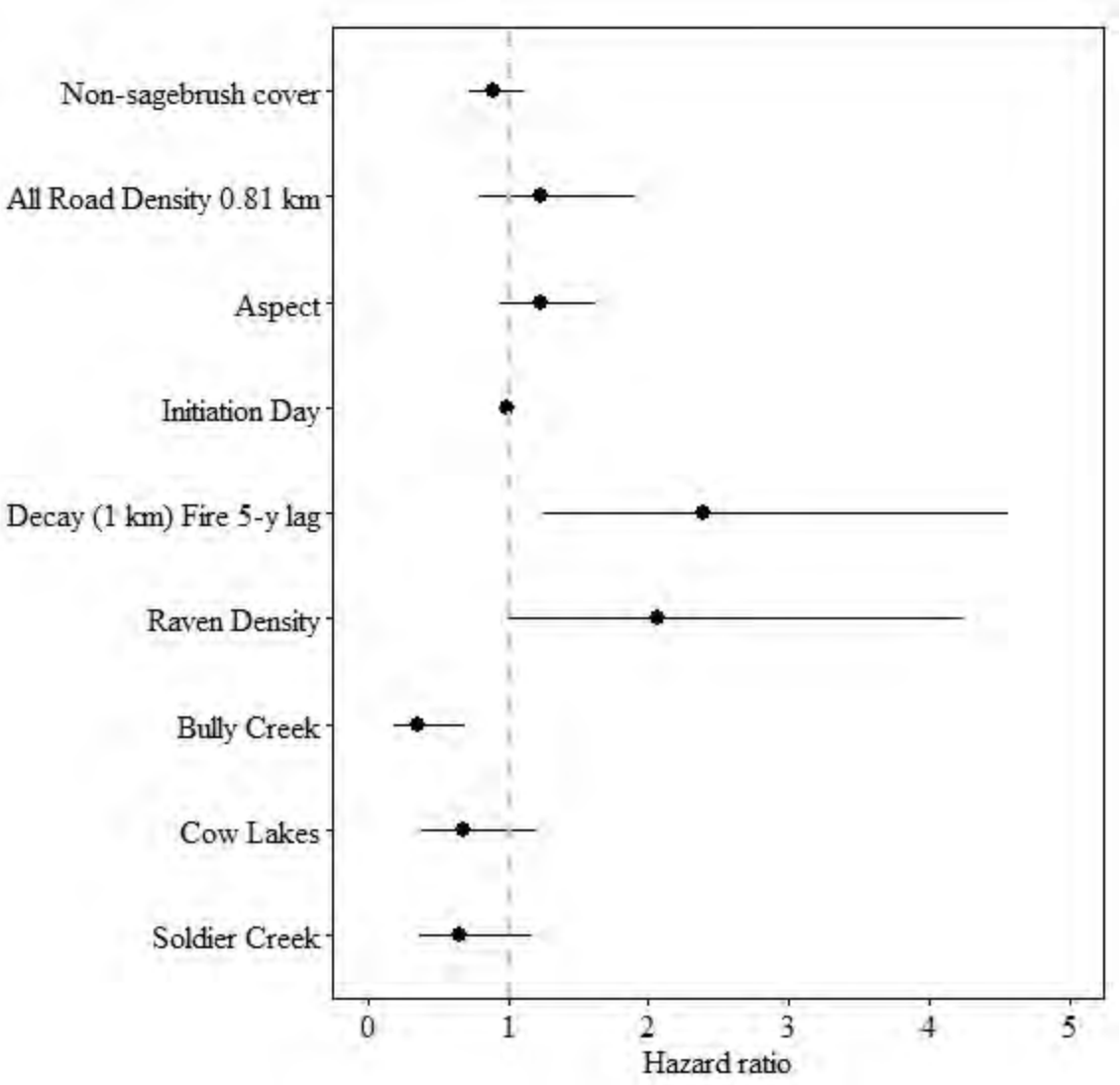

Figure 4. Estimated hazard ratios and 95% confidence intervals for variables in the second AIC-selected CoxPH model of sage-grouse nest survival. Values >1 indicate variables that decrease nest survival and values <1 indicate variables that increase nest survival. Study area hazard ratios were in reference to the Baker PAC. Data collected in Baker and Malheur Counties, Oregon, USA (2018–2022).

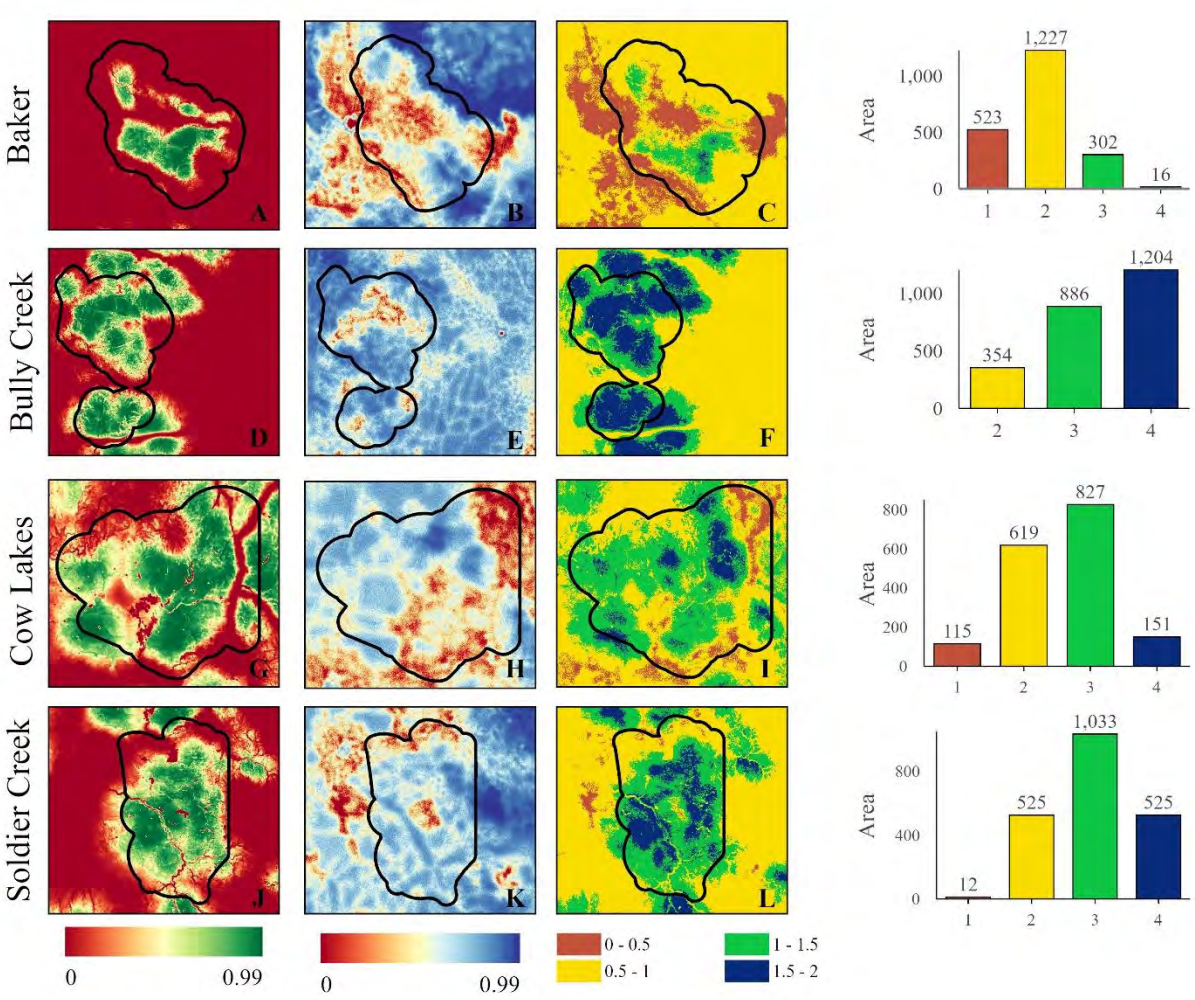

Figure 5: Predicted surfaces from top ΔAIC_c-selected resource selection functions for sage-grouse nest site selection (A, D, G, J), Cox proportional hazards model for nest survival (B, E, H, K), source/sink habitat maps for nest survival, and cumulative area of source/sink habitat (km^2) for the Baker, Bully Creek, Cow Lakes, and Soldier Creek PACs, Baker and Malheur Counties, OR, USA (2018–2022). PAC boundaries include 3.6 km buffer used for resource selection functions. For source/sink habitat maps, values near 0 indicate low RSS, low survival; values near 1 indicate high RSS, low survival or low RSS, high survival; values near 2 indicate high RSS, high survival. Data collected in Baker and Malheur Counties, Oregon, USA (2018–2022).

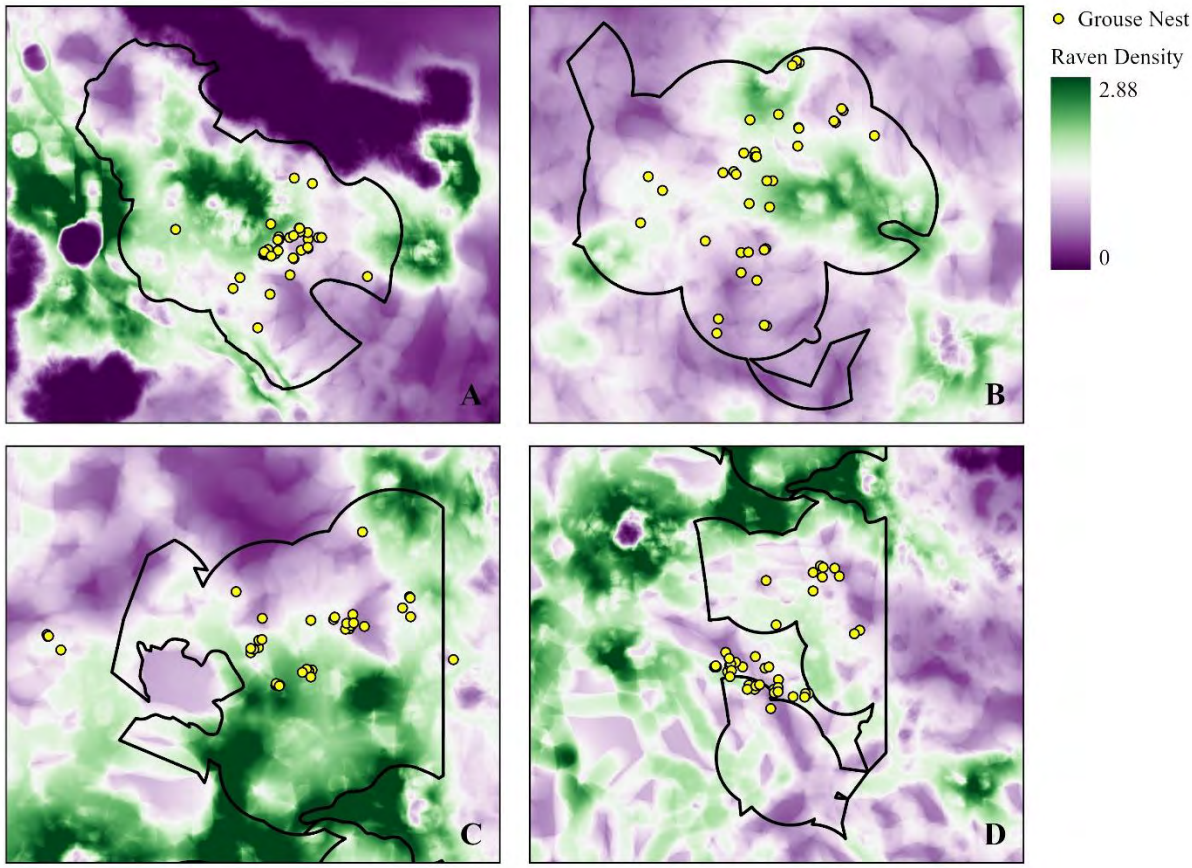

Figure 6. Predicted relative raven densities from (Chapter 1) and sage-grouse nests in the Baker (A), Bully Creek (B), Cow Lakes (C), and Soldier Creek (D) PACs in Baker and Malheur Counties, OR, USA (2018–2022). Data collected in Baker and Malheur Counties, Oregon, USA (2018–2022).

Table 1. Spatial predictor variables used for sage-grouse nest site selection and nest survival. Data collected in Baker and Malheur Counties, Oregon, 2018–2022).

Predictor Variable	Abbreviation	Year(s)	Data Source(s)
Annual herbaceous vegetation Bare ground Perennial herbaceous vegetation Non-sagebrush Sagebrush Total shrub Tree	Annual Bare Per Nonsage Sage Shrub Tree	2016 – 2021	Rangeland Condition Monitoring Assessment and Projection (RCMAP) (Rigge et al. 2021)
Topographic ruggedness index Topographic positioning index Elevation	TRI TPI Elevation	2021	Derived from 10 m Digital Elevation Model (DEM) (USGS 2021)
Distance to fire Proportion of area burned Mean burn severity	DIST_FIRE_Xy[a] BurnPropXy[a] BurnSevXy[a]	1996 – 2021	Derived from difference Normalized Burn Ratios (dNBR) from Monitoring Trends in Burn Severity (MTBS 2022)
Distance to lek	DIST_LEK	2016 – 2022	Oregon Department of Fish and Wildlife (ODFW 2022) Idaho Department of Fish and Game (IDFG 2002)
Density of primary roads Density of all roads	RoadsPrimary RoadsAll	2019, 2022	Oregon Department of Transportation (ODOT 2019) Idaho Transportation Department (ITD 2022)
Distance to landfill Distance to transmission line	DIST_LANDFILL DIST_POWER	2022	Homeland Infrastructure Foundation-Level Data (HIFLD 2022)
Distance to agriculture Proportion of agriculture	DIST_AG Ag	2016, 2017	National Land Cover Database (Dewitz 2019) Cropland Data Layer (USDA 2017)

[a]X in fire variables is equal to 20, 10, or 5 to indicate time lag.

Table 2. Informative variables used in backward selection to create base nest-site selection and nest survival models. Data collected in Baker and Malheur Counties, Oregon, (2018–2022).

Nest-site selection	Nest survival
$Annual_{3.6}$	$Nonsage_{1.47}$
$Bare_{1.47}$	$Riparian_{1.47}$
$Nonsage_{3.6}$	$Shrub_{0.57}$
$Per_{3.6}$	$TRI_{0.81}$
$Sage_{0.09}$	$DIST\_AG_{Euclid}$
$Riparian_{0.18}$	$RoadsAll_{0.81}$
$TRI_{0.18}$	Aspect
Elevation	Initiation day
$RoadsAll_{3.6}$	
$DIST\_LEK_{Euclid}$	

Subcripts indicate spatial scale or distance equation.

Table 3. Model selection rankings for resource selection models with additive and interactive terms of fire and raven density on sage-grouse nest site selection. All models contain the base nest-site selection model. Data collected in Baker and Malheur Counties, Oregon, (2018–2022).

Model (includes base model)	K	AIC_c	ΔAIC_c	w_i
$DIST\_FIRE\_10y_{Euclid}$ + $BurnProp5y_{3.6}$	14	1019.72	0.00	0.26
$DIST\_FIRE\_10y_{Euclid}$ + $BurnSev5y_{3.6}$	14	1020.05	0.33	0.22
$DIST\_FIRE\_10y_{Euclid}$	13	1020.96	1.24	0.14
$DIST\_FIRE\_10y_{Euclid}$ + $BurnProp5y_{3.6}$ + Raven	15	1021.40	1.68	0.11
$DIST\_FIRE\_10y_{Euclid}$ + $BurnSev5y_{3.6}$ + Raven	15	1021.75	2.03	0.09
$DIST\_FIRE\_10y_{Euclid}$ + Raven	14	1022.63	2.91	0.06
$DIST\_FIRE\_10y_{Euclid}$ + $BurnProp5y_{3.6}$*Raven	16	1022.84	3.12	0.05
$DIST\_FIRE\_10y_{Euclid}$ + $BurnSev5y_{3.6}$*Raven	16	1023.00	3.28	0.05
$DIST\_FIRE\_10y_{Euclid}$* Raven	15	1024.51	4.79	0.02
$BurnProp5y_{3.6}$*Raven	15	1039.62	19.90	0.00
$BurnSev5y_{3.6}$*Raven	15	1039.87	20.15	0.00
$BurnProp5y_{3.6}$ + Raven	14	1040.22	20.50	0.00
$BurnSev5y_{3.}$6 + Raven	14	1040.94	21.22	0.00
$BurnProp5y_{3.6}$	13	1042.31	22.59	0.00
$BurnSev5y_{3.6}$	13	1042.95	23.23	0.00
Raven	13	1046.19	26.47	0.00
Base	12	1049.36	29.64	0.00
Null	1	1356.95	337.22	0.00

Table 4. Model selection rankings for Cox proportional hazards (CoxPH) models with additive and interactive terms of fire and raven density on sage-grouse nest survival. All models contain the base nest survival model. Baker and Malheur Counties, Oregon, (2018–2022).

Model (includes base model)	K	AIC_c	ΔAIC_c	w_i
DECAY_FIRE_5y$_{\text{-1 km}}$ + Raven	9	997.43	0.00	0.20
DECAY_FIRE_5y$_{\text{-0.5 km}}$ + Raven	9	997.45	0.03	0.20
DECAY_FIRE_5y$_{\text{-2 km}}$ + Raven	9	998.56	1.14	0.11
DECAY_FIRE_5y$_{\text{-1 km}}$	8	999.16	1.73	0.08
DECAY_FIRE_5y$_{\text{-2 km}}$	8	999.31	1.89	0.08
DECAY_FIRE_5y$_{\text{-0.5 km}}$ * Raven	10	999.65	2.22	0.07
DECAY_FIRE_5y$_{\text{-1 km}}$ * Raven	10	999.69	2.26	0.06
DECAY_FIRE_5y$_{\text{-0.5 km}}$	8	1000.11	2.68	0.05
DECAY_FIRE_5y$_{\text{-5 km}}$ + Raven	9	1000.74	3.31	0.04
DECAY_FIRE_5y$_{\text{-2 km}}$ * Raven	10	1000.80	3.38	0.04
DECAY_FIRE_5y$_{\text{-5 km}}$	8	1001.01	3.58	0.03
Raven	8	1001.94	4.51	0.02
DECAY_FIRE_5y$_{\text{-5 km}}$ * Raven	10	1003.00	5.57	0.01
Base	7	1003.90	6.47	0.01
Null	0	1013.97	16.54	0.00

Table 5. Results of proportional hazards tests on the base and top five AIC-selected nest survival models. Baker and Malheur Counties, Oregon, (2018–2022).

Model	χ^2	df	p
DECAY_FIRE_5y$_{\text{-1 km}}$ + Raven	7.73	9	0.56
DECAY_FIRE_5y$_{\text{-0.5 km}}$ + Raven	7.25	9	0.61
DECAY_FIRE_5y$_{\text{-2 km}}$ + Raven	9.09	9	0.43
DECAY_FIRE_5y$_{\text{-1 km}}$	8.11	8	0.42
DECAY_FIRE_5y$_{\text{-2 km}}$	9.37	8	0.31
Base	8.18	7	0.32

CHAPTER 4 - LANDSCAPE CONFIGURATION IMPACTS SPACE USE AND SURVIVAL OF FEMALE SAGE-GROUSE

ABSTRACT

Composition and configuration of landscapes are essential factors for species distribution and persistence. Disturbance changes landscapes and can impact movement and space use of individuals based on species mobility with tradeoffs between resource acquisition and survival. We examined the effects of composition and configuration of habitat and disturbance on space use (neighborhood size) and survival of adult female sage-grouse during the breeding season using linear and Cox proportional hazards mixed models. Spring neighborhood size decreased as the proportion of non-sagebrush and sagebrush cover increased, but the rate was dependent on the configuration of each cover class. Spring neighborhood size varied as the proportion of anthropogenic footprint increased (e.g., roads, agriculture, exurban development, power distribution), with smaller neighborhoods associated with high interspersion and large neighborhoods associated with low interspersion. Sage-grouse survival was negatively affected by the increasing proportion of anthropogenic cover, regardless of configuration. Sage-grouse survival decreased as interspersion and proportion of juniper cover increased. We also found that females that spent more time on nest had smaller spring neighborhood sizes and were more likely to survive. Our results indicate potential restriction of female sage-grouse to small patches of contiguous habitat (sagebrush, non-sagebrush shrub, and grassland) in multi-use human-altered landscapes with consequences on spring survival.

INTRODUCTION

Human-caused habitat loss and fragmentation are the among the leading drivers of biodiversity loss worldwide (Pimm et al. 2014, Haddad et al. 2015). Landscape composition and configuration are the result of the processes of habitat loss and configuration (Fahrig 2003, Lindenmayer and Fischer 2007, Villard and Metzger 2014, Hadley and Betts 2016) and are essential factors for species distribution and (meta)population persistence (Hanksi 1999, Niebuhr et al. 2015). Alterations to landscapes can cause changes in animal behavior (Baguette and Van Dyck 2007), movement (Laforge et al. 2021), habitat selection (Hins et al. 2009), reproduction (Horn et al. 2005, Kramer et al. 2019), and survival (Robinson 2018).

Movement and space use responses to landscape change vary by species and individual (Niebuhr et al. 2015, Martin and Fahrig 2016). Individuals may increase movement and thereby space use, in fragmented landscapes to acquire resources in multiple patches. For example, in eastern Australia, Gardiner et al. (2019) found that the home ranges of eastern bettongs (*Bettongia gaimardi*), a woodland specialist marsupial, were larger when their habitat was more disaggregated. Alternatively, individuals may restrict space use to patches of preferred habitat. For instance, Bevanda et al. (2015) found that home range sizes of roe deer (*Capreolus capreolus*) decreased as the landscape became patchier. Each strategy has tradeoffs and depends on the individual's mobility (Wiegand et al. 2005, Niebuhr et al. 2015). Augmenting movement or home range size may increase survival or reproductive success through access to additional or higher-quality resources. However, it may also have consequences by increasing energy costs and exposure to predation (Wiegand et al.

2005, Niebuhr et al. 2015). Condensing space use may limit the mortality risk associated with movement, but the individual may incur other fitness costs from a reduced amount or quality of resources (Wiegand et al. 2005, Niebuhr et al. 2015).

The sagebrush (*Artemisia* spp.) biome is one of the most imperiled environments in western North America. Threats to it include land conversion, resource extraction, historical overgrazing, juniper expansion, invasion of non-native grasses, and wildfire (Doherty et al. 2022). Wildfire and invasive annual grasses have driven landscape changes in the Great Basin over the last four decades (Smith et al. 2022). Increased frequency and severity of wildfire has burned approximately 90,000 km^2 between 1984 and 2020 (Miller et al. 2011, Doherty et al. 2022, Crist et al. 2023) while exotic annual grasses, like cheatgrass (*Bromus tectorum*), have increased by eight-fold since 1990, now dominating nearly 77,000 km^2 of the Great Basin (Smith et al. 2022). State transitions of sagebrush to other vegetation types due to wildfire and exotic annual grass invasion have altered habitat quality for sagebrush-obligate species like greater sage-grouse (*Centrocercus urophasianus*, hereafter sage-grouse; Coates et al. 2016, O'Neil et al. 2020).

Loss of sagebrush after European settlement has reduced the amount of potential sage-grouse habitat by ~44% (Schroeder et al. 2004, Doherty et al. 2016). Due to population declines resulting from this range reduction, the sage-grouse is listed as endangered in Canada and was nearly listed under the U. S. Endangered Species Act (Lungle and Pruss 2008, USFWS 2015). Sage-grouse generally exhibit high annual and overwinter survival rates, with most mortalities occurring during the spring, summer, and fall (Moynahan et al. 2006, Connelly et al. 2011, Blomberg et al.

2013a, Dinkins et al. 2017). Adult and yearling (second year) female survival has been identified as a critical vital rate driving population growth for sage-grouse (Taylor et al. 2012, Dahlgren et al. 2016). Landscape factors associated with reduced female survival include juniper expansion (Dinkins et al. 2014a, Coates et al. 2017, Prochazka et al. 2017, Severson et al. 2017) and wildfire (Foster et al. 2019, Tyrrell et al. 2023). Results vary on the effect of anthropogenic disturbance on yearling and adult female survival (Holloran et al. 2010, Dinkins et al. 2014a, Kirol et al. 2015, LeBeau et al. 2017, Pratt and Beck 2021, Coates et al. 2023). In Wyoming, yearling and adult female survival was negatively associated with natural gas development (Holloran et al. 2010), disturbance from major roads and proximity to minor roads (Pratt and Beck 2021), and proximity to powerlines (Dinkins et al. 2014a), while in Idaho survival was negatively associated with geothermal power infrastructure (Coates et al. 2023). However, female survival was positively associated with proximity to anthropogenic edge habitat (Kirol et al. 2015) and road density (Dinkins et al. 2014a) and was not impacted by wind energy infrastructure (LeBeau et al. 2017).

Due to complex movements between seasonal habitats, individual seasonal home ranges can be hard to identify for sage-grouse. Some individuals are year-round residents, others exhibit partial migration, moving between two or more seasonal habitats (Crawford et al. 2004, Connelly et al. 2011, Dinkins et al. 2017, Pratt et al. 2019). Because of this, some sage-grouse may not exhibit range residency within seasonal habitats, making reliable seasonal home range estimation difficult (Calabrese et al. 2016). However, long-distance movements during the breeding season have

been linked to decreased survival (Cross et al. 2017, Ebenhoch et al. 2019), and increased space use during the breeding season was linked to higher corticosterone concentrations (Rabon et al. 2021). Research on how differences in habitat composition and configuration affect female space use and survival during the breeding season is limited. We investigated how composition and configuration of disturbance may influence the amount of area (hereafter, neighborhood) adult female sage-grouse use during the breeding season and potential consequences on survival across six-years (2017–2022) in Baker and Malheur counties, Oregon, USA. We expected neighborhood size and survival to vary based on not just the composition but also the configuration of disturbance (i.e., anthropogenic, invasive annual grass, wildfire). Potential survival consequences from space use related to composition and configuration directly affect habitat management for sage-grouse.

STUDY AREA

We selected our study areas from Oregon sage-grouse Priority Areas of Conservation (PACs) (Figure 1). The Baker, Bully Creek, Crowley, Cow Lakes, and Soldier Creek PACs were selected due to concerns regarding local population declines and significant wildfire activity in the last 20 years. Priority Areas of Conservation were created by the Oregon Department of Fish and Wildlife (ODFW) in 2011 using lek counts and telemetry data to determine areas of high sage-grouse density, seasonal habitats, including winter range, and connectivity corridors (Hagen 2011b, USFWS 2015).

The Baker PAC was located 5 km east of Baker City, in Baker County, OR (44°47'N, 117°49'W) with an area of 1,362 km^2. The Bully Creek, Cow Lakes, Crowley, and Soldier Creek PACs were located in Malheur County, OR. The Bully Creek and Crowley PACs were located 4.1 km northeast (43°51'N, 117°36'W) and 2.5 km south (43°44'N, 118°04'W) of Juntura, OR, respectively. The Bully Creek PAC encompassed an area of 1,133 km^2, while the Crowley PAC had an area of 1,760 km^2. The Cow Lakes and Soldier Creek PACs were located 5.5 km north (42°58'N, 117°03'W) and 3.5 km southwest (43°55'N, 117°07'W) of Jordan Valley, OR, respectively. Cow Lakes had an area of 1,010 km^2, while Soldier Creek encompassed an area of 1,195 km^2. The elevation among the five PACs ranged from 780 m to 1,855 m, with annual average temperatures between -9° C in January to 34° C in July. The average annual rain and snowfall ranged from 25.7 to 34 cm and 47 to 93 cm, respectively. Land ownership varied among the five PACS, with Crowley and Soldier Creek each comprised of ~92% public and ~8% privately owned land, Bully Creek and Cow Lakes PACs each contained ~75% public and ~25% privately owned, and the Baker PAC was ~34% public and ~66% privately owned land.

The dominant overstory vegetation in all of the PACs was Wyoming big sagebrush (*A. tridentata wyomingensis*), low sagebrush (*A. arbuscula*), stiff sagebrush (*A. rigida*), and a small proportion of mountain big sagebrush (*A. t. vaseyana*) at higher elevations. Native understory vegetation consisted of common forbs (*Lupinus, Crepis,* and *Lomatium* spp.) and native bunchgrasses such as bluebunch wheatgrass (*Pseudoroegneria spicata*), giant wildrye (*Leymus cinereus*), Idaho fescue (*Festuca idahoensis*), and Sandberg's bluegrass (*Poa secunda*). Cheatgrass and medusahead

were widespread along with other invasive vegetation such as ventenata (*Ventenata dubia*), crested wheatgrass (*Agropyron cristatum*), Russian thistle (*Kali tragus*), and perennial pepperweed (*Lepidium latifolium*).

Wildfire activity varied among our chosen PACs. The Baker PAC had the lowest burned area, with four large fires (>4 km^2) impacting 64 km^2 (4.7%) of the PAC between 2006 and 2014. However, the Baker sage-grouse population is geographically and genetically isolated due to a population decline in 2014, which it has yet to recover from (Vold 2023). The Soldier Creek PAC had sixteen fires that burned 76 km^2 (6.3%) in the PAC and 2,103 km^2 adjacent to the PAC between 2007 and 2019. The sage-grouse population in the Soldier Creek PAC has remained relatively stable since 2012. The Cow Lakes PAC was impacted by eleven large fires between 2007 and 2020, burning 207 km^2 (20.5%) in the PAC and 1,171 km^2 adjacent to the PAC. Sage-grouse populations were largely stable between 1993 and 2016 but began declining in 2017, reaching a low in 2018 that prompted direct management action by the Bureau of Land Management (BLM) (BLM 2019, Vold 2023). Lastly, the Bully Creek PAC was impacted by eight major fires between 2006 and 2020, burning 455 km^2 (39.2%) of the PAC and another 328 km^2 adjacent to the PAC. The Bully Creek sage-grouse population has remained relatively stable since 2011.

METHODS

Capture and Monitoring

Using a standard spotlight and hoop net technique, we captured female sage-grouse on foot at night (Giesen et al. 1982, Wakkinen et al. 1992). Beginning in 2017, individuals were primarily captured during the spring lekking season (March–May) and late summer (late-July–August), with occasional captures in the winter (November–February). Upon capture, we determined the age of each individual based on primary feather molt as either a yearling (first breeding season) or adult (Braun and Schroeder 2015). We marked all individuals with an Oregon Department of Fish and Wildlife (ODFW) aluminum leg band and one of the following transmitters: 1) 22 g rump-mounted ARGOS/GPS Solar PTT-100 (Microwave Telemetry Inc., Columbia, MD 21045 USA), 2) A RI-2DM 22 g VHF necklace (Holohil Systems Ltd., Carp, Ontario, Canada) with a PinPoint-75 Avian GPS store-on-board (SOB) 4.1 g tags or PinPoint-120 Avian GPS SOB 4.8 g tags (Lotek Wireless Inc., St. John's, NL A1A 5C6 Canada) with a total weight between 26.1 and 26.8 g, or 3) a Holohil VHF necklace with an attached 5.6 g Pica solar-powered GPS logger capable of remote download with base stations (Ecotone Telemetry, Gdynia, Poland) with a total weight of 27.6 g. Argos PTT units recorded five locations/day from 1 March through 31 October and two locations/day from 1 November to 28/29 February. Ecotone units recorded six locations/day year-round, which were remotely downloaded with handheld base stations when birds were ground-tracked. Lotek units recorded two (PinPoint-75) or three (PinPoint-120) locations/day for one year, and then individuals were recaptured to retrieve data and affix a new SOB unit.

We tracked Argos PTT marked individuals via downloaded locations. We located individuals marked with VHF/Lotek and VHF/Ecotone units weekly from mid-April through late-July during the breeding season using VHF receivers (Communications Specialists, R-1000, Orange, CA, USA) and 3-way antennas (Communications Specialists, Orange, CA, USA). These individuals were monitored monthly by air for the rest of the year. VHF necklaces were equipped with a mortality switch that doubled the beats per minute (bpm) when the unit was stationary for more than eight hours. Once this mortality signal was heard, transmitters were recovered as soon as possible. To minimize disturbance to nesting females, individuals marked with Argos PTT units were only investigated for mortalities between 1 April and 30 June if downloaded data indicated no movement for >30 days, but were recovered as soon as possible the rest of the year if downloaded data indicated no movement for more than three days. The mortality date for all individuals was recorded from GPS data as the first day movement ceased.

Land cover and fire variables

We compiled land cover data from 30 x 30 m LANDFIRE 2020 Existing Vegetation (LANDFIRE 2020). We condensed land cover types to seven cover classes associated with breeding season habitat selection and survival of female sage-grouse: anthropogenic, invasive, juniper, matrix, non-juniper tree cover, other, and sagebrush. The anthropogenic cover class included all agriculture, all development (low, medium, and high intensity) and road cover types. The invasive cover class represented all cover types of annual and perennial invasive vegetation. Juniper

represented all juniper and juniper-pinyon cover types, while non-juniper cover represented all other forest and woodland cover classes. Non-sagebrush cover consisted of grassland, non-sagebrush shrubland, riparian areas, and natural bare ground (e.g., volcanic rock, cliffs, badlands) present within our study areas. The sagebrush cover class was comprised of all big, low, and silver sagebrush cover types. All remaining cover types were classified as other.

Differenced normalized burn ratio (dNBR) rasters of wildfires >4 km^2 that occurred between 2006 and 2020 were obtained from Monitoring Trends in Burn Severity (MTBS) for all fires occurring within and adjacent to our study areas (MTBS 2023). We quantified the proportion of burned area at 5- and 10-year lags by reclassifying dNBR so that all burn severity values of 1, 2, 3, and 4 were set to 1, and all other values were set to 0. Fire variables were temporally aligned; for example, space use and survival data from 2017 were given values from fire data for 5- and 10-year lags from 2011–2016 and 2006–2016, respectively.

Estimating Neighborhoods

Annual breeding season neighborhoods were identified for each female sage-grouse between 1 March and 30 June. This period encompasses lekking, nesting, and early brood-rearing in Oregon (Hagen 2011). Individuals needed to have >30 days of recorded data during this period to be included in the data set. A new neighborhood was created every year for individuals who survived for multiple seasons. All data recorded within 24 hours after capture was removed before analysis to eliminate

capture-induced movements. Apparent movements from winter habitat to breeding grounds or from breeding grounds to summer habitat were removed prior to analysis.

We quantified breeding season neighborhoods with 100% minimum convex polygons (MCPs) in ArcGIS Pro 3.2.0 (Esri Inc., 2013, Redlands, California, USA). We chose MCPs because kernel density estimators created disjointed polygons for most individuals, whereas MCPs provided a single, contiguous landscape that was specific and available for each individual (Hins et al. 2009, Robinson 2018).

Landcover quantification

We used the package 'landscapemetrics' version 2.0.0 (Hesselbarth et al. 2019) in R version 4.2.2 (R Core Team 2022) to calculate our habitat amount and fragmentation variables at the cover class scale. To quantify the composition of each sage-grouse neighborhood, we created proportion variables for each of our seven land cover classes by dividing the area of each neighborhood by the total area of each cover class present. If a land cover class was absent, the proportion was recorded as 0. We quantified the configuration of each cover class with the Clumpiness Index and the Interspersion and Juxtaposition Index (IJI). Clumpiness is a class-specific metric that uses cell adjacencies to calculate aggregation, or clumpiness, of the target land cover or fire class. It scales between -1 and 1, with -1 representing complete disaggregation of a cover class, 0 representing a random configuration, and 1 representing total aggregation (Figure 2; McGarigal et al. 2023). Clumpiness was recorded as not applicable (NA) if a cover type was absent. IJI is an aggregation metric that describes the intermixing of classes. IJI is reported as a percentage, and measures the ratio

between the amount of edge of the target cover class and the number of bordering cover classes relative to that same ratio for all other cover classes present in the landscape (Figure 2; McGarigal et al. 2023). Values close to 0 indicate that the target cover class is only adjacent to a single other class and approaches 100 when the target class is equally adjacent to all other classes present. IJI requires ≥3 cover classes, so it was not calculated for fire variables.

Modeling strategy

We wanted to assess if configuration effects differed as the amount of disturbance or habitat varied. Therefore, configuration metrics were only evaluated as interactions with proportion variables (Trzcinski et al. 1999, Hadley and Betts 2016). For our neighborhood size and survival analyses, we first selected the best fitting landscape metric (proportion only, proportion × clumpiness, or proportion × IJI) for each cover class using Akaike's Information Criterion corrected for small sample sizes (AIC_c). We also evaluated age (yearling or adult), year, study area, transmitter type, and proportion of time spent on nest. Variables or interactions for each cover class with the lowest AIC_c, and those within $\Delta 2$ AIC_c, were deemed informative and moved forward if an 85% confidence interval did not overlap zero (Arnold 2010). We then evaluated all possible combinations of informative variables using AIC_c. All continuous variables were z-standardized, so model coefficients were directly comparable. To account for individuals represented in multiple years, we included a random effect of Hen ID in both neighborhood size and survival analyses.

Neighborhood composition and adult survival

We used linear mixed models (lmm) to assess how habitat composition and configuration affected log-transformed neighborhood area (km^2) (Hinam and St. Clair 2008, LaForge et al. 2021). We evaluated cumulative 121-day spring breeding season adult survival using mixed effects Cox proportional hazards (CoxPH) models (Cox 1972) using the "survival" v 3.5.5 and "coxme" v 2.2-18.1 packages (Therneau 2023). This time-to-event survival model assesses the probability of an event occurring, in this case, mortality. CoxPH models produce hazard ratios (H.R.s) with values <1 indicating the variable increases survival and >1 indicating the variable reduces survival. We used chi-squared tests and the Schoenfeld residual scores for each variable and the final model to ensure they did not violate the proportional hazards assumption.

RESULTS

We captured and GPS-marked 115 female sage-grouse between 2017 and 2022. We marked 56 individuals with Argos PTT units, 33 with Lotek SOB units, and 26 with Ecotone SOB units. There were 76 individuals with at least 30 days of recorded data between 1 March and 30 June. The mean number of locations per neighborhood was 372.17 (range = 75–723). The mean neighborhood size was 38.34 km^2 (range = 0.37 – 242.96 km^2).

Neighborhood composition and configuration

After variable selection, we were left with interactions between proportion of anthropogenic footprint and IJI, proportion of non-sagebrush cover and IJI, proportion of other cover and IJI, proportion of sagebrush cover and IJI, proportion of burned with a five-year lag and clumpy, and proportion of time spent on nest. The model including only the five interactions and the full model were removed from consideration due to multicollinearity issues. The top ranked ΔAIC_c-selected model included interactions between the proportion of anthropogenic footprint and IJI, proportion of non-sagebrush cover and IJI, proportion of sagebrush and IJI, and proportion of time spent on nest (Table 1). The second ranked model was within $\Delta 2$ AIC_c of the top ranked model and contained the same three interactions without proportion of time spent on nest (Table 1). We only report results from the top ranked model since the second ranked model is nested within it. Spring neighborhood size decreased as the proportion of time spent on nest increased (Table 2; Figure 3). Neighborhood size varied depending on configuration as the proportion of anthropogenic footprint increased (Table 2; Figure 4). When anthropogenic footprint was well interspersed, neighborhood size decreased, but when the anthropogenic footprint was not interspersed, neighborhood size increased (Table 2; Figure 4). Spring neighborhood size decreased as the proportion of non-sagebrush cover increased, but at a slower rate when non-sagebrush cover was not highly interspersed (Table 2; Figure 5). Lastly, spring neighborhood size decreased as the proportion of sagebrush cover increased, but at slower rate when sagebrush cover was not highly interspersed (Table 2; Figure 6).

Female survival

After variable selection, we were left with proportion of anthropogenic footprint, the interaction between proportion of juniper cover and IJI, and proportion of time spent on nest. The top ΔAIC_c selected model was the full model which indicated that with every square kilometer increase in anthropogenic footprint, mortality risk increased by 31% (85% CI: 7–47%; Figure 7; Tables 3 and 4) regardless of configuration. Mortality risk varied with the proportion and configuration of juniper cover (Figure 7, Table 4), and females that spent more time on nest had an 37% reduction in mortality risk (85% CI: 14–94%). Our final model and all variables within upheld the proportional hazards assumption (Table 5).

DISCUSSION

Our results demonstrate that spring neighborhood size and survival were associated with the amount and configuration of disturbance on the landscape. The anthropogenic footprint present within sage-grouse neighborhoods affected both space use and survival. Neighborhood size decreased when the anthropogenic footprint was well interspersed and increased when the footprint was dispersed. A highly interspersed anthropogenic footprint likely corresponded to road networks, transmission or distribution lines, resource extraction infrastructure, or small parcels of agriculture that were spread out within a neighborhood (more edge) whereas a low interspersed footprint corresponded to a reduced human footprint with less edge along multiple cover classes within the neighborhood. The smaller neighborhood sizes in

our study provide evidence that sage-grouse were avoiding human disturbance by remaining in smaller areas of habitat rather than moving through or around disturbed areas. Avoidance of anthropogenic structures and disturbance has been documented in oil and gas fields in Wyoming (Dinkins et al. 2014b, Fedy et al. 2015) and Colorado (Walker 2022), geothermal energy infrastructure in Nevada (Coates et al. 2023), and in multi-use landscapes in Oregon (Chapter 2). Additionally, Bush et al. (2011), found that agricultural areas in Saskatchewan were barriers to dispersal for both males and females during the spring breeding season. Spring female survival decreased as the proportion of anthropogenic footprint increased, regardless of configuration (Figure 7). This is contrary to findings by Kirol et al. (2015) who found that female survival increased at closer proximities to anthropogenic edge (infrastructure sites and roads), and Dinkins et al. (2014a) who found that female survival was positively associated with road density. Our anthropogenic category was broad, encompassing development at all intensities, agriculture (cropland, pastures, orchards, vineyards), and roads; therefore, we may not have captured potential positive relationships to specific types of human disturbance.

Consistent with current literature, pinyon-juniper cover negatively affected spring female survival (Coates et al. 2017, Prochazka et al. 2017, Severson et al. 2017). Our results provide evidence that female survival decreases with increasing cover of juniper when it is highly interspersed. Low interspersion means that juniper cover is mainly isolated, with less edge, probably corresponding to older, more clustered trees, which sage-grouse avoid (Coates et al. 2017, Severson et al. 2017, Rabon 2020). High interspersion is characteristic of Phase I and Phase II juniper

stands (Miller et al. 2005). This configuration and age class is used by sage-grouse and associated with a higher risk of mortality (Coates et al. 2017, Prochazka et al. 2017, Rabon et al. 2020).

We did not find evidence that the proportion or configuration of wildfire influenced spring neighborhood sizes or survival. Foster et al. (2019), Dudley et al. (2022), and Tyrrell et al. (2023), found that female survival decreased in the first 1-2 years following a wildfire. Only one fire (202 km^2, 0.3%) burned in known sage-grouse breeding habitat in our study areas between 2017 and 2022, so survival consequences may have been minimal or not detected. Additionally, our fire variables were categorized at five- and ten-year lags which may reflect changes to habitat selection related to disturbance. Schuyler et al. (2022) found that female sage-grouse begin selecting for areas of lower burn severity and higher shrub cover five to seven years post-fire. Our results indicated that spring neighborhood sizes decreased as the cover of both non-sagebrush and sagebrush cover increased, but the rate varied depending on the configuration (Figures 5 and 6). This indicates that female sage-grouse may potentially be restricted to patches of intact sagebrush or non-sagebrush habitat within the mosaic of fire footprints. Additionally, our non-sagebrush cover variable included grassland which may have been confounded with our fire variables. We quantified burned area using data from MTBS which is also used by LANDFIRE to quantify vegetation changes due to fire disturbance. Grass is the first to recolonize burned areas in sagebrush ecosystems (Ellsworth et al. 2016); therefore, grassland cover may have reflected the existing vegetation type in burned areas.

We collected location data with three types of GPS transmitters which included backpack-style solar powered PTT units. Foster et al. (2018) and Severson et al. (2019) both found that these units reduced annual and seasonal survival for female sage-grouse when compared to individuals marked with necklace-style VHF radio transmitters. In light of this new information, we discontinued the use of PTTs after spring trapping in 2020. Our results indicated that transmitter type was not an informative predictor of female spring survival. However, individuals fitted with PTT units accounted for 58% (n=44) of our sample size so we may not have detected an effect.

Our results indicated female sage-grouse who spent more time on nest were more likely to survive the spring breeding season, which was contrary to findings from Blomberg et al. (2013b), Dinkins et al. (2014a), and Smith et al. (2018). These three studies addressed cumulative reproductive effort on summer survival of female sage-grouse, whereas ours assessed survival strictly during the spring and did not assess potential impacts on survival in subsequent seasons. Our proportion of time spent on nest variable was not used to address cumulative reproductive effort but rather accounted for reduced movement by females who spent more time incubating and therefore had smaller spring neighborhoods and potentially less exposure to predators in the spring.

Predation is the leading cause of sage-grouse mortality (Hagen 2011b, Blomberg et al. 2013b, Davis et al. 2014). However, there are no predators that specialize on sage-grouse, but several of the generalist avian and mammalian species that prey on sage-grouse are subsidized by humans, including coyotes (*Canis latrans*;

Manlick and Pauli 2020, Reed et al. 2023), red foxes (*Vulpes vulpes*; Manlick and Pauli 2020), and *Buteo* hawks (Chapter 2). Interspersion of the anthropogenic footprint within sage-grouse neighborhoods likely increases predation risk by both increasing predator abundance and facilitating access to previously unavailable areas. For example, some mammalian predators use linear right-of-ways, which can reduce landscape resistance to movement and therefore reduce energy costs when searching for prey (Latham et al. 2011). Additionally, infrastructure along with pinyon-juniper expansion provides perching and nesting sites for avian species in sagebrush ecosystems which have limited natural elevated substrates. Anthropogenic food subsidies (e.g., livestock, agricultural waste, high rodent populations) support higher densities of predators than the surrounding landscape (Oro et al. 2013). Habitat management for sage-grouse should continue defending and growing contiguous areas of sagebrush and removing juniper around spring breeding areas. However, management should also focus on mitigating anthropogenic alterations to the landscape to reduce the impacts of subsidized predators on sage-grouse and other species of conservation concern.

LITERATURE CITED

Arnold. T. 2010. Uninformative parameters and model selection using Akaike's Information Criterion. Journal of Wildlife Management 74:1175–1178.

Baguette, M., and H. Van Dyck. 2007. Landscape connectivity and animal behavior: functional grain as a key determinant for dispersal. Landscape Ecology 22:1117–1129.

Bevanda, M., E. A. Fronhofer, M. Heurich, J. Müller, and B. Reineking. 2015. Landscape configuration is a major determinant of home range size variation. Ecosphere 6:1–12.

Blomberg, E. J., D. Gibson, J. S. Sedinger, M. L. Casazza, and P. S. Coates. 2013a. Intraseasonal variation in survival and probable causes of mortality in greater sage-grouse *Centrocercus urophasianus*. Wildlife Biology 19:347–357.

Blomberg, E. J., J. S. Sendinger, D. V. Nonne, and M. T. Atamian. 2013b. Seasonal reproductive costs contribute to reduced survival of female greater sage-grouse. Journal of Avian Biology 44:149–158.

Braun, C. E., and M. A. Schroeder. 2015. Age and sex identification from wings of sage-grouse. Wildlife Society Bulletin 39:182–187.

Bureau of Land Management (BLM). 2019. Notice of availability of record of decision and approved resource management plan amendment for greater sage-grouse conservation, Wyoming. Federal Register 84:10322–10323.

Bush, K. L., C. K. Dyte, B. J. Moynahan, C. L. Aldridge, H. S. Sauls, A. M. Battazzo, B. L. Walker, K. E. Doherty, J. Tack, J. Carlson, D. Eslinger, J. Nicholson, M. S. Boyce, D. E. Naugle, C. A. Paszkowski, and D. W. Coltman. 2011. Population structure and genetic diversity of greater sage-grouse (*Centrocercus urophasianus*) in fragmented landscapes at the northern edge of their range. Conservation Genetics 12:527–542.

Calabrese, J. M., C. H. Fleming, and E. Gurarie. 2016. ctmm: an R package for analyzing animal relocation data as a continuous-time stochastic process. Methods in Ecology and Evolution 7:1124–1132.

Coates, P. S., M. A. Ricca, B. G. Prochazka, M. L. Brooks, K. E. Doherty, T. Kroger, E. J. Blomberg, C. A. Hagen, and M. L. Casazza. 2016. Wildfire, climate, and invasive grass interactions negatively impact an indicator species by reshaping sagebrush ecosystems. Proceedings of the National Academy of Sciences 113:12745–12750.

Coates, P. S., B. G. Prochazka, M. A. Ricca, K. B. Gustafson, P. Ziegler, and M. L. Casazza. 2017. Pinyon and juniper encroachment into sagebrush ecosystems impacts distribution and survival of greater sage-grouse. Rangeland Ecology and Management 70:25–38.

Coates, P. S., B. G. Prochazka, S. T. O'Neil, S. C. Webster, S. Espinosa, M. A. Ricca, S. R. Mathews, M. Casazza, and D. J. Delehanty. 2023. Geothermal energy production adversely affects a sensitive indicator species within sagebrush ecosystems in wester North America. Biological Conservation 280:109889.

Connelly, J. W., C. A. Hagen, and M. A. Schroeder. 2011. Characteristics and dynamics of greater sage-grouse populations. Pages 53–67 *in* S. T. Knick and J. W. Connelly, editors. Greater sage-grouse: ecology and conservation of a landscape species and its habitats. Studies in Avian Biology, Volume 38, University of California Press, Berkeley, USA.

Cox, D. R. 1972. Regression models and life tables (with discussion). Journal of the Royal Statistical Society, Series B 34:187–220.

Crawford, J. A., Olson, R. A., N. E. West, J. C. Mosley, M. A. Schroeder, T. D. Whitson, R. F. Miller, M. A. Gregg, and C. S. Boyd. 2004. Ecology and management of sage-grouse and sage-grouse habitat. Journal of Range Management 57:2–19.

Crist, M. R., R. Belger, K. W. Davies, D. M. Davis, J. R. Meldrum, D. J. Shinneman, T. E. Remington, J. Welty, and K. E. Mayer. 2023. Trends, impacts, and cost of catastrophic and frequent wildfires in the sagebrush biome. Rangeland Ecology and Management 89:3–19.

Cross, T. B., D. E. Naugle, J. C. Carlson, and M. K. Schwartz. 2017. Genetic recapture identifies long-distance breeding dispersal in greater sage-grouse (*Centrocercus urophasianus*). The Condor 119:155–166.

Dahlgren, D. K., M. R. Guttery, T. A. Messmer, D. Caudill, R. D. Elmore, R. Chi, and D. N. Koons. 2016. Evaluating vital rate contributions to greater sage-grouse population dynamics to inform conservation. Ecosphere 7:e01249.

Davis, D. M., K. P. Reese, S. C. Gardner. 2014. Demography, reproductive ecology, and variation in survival of greater sage-grouse in northeastern California. The Journal of Wildlife Management 78:1343–1355.

Dinkins, J. B., M. R. Conover, C. P. Kirol, J. L. Beck, and S. N. Frey. 2014a. Greater sage-grouse (*Centrocerus urophasianus*) hen survival: effects of raptors, anthropogenic and landscape features, and hen behavior. Canadian Journal of Zoology 92:319–330.

Dinkins, J. B., M. R. Conover, C. P. Kirol, J. L. Beck, and S. N. Frey. 2014b. Greater sage-grouse (*Centrocerus urophasianus*) select habitat based on avian predators, landscape composition, and anthropogenic features. Condor 116:629–642.

Dinkins, J. B., K. L. Lawson, K. T. Smith, J. L. Beck, C. P. Kirol, A. C. Pratt, M. R. Conover, and F. C. Blomquist. 2017. Quantifying overlap and fitness consequences of migration strategy with seasonal habitat use and a conservation policy. Ecosphere 8:e01991.

Doherty, K., D. M. Theobald, J. B. Bradford, L. A. Wiechman, G. Bredrosian, C. S. Boyd, M. Cahill, P. S. Coates, M. K. Creutzburg, M. R. Crist, S. P. Finn, A. V. Kumar, C. E. Littlefield, J. D. Maestas, K. L. Prentice, B. G. Prochazka, T. E. Remington, W. D. Sparklin, J. C. Tull, Z. Wurtzbach, and K. A. Zeller. 2022. A sagebrush conservation design to proactively restore America's sagebrush biome. U.S. Geological Survey Open-File Report 2022–1081, 38p.

Dudley, I. F., P. S. Coates, B. G. Prochazka, D. M. Davis, S. C. Gardner, and D. J. Delehanty. 2022. Maladaptive nest-site selection and reduces nest survival in female sage-grouse following wildfire. Ecosphere 13:e4282.

Ebonhoch, K., D. Thornton, L. Shipley, J. A. Manning, and K. White. 2019. Effects of post-release movements on survival of translocated sage-grouse. Journal of Wildlife Management 83:1314–1325.

Ellsworth, L. M., D. W. Wrobleski, J. B. Kaufman, and S. A. Reis. 2016. Ecosystem resilience is evident 17 years after fire in Wyoming big sagebrush ecosystems. Ecosphere 7:e01618.

Fahrig, L. 2003. Effects of habitat fragmentation on biodiversity. Annual Review of Ecology, Evolution, and Systematics 34:487–515.

Fedy, B. C, C. P. Kirol, A. L. Sutphin, and T. L. Maechtle. 2015. The influence of mitigation on sage-grouse habitat selection within an energy development field. PLoS ONE 10:e0121603.

Foster, L. J., K. M. Dugger, C. A. Hagen, and D. A. Budeau. 2018. Potential effects of GPS transmitter on greater sage-grouse survival in a post-fire landscape. Wildlife Biology 2018:1–5.

Foster, L. J., K. M. Dugger, C. A. Hagen, and D. A. Budeau. 2019. Greater sage-grouse vital rates after wildfire. Journal of Wildlife Management 83:121–134.

Gardiner, R., K. Proft, S. Comte, M. Jones, and C. N. Johnson. 2019. Home range size scales to habitat amount and increasing fragmentation in a mobile woodland specialist. Ecology and Evolution 9:14005–14014.

Giesen, K. M., T. J. Schoenberg, and C. E. Braun. 1982. Methods for trapping sage grouse in Colorado. Wildlife Society Bulletin 10:224–231.

Haddad, N. M., L. A. Brudvig, J. Colbert, K. F. Davies, A. Gonzalez, R. D. Holt, T. E. Lovejoy, J. O. Sexton, M. P. Austin, C. D. Collins, W. M. Cook, E. I. Damschen, R. M. Ewers, B. L. Foster, C. N. Jenkins, A. J. King, W. F. Laurance, D. J. Levey, C. R. Margules, B. A. Melbourne, A. O. Nicholls, J. L. Orrock, D. X. Song, and J. R. Townshend. 2015. Habitat fragmentation and its lasting impact on Earth's ecosystems. Science Advances 1:e1500052.

Hadley, A. S., and M. G. Betts. 2016. Refocusing habitat fragmentation research using lessons from the last decade. Current Landscape Ecology Reports 1:55–66.

Hagen, C. A. 2011a. Greater sage-grouse conservation assessment and strategy for Oregon: a plan to maintain and enhance populations and habitat. Oregon Department of Fish and Wildlife, Salem, Oregon, USA.

Hagen, C. A. 2011b. Predation on greater sage-grouse: Facts, processes, and effects. Chapter 6 *in* S. T. Knick and J. W. Connelly, editors. Greater sage-grouse: ecology and conservation of a landscape species and its habitats. Studies in Avian Biology, Volume 38, University of California Press, Berkeley, USA.

Hanski, I. 1999. Metapopulation ecology. Oxford University Press.

Hesselbarth, M. H., M. Sciaini, K. A. With, K. Wiegand, and J. Nowosad. 2019. landscapemetrics: an open-source R tool to calculate landscape metrics. Ecography 42:1648–1657.

Hinam, H. L., and C. C. St. Clair. 2008. High levels of habitat loss and fragmentation limit reproductive success by reducing home range size and provisioning rates of northern saw-whet owls. Biological Conservation 141:524–535.

Hins, C., J. P. Ouellet, C. Dussault, and M. H. St-Laurent. 2009. Habitat selection by forest-dwelling caribou in managed boreal forest of eastern Canada: evidence of a landscape configuration effect. Forest Ecology and Management 257:636–643.

Holloran, M. J., R. C. Kaiser, W. A. Hubert. 2010. Yearling greater sage-grouse response to energy development in Wyoming. The Journal of Wildlife Management 74:65–72.

Horn, D. J., M. L. Phillips, R. R. Koford, W. R. Clark, M. A. Sovada, and R. J. Greenwood. 2005. Landscape composition, patch size, and distance to edges:

interactions affecting duck reproductive success. Ecological Applications 15:1367–1376.

Kirol, C. P., J. L. Beck, S. V. Huzurbazar, M. J. Holloran, and S. N. Miller. 2015. Identifying greater sage-grouse source and sink habitats for conservation planning in an energy development landscape. Ecological Applications 25:968–990.

Kramer, G. R., K. O. Daly, H. M. Streby, and D. E. Andersen. 2018. Association between American woodcock seasonal productivity and landscape composition and configuration in Minnesota. Proceedings of the American Woodcock Symposium 11:107–121.

Laforge, A., F. Archaux, A. Coulon, C. Sirami, J. Froidevaux, N. Gouix, S. Ladet, H. Martin, K. Barré, C. Roemer, F. Claireau, C. Kerbiriou, and L. Barbaro. 2021. Landscape composition and life-history traits influence bat movement and space use: analysis of 30 years of published telemetry data. Global Ecology and Biogeography 30:2442–2454.

LANDFIRE. 2020. Existing Vegetation layer, LANDFIRE 2020. U. S. Department of the Interior, U. S. Geological Survey, and U. S. Department of Agriculture.

Latham, A. D. M., M. C. Latham, M. S. Boyce, and S. Boutin. 2011. Movement responses by wolves to industrial linear features and their effect on woodland caribou in northeastern Alberta. Ecological Applications 21:2854–2865.

LeBeau, C. W., G. D. Johnson, M. J. Holloran, J. L. Beck, R. M. Nielson, M. A. Kaufman, E. J. Rodemaker, and T. L. McDonald. 2017. Greater sage-grouse habitat selection, survival, and wind energy infrastructure. Journal of Wildlife Management 81:690–711.

Lindenmayer, D. B., and J. Fischer. 2077. Tackling the habitat fragmentation panchreston. Trends in Ecology and Evolution 22:127–132.

Lungle, K. and S. Pruss. 2008. Recovery Strategy for the Greater Sage-Grouse (*Centrocercus urophasianus urophasianus*) in Canada. In Species at Risk Act Recovery Strategy Series. Parks Canada Agency. Ottawa, Ontario, 43 pp.

Manlick, P. J., and J. N. Pauli. 2020. Human disturbance increases trophic niche overlap in terrestrial carnivore communities. PNAS 117:26842–26848.

Martin, A. E., and L. Fahrig. 2016. Reconciling contradictory relationships between mobility and extinction risk in human-altered landscapes. Functional Ecology 30:1558–1567.

McGarigal, K. S., S. A. Cushman, and E. Ene. 2023. FRAGSTATS v4: spatial pattern analysis program for categorical and continuous maps. University of Massachusetts.

Miller, R. F., J. D. Bates, T. J. Svejcar, F. B. Pierson, and L. E. Eddleman. 2005. Biology, ecology, and management of western juniper (*Juniperus occidentalis*). Technical Bulletin 152 Oregon State University Extension, Corvallis, Oregon, USA.

Miller, R. F., S. T. Knick, D. A. Pyke, C. W. Meinke, S. E. Hanser, M. J. Wisdom, and A. L. Hild. 2011. Characteristics of sagebrush habitats and limitations to long-term conservation. Pages 145–184 *in* S. T. Knick and J. W. Connelly, editors. Greater sage-grouse: ecology and conservation of a landscape species and its habitats. Studies in Avian Biology, Volume 38, University of California Press, Berkeley, USA.

Moynahan, B. J., M. S. Lindberg, and J. W. Thomas. 2006. Factors contributing to process variance in annual survival of female sage-grouse in Montana. Ecological Applications 16:1529–1538.

Monitoring Trends in Burn Severity. 2023. MTBS Data Access: Fire Level Geospatial Data (2017, July - last revised). MTBS Project USDA Forest Service/U.S. Geological Survey. Available online: http://mtbs.gov/direct-download.

Moynahan, B. J., M. S. Lindberg, and J. W. Thomas. 2006. Factors contributing to process variance in annual survival of female greater sage-grouse in Montana. Ecological Applications 16:1529–1538.

Niebuhr, B. B. S., M. E. Wosniack, M. C. Santos, E. P. Raposo, G. M. Viswanathan, M. G. E. da Luz, and M. R. Pie. 2015. Survival in patchy landscapes: the interplay between dispersal, habitat loss and fragmentation. Scientific Reports 5:11898.

O'Neil, S. T., P. S. Coates, B. E. Brussee, M. A. Ricca, S. P. Espinosa, S. C. Gardner, and D. J. Delehanty. 2020. Wildfire and the ecological niche: diminishing habitat suitability for an indicator species within semi-arid ecosystems. Global Change Biology 26:6296–6312.

Oro, D., M. Genovart, G. Tavechhia, M. S. Fowler, and A. Martínez-Abraín. 2013. Ecological and evolutionary implications of food subsidies from humans. Ecology Letters 16:1501–1514.

Pimm, S. L., C. N. Jenkins, R. Abell, T. M. Brooks, J. L. Gittleman, L. N. Joppa, P. H. Raven, C. M. Roberts, and J. O. Sexton. 2014. The biodiversity of species

and their rates of extinction, distribution, and protection. Science 344:1246752.

Pratt, A. C., K. T. Smith, and J. L. Beck. 2019. Prioritizing seasonal habitats for comprehensive conservation of a partially migratory species. Global Ecology and Conservation 17:e00594.

Pratt, A. C., and J. L. Beck. 2021. Do greater sage-grouse exhibit maladaptive habitat selection? Ecosphere 12:e03354.

Prochazka, B. G., P. S. Coates, M. A. Ricca, M. L. Cassaza, K. B. Gustafson, and J. M. Hull. 2017. Encounters with pinyon-juniper influence riskier movements in greater sage-grouse across the Great Basin. Rangeland Ecology and Management 70:39–49.

R Core Team. 2022. R: a language and environment for statistical computing. R Foundation for Statistical Computing, Vienna, Austria.

Rabon, J. C. 2020. Habitat selection and physiological condition of female greater sage-grouse in relation to western juniper. Thesis. University of Idaho.

Rabon, J. C., C. M. V. Nuñez, P. S. Coates, M. A. Ricca, and T. N. Johnson. 2021. Ecological correlates of fecal corticosterone metabolites in female greater sage-grouse (*Centrocerus urophasianus*). Canadian Journal of Zoology 99:812–822.

Reed, P. M., J. F. Dwyer, and T. Stankowich. 2023. Supplementation of season natural resources with year-round anthropogenic resources by coyotes in natural fragments within a high-density urban area. Wildlife Biology 2023:e01095.

Robinson, S. G. 2018. Effects of landscape characteristics on annual survival of lesser prairie-chickens. The American Midland Naturalist 180:66–86.

Schroeder, M. A., C. L. Aldridge, A. D. Apa, J. R. Bohne, C. E. Braun, S. D. Bunnell, J. W. Connelly, P. A. Deibert, S. C. Gardner, M. A. Hilliard, G. D. Kobriger, S. M. Mcadam, C. W. Mccarthy, J. J. Mccarthy, D. L. Mitchell, E. V Rickerson, and S. J. Stiver. 2004. Distribution of sage-grouse in North America. Condor 106:363–376.

Schuyler, E. M., C. A. Hagen, C. R. Anthony, L. J. Foster, and K. M. Dugger. 2022. Temporal mismatch in space use by a sagebrush obligate species after large-scale wildfire. Ecosphere 13:e4179.

Severson, J. P., C. A. Hagen, J. D. Tack, J. D. Maestas, D. E. Naugle, J. T. Forbes, and K. P. Reese. 2017. Better living through conifer removal: a demographic analysis of sage-grouse vital rates. PLoS ONE 12:e0174347.

Severson, J. P., P. S. Coates, B. G. Prochazka, M. A. Ricca, M. L. Casazza, and D. J. Delehanty. 2019. Global positioning system tracking devices can decrease greater sage-grouse survival. The Condor 121:1–15.

Smith, K. T., J. L. Beck, and C. P. Kirol. Reproductive state leads to intraspecific habitat partitioning and survival differences in greater sage-grouse: implications for conservation. Wildlife Research 45:119–131.

Smith, J. T., B. W. Allred, C. S. Boyd, K. W. Davies, M. O. Jones, A. R. Kleinhesselink, J. D. Maestas, S. L. Morford, and D. E. Naugle. 2022. The elevational ascent and spread of exotic annual grass dominance in the Great Basin, USA. Diversity and Distributions 28:83–96.

Taylor, R. L., B. L. Walker, D. E. Naugle, and L. S. Mills. 2012. Managing multiple vital rates to maximize greater sage-grouse population growth. The Journal of Wildlife Management 76:336-347.

Therneau, T. 2023. A package for survival analysis in R. R package version 3.5-5, https://CRAN.R-project.org/package=survival.

Trzcinski, M. K., L. Fahrig, and G. Merriam. 1999. Independent effects of forest cover and fragmentation on the distribution of forest breeding birds. Ecological Applications 9:586–593.

Tyrrell, E. A., P. S. Coates, B. G. Prochazka, B. E. Brussee, S. P. Espinosa, and J. M. Hull. 2023. Wildfire immediately reduces nest and adult survival of greater sage-grouse. Scientific Reports 13:10970.

U.S. Fish and Wildlife Service. 2015. 50 CFR Part 17 Endangered and Threatened Wildlife and Plants; 12-month findings for petitions to list the greater sage-grouse (*Centrocercus urophasianus*) as threatened or endangered. Docket No. FWS-R6-E.S.-2015-0146. U.S. Department of Interior, Fish and Wildlife Service, Washington, DC, USA.

Villard, M. A., and J. P. Metzger. 2014. Beyond the fragmentation debate: a conceptual model to predict when habitat configuration really matters. Journal of Applied Ecology 51:309–318.

Vold, S. T. 2023. Oregon greater sage-grouse population monitoring: 2023 annual report. Oregon Department of Fish and Wildlife, Hines, OR, USA.

Wakkinen W. L., K. P. Reese, J. W. Connelly, and R. A. Fischer. 1992. An improved spotlighting technique for capturing sage grouse. Wildlife Society Bulletin 20:425–426.

Walker, B. L. 2022. Resource selection by greater sage-grouse varies by season and infrastructure type in a Colorado oil and gas field. Ecosphere 13:e4018.

Wiegand, T., E. Revilla, and K. A. Moloney. 2005. Effects of habitat loss and fragmentation on populations dynamics. Conservation Biology 19:108–121.

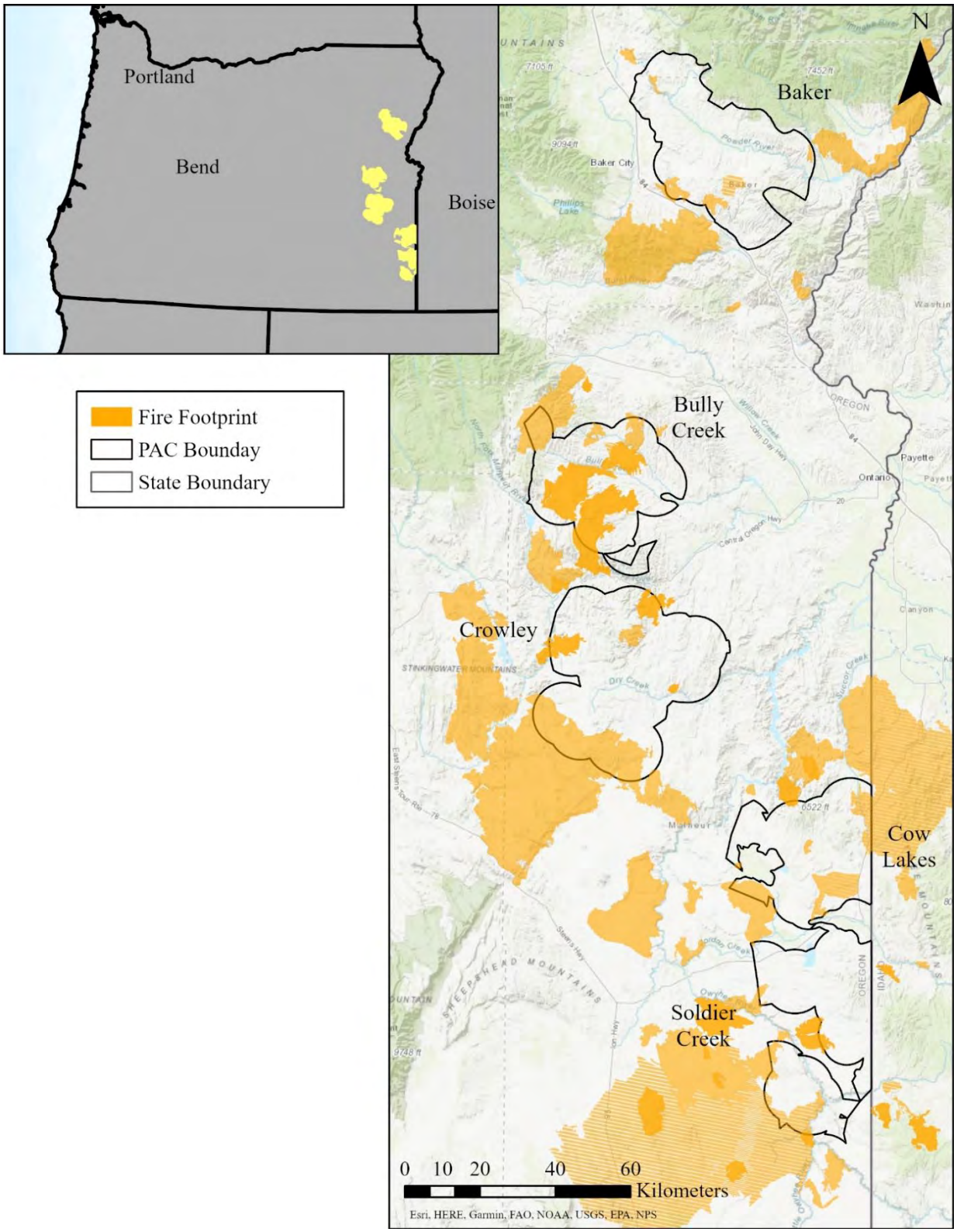

Figure 1. Map of sage-grouse Priority Areas of Conservation (PACs) in Baker and Malheur Counties, OR, USA. Orange polygons represent fire footprints between 2006 and 2020.

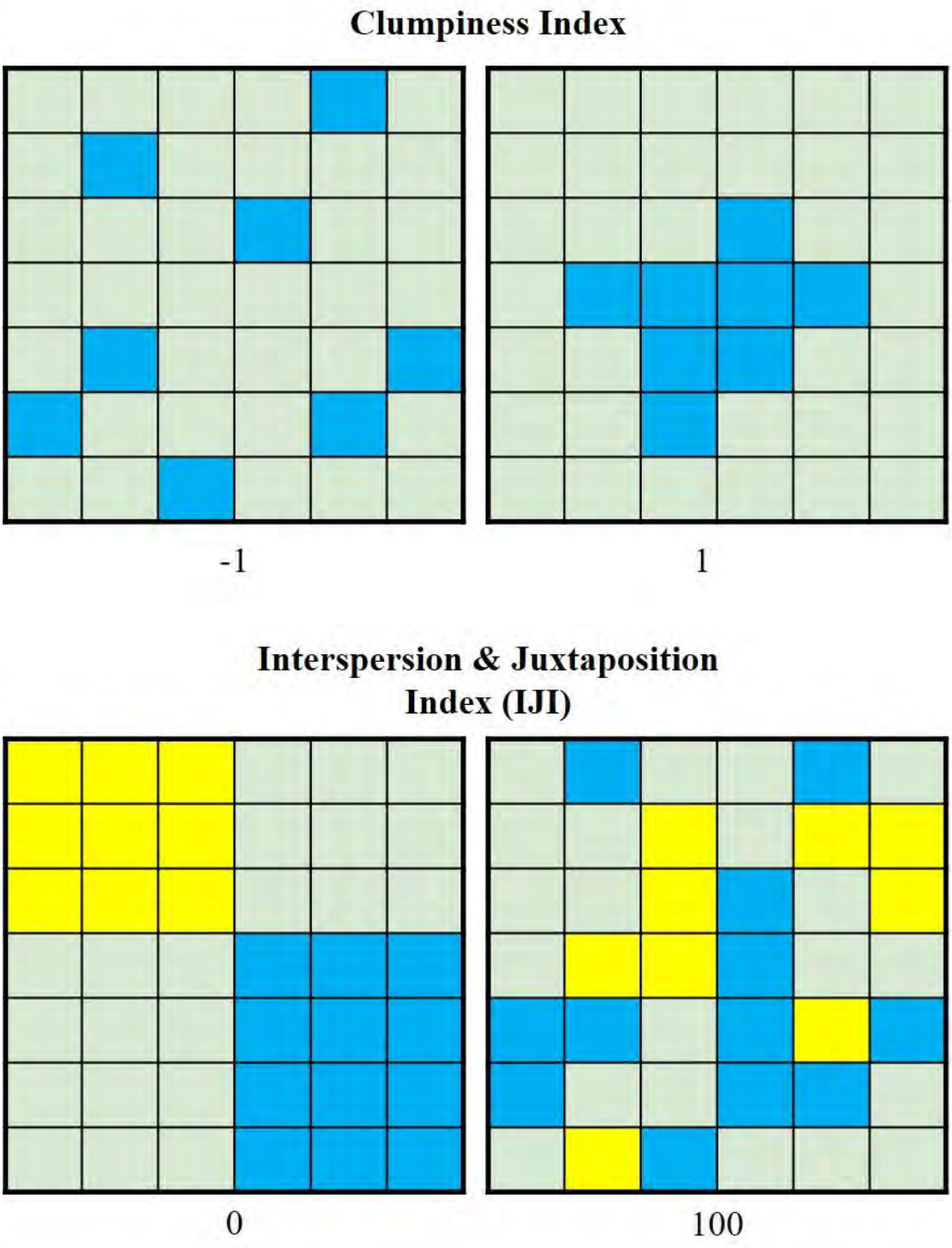

Figure 2. Visual depictions of low and high values of clumpiness and interspersion and juxtaposition indices.

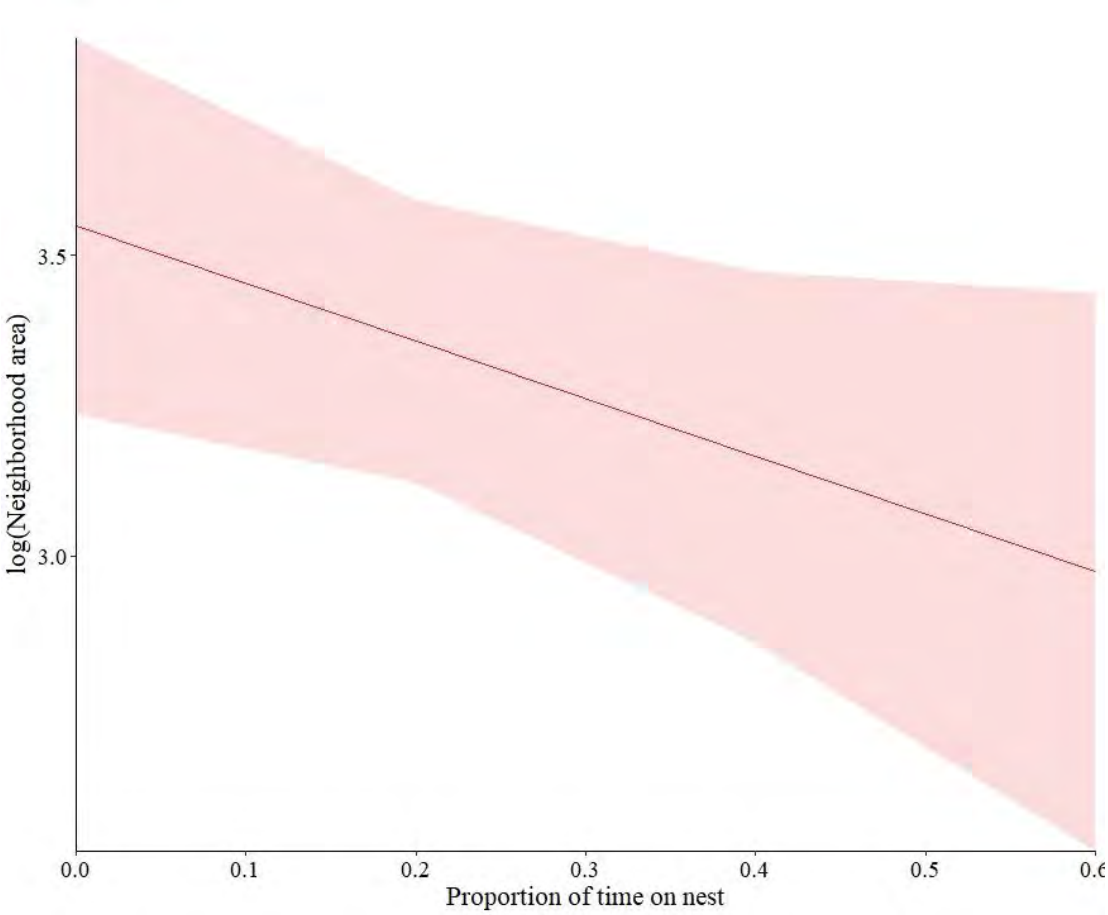

Figure 3. Effects plot and 85% confidence interval (shaded areas) from top ΔAIC_c ranked linear mixed model of the proportion of time spent on nest on the log(area) (km^2) of sage-grouse spring neighborhood size. Data collected in Baker and Malheur Counties, Oregon, USA (2017–2022).

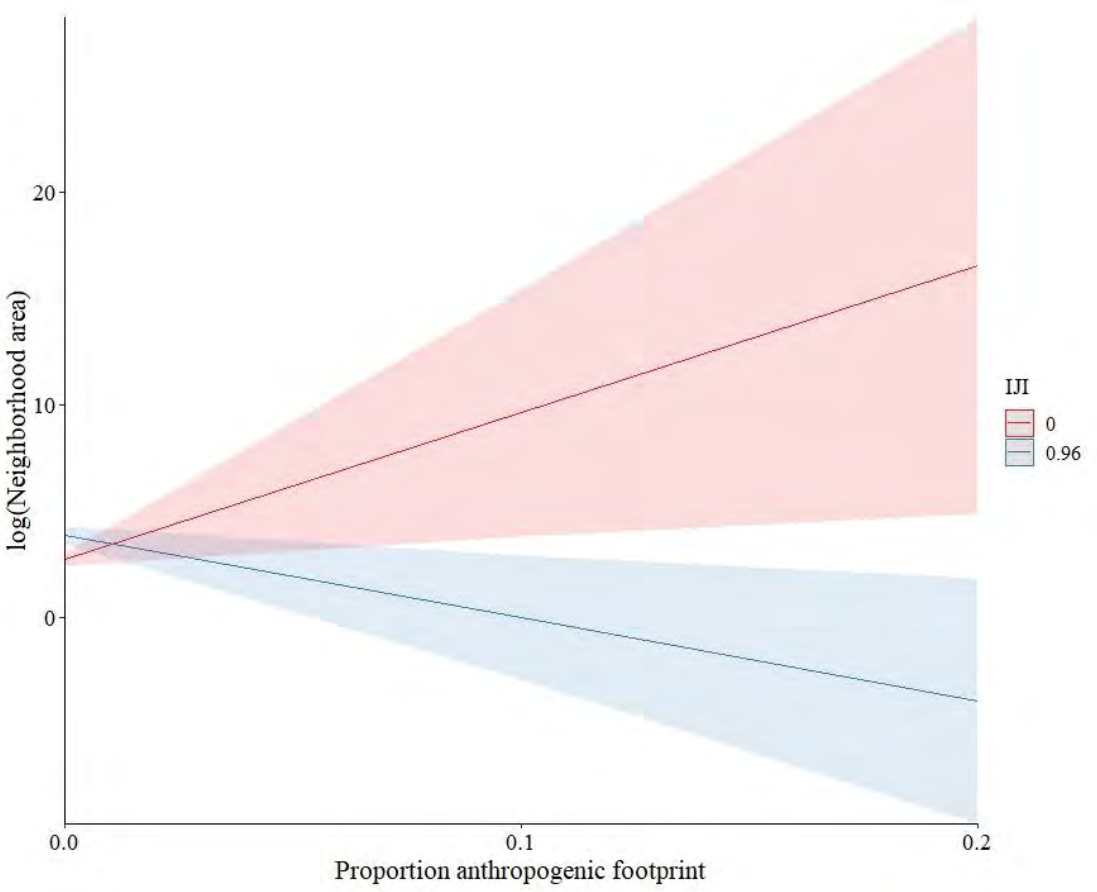

Figure 4. Effects plot and 85% confidence intervals (shaded areas) from top ΔAIC_c ranked linear mixed model of the interaction between proportion of anthropogenic footprint and the interspersion and juxtaposition index (IJI) on the log(area) (km^2) of sage-grouse spring neighborhood size. Values of IJI represent the lowest and highest values in the data, with values closer to 1 indicating high interspersion. Data collected in Baker and Malheur Counties, Oregon, USA (2017–2022).

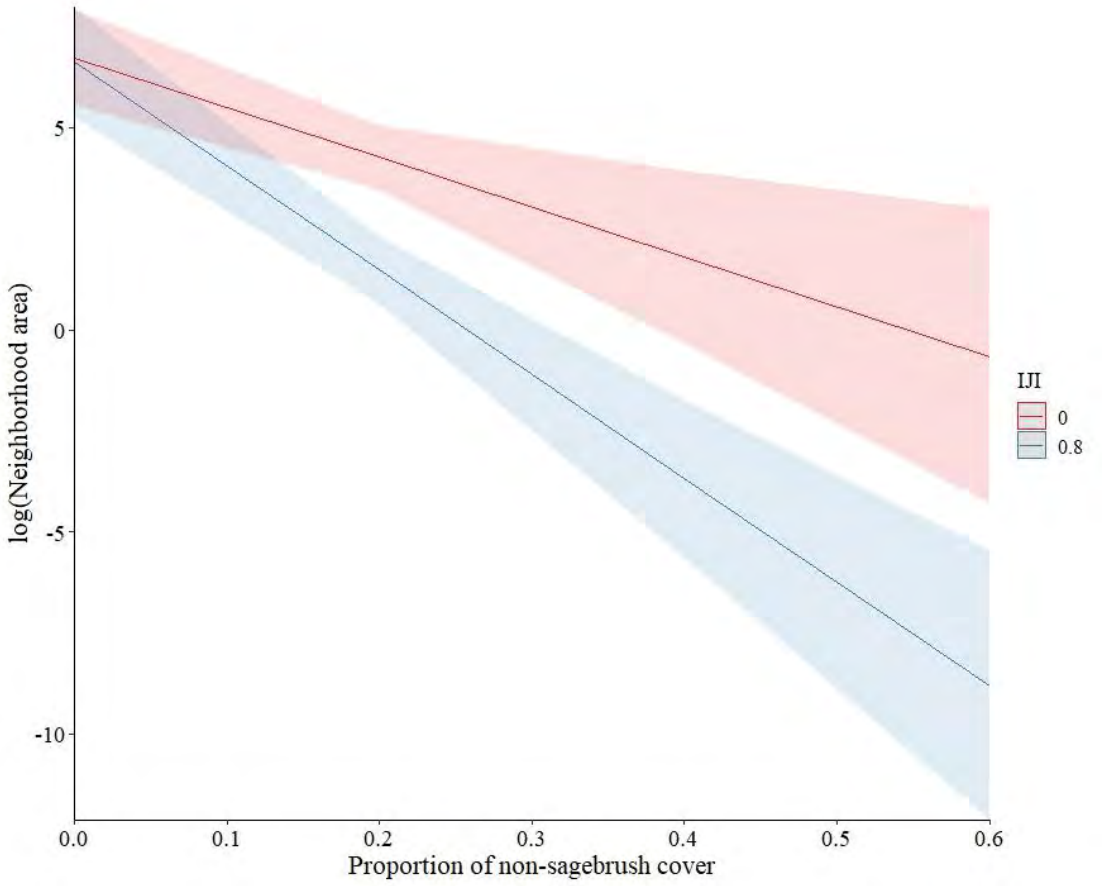

Figure 5. Effects plot and 85% confidence intervals (shaded areas) from top ΔAIC_c ranked linear mixed model of the interaction between proportion of non-sagebrush cover and the interspersion and juxtaposition index (IJI) on the log(area) (km^2) of sage-grouse spring neighborhood size. Values of IJI represent the lowest and highest values in the data, with values closer to 1 indicating high interspersion. Data collected in Baker and Malheur Counties, Oregon, USA (2017–2022).

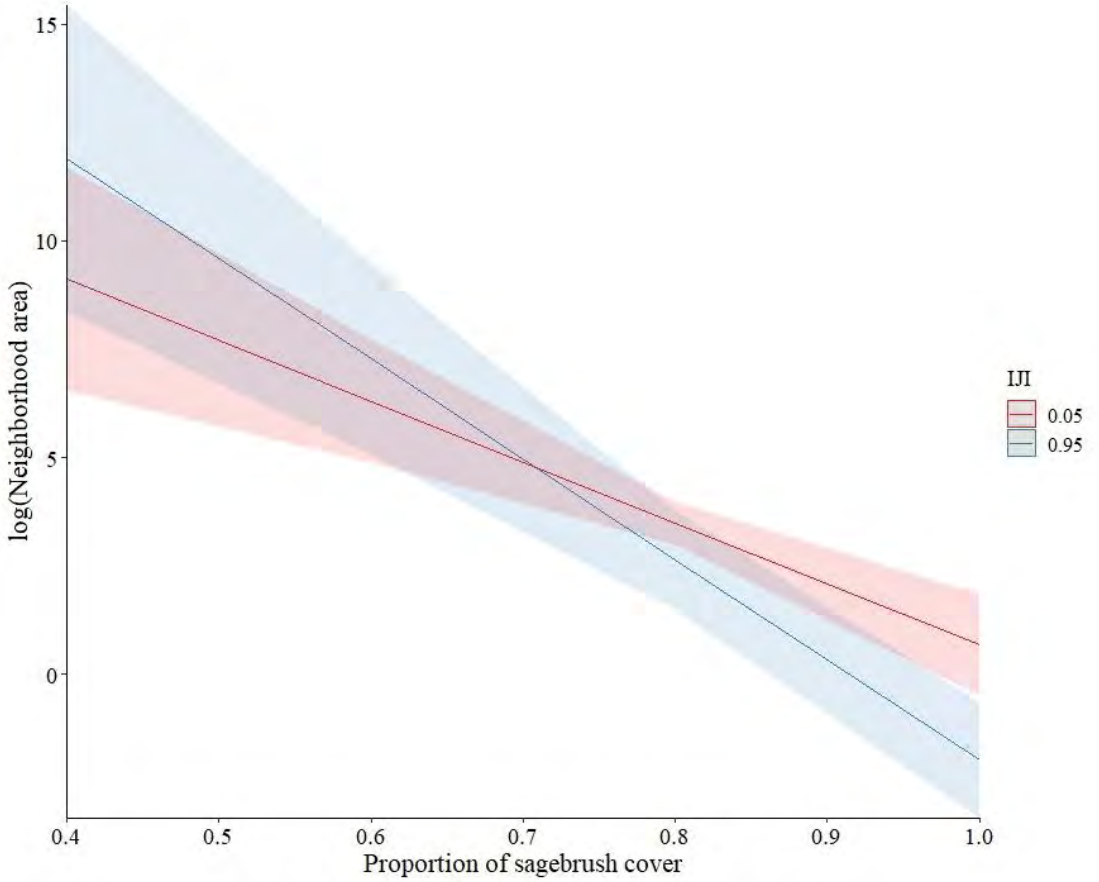

Figure 6. Effects plot and 85% confidence intervals (shaded areas) from top ΔAIC_c ranked linear mixed model of the interaction between proportion of sagebrush cover and the interspersion and juxtaposition index (IJI) on the log(area) (km^2) of sage-grouse spring neighborhood size. Values of IJI represent the lowest and highest values in the data, with values closer to 1 indicating high interspersion. Data collected in Baker and Malheur Counties, Oregon, USA (2017–2022).

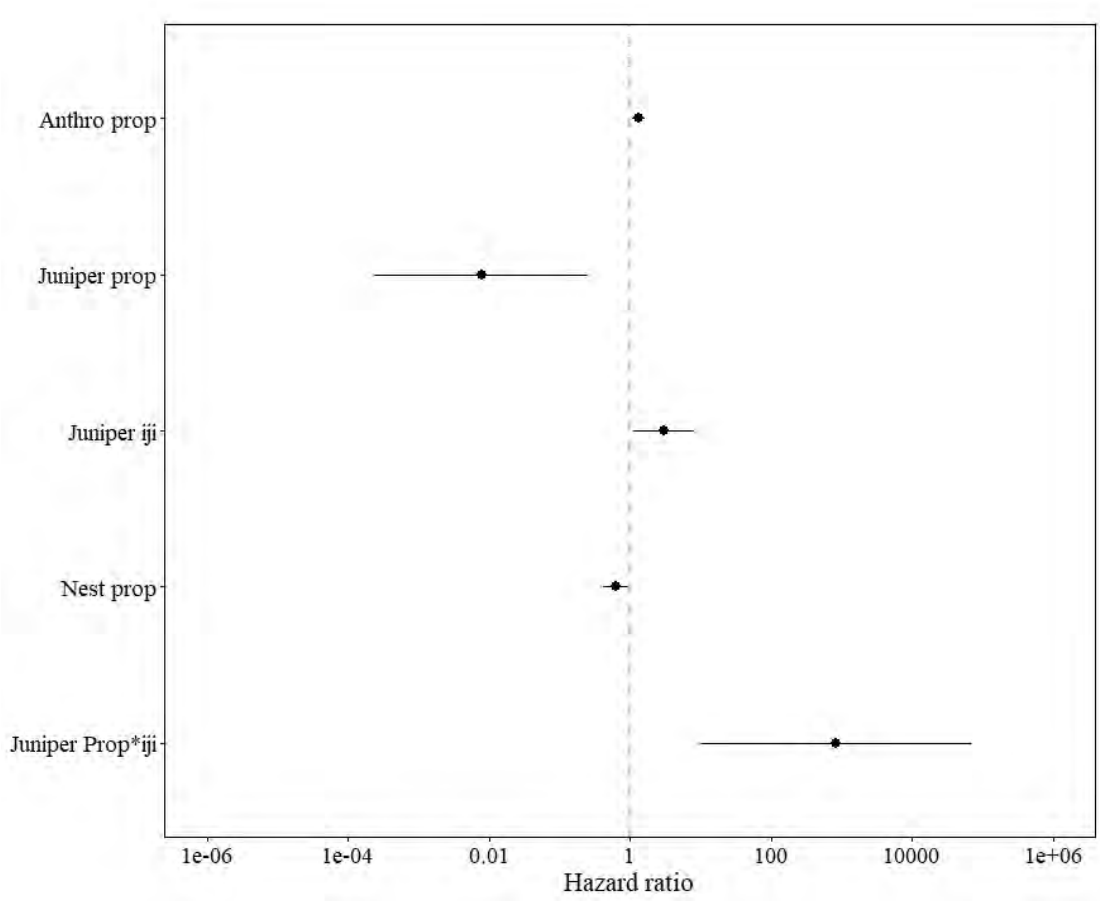

Figure 7. Estimated hazard ratios and 85% confidence intervals for variables the top ΔAIC_c CoxPH mixed-model of female sage-grouse survival. Values >1 indicate variables that decrease survival and values <1 indicate variables that increase survival. Data collected in Baker and Malheur Counties, Oregon, USA (2017–2022).

Table 1. Model selection rankings using Akaike's Information Criterion adjusted for small sample sizes (ΔAIC_c), number of parameters (K), and Akaike weights (w_i) for the top five ranked and the null linear mixed models after variable selection of composition, configuration, and categorical variables on sage-grouse spring neighborhood size. Nest_prop = proportion of time spent on nest, NS = non-sagebrush cover. Data collected in Baker and Malheur Counties, Oregon, (2017–2022).

Model	K	AIC_c	ΔAIC_c	w_i
Anthro_prop*Anthro_iji + NS_prop*NS*iji + Sage_prop*Sage*iji + Nest_prop	13	234.30	0.00	0.43
Anthro_prop*Anthro_iji + NS_prop*NS*iji + Sage_prop*Sage*iji	12	235.16	0.86	0.28
Anthro_prop*Anthro_iji + NS_prop*NS_iji + Other_prop*Other_iji + Sage_prop*Sage_iji + Nest_prop	16	236.54	2.24	0.14
Anthro_prop*Anthro_iji + NS_prop*NS_iji + Other_prop*Other_iji + Sage_prop*Sage_iji	15	236.69	2.39	0.13
NS_prop*NS_iji + Other_prop*Other_iji + Sage_prop*Sage_iji + Fire5y_prop*Fire5y_clumpy + Nest_prop	16	243.39	9.09	0.00
Null	3	342.74	108.44	0.00

Table 2. Standardized parameter estimates, standard errors (SE), t-values, and 85% confidence intervals for variables from the top ΔAIC_c ranked linear mixed model of composition and configuration of land cover and disturbance on sage-grouse neighborhood size. Nest_prop = proportion of time spent on nest, NS = non-sagebrush cover class. Data collected in Baker and Malheur Counties, Oregon, (2017–2022).

Variable	Estimate	SE	t-value	85% CI
Intercept	3.37	0.12	28.36	3.19–3.54
Anthro_prop	0.54	0.26	2.06	0.16–0.92
Anthro_IJI	0.08	0.14	0.64	-0.16–0.29
NS_prop	-2.04	0.32	-6.28	-2.51– -1.55
NS_iji	-0.45	0.13	-3.55	-0.64– -0.26
Sage_prop	-2.25	0.33	-6.84	-2.73– -1.77
Sage_iji	-0.12	0.12	-0.95	-0.30– - 0.07
Nest_prop	-0.12	0.06	-1.88	-0.21– -0.03
Anthro_prop*Anthro_iji	-0.64	0.26	-2.52	-1.02– -0.27
NS_prop*NS_iji	-0.26	0.10	-2.71	-0.40– -0.12
Sage_prop*Sage_iji	-0.18	0.09	-2.10	-0.32– -0.05

Table 3. Model selection rankings using Akaike's Information Criterion adjusted for small sample sizes (ΔAIC_c), number of parameters (K), and Akaike weights (w_i) for CoxPH mixed models after variable selection of composition, configuration, and ecology variables on cumulative spring survival of female sage-grouse. Nest_prop = proportion of time spent on nest. Data collected in Baker and Malheur Counties, Oregon, (2017–2022).

Model	K	AIC_c	ΔAIC_c	w_i
Anthro_prop + Juniper_prop*iji + Nest_prop	6	178.84	0.00	0.36
Juniper_prop*iji + Nest_prop	5	179.37	0.54	0.28
Anthro_prop + Juniper_prop*iji	5	179.38	0.55	0.28
Juniper_prop*iji	4	182.45	3.61	0.06
Anthro_prop + Nest_prop	3	185.91	7.07	0.01
Anthro_prop	2	186.03	7.19	0.01
Nest_prop	2	187.03	8.21	0.01
Null	1	189.53	10.69	0.00

Table 4. Standardized parameter estimates, standard errors (SE), t-values, and 85% confidence intervals for variables from the top ΔAIC_c ranked CoxPH mixed model of composition and configuration of land cover and disturbance on spring survival of female sage-grouse. Nest_prop = proportion of time spent on nest. Data collected in Baker and Malheur Counties, Oregon, (2017–2022).

Variable	Estimate	SE	p-value	85% CI
Anthro_prop	0.27	0.14	0.049	0.07–0.47
Juniper_prop	-4.87	2.41	0.044	-8.34– -1.39
Juniper_IJI	1.11	0.69	0.110	0.12–2.10
Nest_prop	-0.46	0.28	0.100	-0.86– -0.06
Juniper_prop*IJI	6.72	3.07	0.029	2.30–11.15

Table 5. Results of proportional hazards tests on the top ΔAIC_c ranked CoxPH mixed model for spring survival of female sage-grouse. Data collected in Baker and Malheur Counties, Oregon, (2018–2022).

Variable	χ^2	df	p
Anthro_prop	2.18	1	0.14
Juniper_prop	2.47	1	0.12
Juniper_IJI	3.52	1	0.06
Nest_prop	2.41	1	0.12
Juniper_prop*IJI	1.33	1	0.25
Global model	10.16	5	0.07

CHAPTER 5 – CONCLUSIONS

Negative effects to sage-grouse demographic rates and habitat selection in the Great Basin have been linked to wildfire (Coates et al. 2016, Foster et al. 2019, Dudley et al. 2022, Tyrrell et al. 2023, O'Neil et al. 2023), invasive annual grasses (Coates et al. 2016, O'Neil et al. 2020), conifer expansion (Coates et al. 2017, Prochazka et al. 2017, Severson et al. 2017, Olsen et al. 2021), and raven densities (Coates et al. 2020, O'Neil et. al. 2023). My research examined how anthropogenic subsidies and wildfire effected predator-prey dynamics within sagebrush ecosystems. My findings indicated that the presence of anthropogenic subsidies create predator hotspots that negatively impact adjacent sage-grouse populations.

The density and occupancy of ravens, red-tailed hawks, and Swainson's hawks were positively associated with anthropogenic elements including agriculture, landfills, road density, and transmission lines. Yearly estimated relative raven densities in my study areas ranged from 0.85–1.64 km^{-2}, well above the 0.4–0.5 km^{-2} associated with below average nest survival in sage-grouse (Coates et al. 2020, O'Neil et al. 2023). Raven density was negatively associated with sage-grouse nest survival, and nest survival was below the range wide average (0.38; Taylor et al. 2012), in the Baker (0.15), Cow Lakes (0.27), and Soldier Creek (0.29) PACs. Swainson's hawk densities (0.11–0.28 km^{-2}) were similar to those found in other anthropogenically subsidized areas like the Central Valley of California (Furnas et al. 2022) and red-tailed hawk densities (0.52 km^{-2}) were comparable to lower estimates found on known winter ranges when individuals are more tolerant of conspecifics (Williams et al. 2000). In addition to supporting high densities, my results found that interspecies interactions were independent or largely positive in relation to

anthropogenic subsidies, suggesting that the three species are highly tolerant of allospecifics when resources are abundant.

I found that the proportion of anthropogenic footprint, regardless of configuration, within spring neighborhoods of female sage-grouse negatively affected adult female survival. Anthropogenic landscape elements, such as linear right-of-ways, tall infrastructure, and food subsidies, are likely facilitating infiltration of sagebrush ecosystems that would otherwise be inaccessible or unable to support dense predator communities. This may also be true for juniper expansion as female survival was negatively associated with interspersed cover of juniper, which provides nesting and perching opportunities for avian predators.

My results indicate that female sage-grouse were selecting nest sites closer to and within burned areas, but that closer proximity to fire reduced nest survival in most areas. While this is consistent with current literature (O'Neil et al. 2020, Dudley et al. 2022, Tyrrell et al. 2023), nest survival rates in the Bully Creek PAC were considerably higher (0.51) than the range wide average (0.38), despite having the largest fire footprint and average raven densities >0.50 km^2. A map comparing the locations of sage-grouse nests in Bully Creek to predicted raven densities illustrated that most nests were located within or near burned areas that were away from high local raven densities that were associated with anthropogenic resources. This comparison suggested that fire was not as detrimental to sage-grouse nest survival if nest were located >8 km from subsidies that support high densities of generalist predators. In the absence of anthropogenic subsidies, fire could reduce avian predator

abundance by removing elevated perching and nesting substrates (e.g., buildings, windmills, power poles, and lone trees) required by most species.

My results support ongoing efforts to restore sagebrush, subdue invasive annual grasses, and remove juniper from sage-grouse conservation areas. However, more focus needs to be put on removing, or heavily mitigating existing anthropogenic infrastructure to prevent use by generalist predators (Brunk et al. 2021, Marzluff et al. 2021). Food subsidies such as road kill, dead livestock, and agricultural waste should be removed or properly stored. Predation is the primary source of mortality for sage-grouse adults, chicks, and nests (Coates et al. 2008, Hagen 2011, Blomberg et al. 2013, Davis et al. 2014), therefore addressing the human-caused increase in predator densities and access to remote sagebrush ecosystems should be prioritized for sage-grouse management.

LITERATURE CITED

Blomberg, E. J., J. S. Sendinger, D. V. Nonne, and M. T. Atamian. 2013. Seasonal reproductive costs contribute to reduced survival of female greater sage-grouse. Journal of Avian Biology 44:149–158.

Brunk, K. M., E. H. West, M. Z. Peery, and A. M. Pidgeon. 2021. Reducing anthropogenic subsidies can curb density of overabundant predators in a protected area. Biological Conservation 256:109081.

Coates, P. S., J. W. Connelly, and D. J. Delehanty. 2008. Predators of greater sage-grouse nests identified by video monitoring. Journal of Field Ornithology 79:421–428.

Coates, P. S., M. A. Ricca, B. G. Prochazka, M. L. Brooks, K. E. Doherty, T. Kroger, E. J. Blomberg, C. A. Hagen, and M. L. Casazza. 2016. Wildfire, climate, and invasive grass interactions negatively impact an indicator species by reshaping sagebrush ecosystems. Proceedings of the National Academy of Sciences 113:12745–12750.

Coates, P. S., B. G. Prochazka, M. A. Ricca, K. B. Gustafson, P. Ziegler, and M. L. Casazza. 2017. Pinyon and juniper encroachment into sagebrush ecosystems impacts distribution and survival of greater sage-grouse. Rangeland Ecology and Management 70:25–38.

Coates, P. S., S. T. O'Neil, B. E. Brussee, M. A. Ricca, P. J. Jackson, J. B. Dinkins, K. B. Howe, A. M. Moser, L. J. Foster, and D. J. Delehanty. 2020. Broad-scale impacts of an invasive native predator on a sensitive native prey species within the shifting avian community of the North American Great Basin. Biological Conservation 243:108409.

Dudley, I. F., P. S. Coates, B. G. Prochazka, D. M. Davis, S. C. Gardner, and D. J. Delehanty. 2022. Maladaptive nest-site selection and reduces nest survival in female sage-grouse following wildfire. Ecosphere 13:e4282.

Foster, L. J., K. M. Dugger, C. A. Hagen, and D. A. Budeau. 2019. Greater sage-grouse vital rates after wildfire. Journal of Wildlife Management 83:121–134.

Furnas, B. J., D. H. Wright, E. N. Tennant, R. M. O'Leary, M. J. Keuhn, P. H. Bloom, and C. L. Battisone. 2022. Rapid growth of the Swainson's Hawk population in California since 2005. Ornithological Applications 124:1–12.

Hagen, C. A. 2011. Predation on greater sage-grouse: Facts, processes, and effects. Chapter 6 *in* S. T. Knick and J. W. Connelly, editors. Greater sage-grouse: ecology and conservation of a landscape species and its habitats. Studies in Avian Biology, Volume 38, University of California Press, Berkeley, USA.

Marzluff, J. M., M. Loretto, C. K. Ho, G. W. Coleman, and M. Restani. 2021. Thinking like a raven: restoring integrity, stability, and beauty to western ecosystems. Human-Wildlife Interactions 15:22.

Olsen, A. C., J. P. Severson, J. D. Maestas, D. E. Naugle, J. T. Smith, J. D. Tack, K. H. Yates, and C. A. Hagen. 2021. Reversing tree expansion in sagebrush steppe yields population-level benefit for imperiled sage-grouse. Ecosphere 12:e03551.

O'Neil, S. T., P. S. Coates, B. E. Brussee, M. A. Ricca, S. P. Espinosa, S. C. Gardner, and D. J. Delehanty. 2020. Wildfire and the ecological niche: diminishing habitat suitability for an indicator species within semi-arid ecosystems. Global Change Biology 26:6296–6312.

O'Neil, S. T., P. S. Coates, S. C. Webster, B. E. Brussee, S. J. Dettenmaier, J. C. Tull, P. J. Jackson, M. L. Casazza, and S. P Espinosa. 2023. A spatially explicit modeling framework to guide management of subsidized avian predator densities. Ecosphere 14:e4618.

Prochazka, B. G., P. S. Coates, M. A. Ricca, M. L. Cassaza, K. B. Gustafson, and J. M. Hull. 2017. Encounters with pinyon-juniper influence riskier movements in greater sage-grouse across the Great Basin. Rangeland Ecology and Management 70:39–49.

Severson, J. P., C. A. Hagen, J. D. Tack, J. D. Maestas, D. E. Naugle, J. T. Forbes, and K. P. Reese. 2017. Better living through conifer removal: a demographic analysis of sage-grouse vital rates. PLoS ONE 12:e0174347.

Taylor, R. L., B. L. Walker, D. E. Naugle, and L. S. Mills. 2012. Managing multiple vital rates to maximize greater sage-grouse population growth. The Journal of Wildlife Management 76:336-347.

Tyrrell, E. A., P. S. Coates, B. G. Prochazka, B. E. Brussee, S. P. Espinosa, and J. M. Hull. 2023. Wildfire immediately reduces nest and adult survival of greater sage-grouse. Scientific Reports 13:10970.

Williams, C. K., R. D. Applegate, R. S. Lutz, and D. H. Rusch. 2000. A comparison of raptor densities and habitat use in Kansas cropland and rangeland ecosystems. Journal of Raptor Research 34:203–209.